ADVANCED FUNCTIONAL MATERIALS
www.afm-journal.de

The Synergy of Artificial Intelligence and 3D Bioprinting: Unlocking New Frontiers in Precision and Tissue Fabrication

*Joao Vitor Silva Robazzi, Irem Deniz Derman, Deepak Gupta, Logan Haugh, Yogendra Pratap Singh, Vaibhav Pal, Yasar Ozer Yilmaz, Suihong Liu, Andre Luis Dias, Rogerio Andrade Flauzino, and Ibrahim Tarik Ozbolat**

This review examines the transformative role of artificial intelligence (AI) in 3D bioprinting, focusing on how advanced AI technologies enhance its precision, functionality, and scalability. AI, through branches, such as machine learning (ML), computer vision (CV), robotics, natural language processing (NLP), and expert systems (ES), provides critical improvements in real-time process monitoring, error correction, and optimization of bioprinting parameters. The integration of AI enables automated quality control and predictive maintenance, improving bioprinting outcomes by increasing cell viability and structural fidelity, and reducing the amount of bioink wasted. Specifically, ML algorithms are employed to predict optimal bioprinting conditions and streamline the bioprinting workflow, while deep learning enhances the ability to process complex datasets for precision tissue biofabrication. Furthermore, AI-powered robotics and CV systems ensure accurate bioink placement and facilitate the construction of complex tissues. Despite the remarkable progress, challenges remain, particularly in the areas of process monitoring, quality control, and the scalability of bioprinting systems. This review also aims to guide scientists, engineers, and healthcare providers in understanding the complexities and potential of AI-enhanced bioprinting, fostering a deeper appreciation of its role in the future of regenerative medicine and personalized healthcare.

1. Introduction

3D Bioprinting, an advanced technology in tissue engineering and regenerative medicine, has revolutionized the fabrication of complex biological constructs,[1] by precisely layering biomaterials and cells. This technology holds great promise for producing tissues and organs tailored for transplantation as well as disease modeling, drug testing, and personalized medicine. The ability to bioprint complex structures such as vascular networks opens the door for previously unimaginable medical applications. Despite these breakthroughs, the path toward scalable, functional, and clinically applicable bioprinted tissues remains challenging. Several obstacles are hindering the full potential of bioprinting. These limitations can be broadly categorized into technical, biological, and scalability challenges. One of the most significant technical barriers lies in achieving precise control over the deposition of cells. Accurate positioning of cells is crucial

J. V. S. Robazzi, I. D. Derman, D. Gupta, Y. P. Singh, V. Pal, Y. O. Yilmaz, S. Liu, I. T. Ozbolat
Engineering Science and Mechanics Department
Penn State University
University Park, PA 16802, USA
E-mail: ito1@psu.edu

J. V. S. Robazzi, I. D. Derman, D. Gupta, Y. P. Singh, Y. O. Yilmaz, S. Liu, I. T. Ozbolat
The Huck Institutes of Life Sciences
Penn State University
University Park, PA 16802, USA

The ORCID identification number(s) for the author(s) of this article can be found under https://doi.org/10.1002/adfm.202509530

DOI: 10.1002/adfm.202509530

J. V. S. Robazzi, A. L. Dias
Department of Electrical and Computer Engineering
Federal Institute of Sao Paulo
Sertaozinho 14169, Brazil

J. V. S. Robazzi, R. A. Flauzino
Department of Electrical and Computer Engineering
University of Sao Paulo
Sao Carlos 13566, Brazil

I. D. Derman
Department of Polymer Science and Technology
Istanbul Technical University
Istanbul 34469, Turkey

L. Haugh, I. T. Ozbolat
Biomedical Engineering Department
Penn State University
University Park, PA 16802, USA

V. Pal
Department of Chemistry
Penn State University
University Park, PA 16802, USA

for ensuring the desired function of the final construct, especially for heterocellular tissues with different cell types and gradients. However, the complexity of working with living cells introduces variability that can affect print fidelity and consistency. Furthermore, current bioprinters are limited by the resolution of nozzle-based systems, which restricts the precision required to build the micro-architecture of native tissues, such as capillaries, nerve networks, and osseous tissue.[2]

Additionally, achieving real-time feedback and error correction during bioprinting is still underdeveloped. Factors such as non-uniform bioink extrusion in extrusion-based bioprinting (EBB), droplet size variations, and nozzle clogging in droplet-based bioprinting (DBB), pose significant risks, reducing the reproducibility of bioprinted constructs. Moreover, the bioinks must balance bioprintability with biological compatibility, often requiring optimization to avoid mechanical instability and maintain cell viability and function. Cells can be subjected to stress during the bioprinting process due to shear forces or exposure to ultraviolet light (UV) and chemicals during crosslinking. These factors can compromise cell viability and affect their long-term function. Moreover, replicating the complex vascular network required for nutrient and oxygen diffusion in thick tissues remains a major challenge. Another biological constraint lies in recapitulating the dynamic microenvironment of native tissues. Cells interact with their surroundings and neighboring cells through biochemical signaling, which influences their proliferation and differentiation. Current bioprinting methods struggle to incorporate these dynamic aspects, limiting the bioactivity and proper maturation of bioprinted tissues.

Although bioprinting has shown promise in laboratory settings, transitioning to clinics remains a challenge. Scaling up the production of tissues or organs introduces logistical challenges, such as controlling batch-to-batch variation, automating production processes, and managing supply chain requirements for biomaterials. Bioprinting times can also be prohibitively long, especially for organ-sized constructs, which affects cell viability, further hindering scalability. The use of multi-material bioprinting, co-culturing different cell types, and the creation of perfusable vascular networks are essential to mimic functional organs. However, balancing the mechanical properties of bioinks with biological needs while maintaining bioprinting precision becomes increasingly complex when scaling up bioprinted constructs.

AI has been considered a powerful tool to address many of these challenges. AI-driven models can optimize bioprinting parameters to enhance precision and reduce variability. AI algorithms can analyze large datasets from pre- and post-bioprinting stages, improving bioprinting fidelity through predictive modeling. Moreover, AI can monitor bioprinting in real-time, enabling error detection and correction during bioprinting. These advancements collectively improve the reliability and reproducibility of bioprinted constructs. AI also plays a vital role in optimizing bioink formulations and predicting cell behavior based on large datasets, thus enhancing the biological relevance of bioprinted tissues. In addition, AI-powered robotic systems facilitate high-throughput bioprinting, paving the way for scalable production. Different AI algorithms can be explored to automate the adaptation of bioprinting conditions, making real-time adjustments based on feedback. With these capabilities, AI is poised to unlock new levels of precision and scalability in bioprinting, accelerating its transition from bench to bedside.[3]

AI involves the development of algorithms and systems that allow machines to perform tasks typically requiring human intelligence. AI systems process vast amounts of data, recognizing patterns and making informed decisions based on that data. Key subfields of AI, including CV, robotics, NLP, ES, and ML, allow machines to perform complex tasks by learning from data or applying rule-based decision-making.[4,5] ML enables systems to adapt and improve performance autonomously, without explicit programming. When combined with the other subfields, AI becomes a powerful tool for solving data-driven challenges across industries, including healthcare. In bioprinting, AI allows optimization of bioprinting processes by analyzing diverse data sources, such as imaging data, bioink properties, and environmental conditions.[6,7] CV systems can process and interpret real-time visual data to detect irregularities during the layer-by-layer formation of tissue constructs. This integration of real-time analysis and adaptive control leads to improved precision, reduced waste of bioinks and cells, and more reproducible fabrication of complex tissues. Evaluating the effectiveness of AI in bioprinting involves assessing how well these systems can predict, monitor, and improve bioprinting while maintaining cell survival rates and function.[8,9] For instance, ML algorithms can be trained to predict optimal bioprinting parameters such as speed, pressure, and temperature for various bioinks, based on past experiments. The performance of these models is evaluated by comparing predicted outcomes with actual results, including cell viability, mechanical strength, and the physiological integration and functionality of bioprinted tissues within their intended biological context. With each new print, AI systems refine their algorithms, constantly improving their predictive capabilities. Reinforcement learning (RL) plays a key role here, where AI agents learn through a trial-and-error process, continuously optimizing bioprinting parameters by receiving feedback from the process in real-time.[10]

For example, CV systems integrated with ML can inspect each layer of bioprinted constructs, ensuring consistency in thickness, patterning, and bioink distribution.[11] Any deviations from the desired output can be immediately corrected through real-time adjustments, minimizing errors and improving reproducibility.

Y. O. Yilmaz
Department of Nanoscience and Nanoengineering
Istanbul Technical University
Istanbul 34469, Turkey
I. T. Ozbolat
Materials Research Institute
Penn State University
University Park, PA 16802, USA
I. T. Ozbolat
Cancer Institute
Penn State University
University Park, PA 16802, USA
I. T. Ozbolat
Neurosurgery Department
Penn State University
University Park, PA 16802, USA
I. T. Ozbolat
Department of Medical Oncology
Cukurova University
Adana 01330, Turkey

Moreover, AI-driven systems such as ES offer significant improvements in handling the inherent variability in biological systems.[12] Unlike traditional logic systems that require exact inputs, fuzzy logic, an expert system algorithm, can handle uncertainty and variability, making it ideal for biofabrication, where environmental conditions and biological responses can fluctuate.

The synergy between AI and 3D bioprinting is still in its early stages, but its potential is immense. As AI technologies continue to evolve, they will enable more sophisticated models that can anticipate the biological behavior of bioprinted tissues over time, leading to more biologically-relevant and clinically useful tissues. This integration of AI-driven automation, data analysis, and real-time optimization has the potential to revolutionize the field, making it possible to bioprint tissues with higher precision, faster production rates, and improved function.

This review explores how advances in AI are transforming 3D bioprinting by addressing important technical and biological challenges to make it more precise, functional, and scalable. First, we discuss recent developments in AI-driven bioprinting and examine specific AI functions that enhance the process, such as CV for real-time monitoring, robotics for precise handling, NLP as an interface tool, and ES for decision-making. Next, we explore how ML methods, including supervised, unsupervised, and RL, are used to optimize bioprinting settings and results by learning from previous experiments. In addition, the Review discusses the integration of AI with different bioprinting techniques, such as EBB, DBB, laser-assisted and light-based bioprinting, and other emerging techniques. Finally, we consider challenges and opportunities in bringing AI-enhanced bioprinting into clinical use and conclude with future perspectives in this promising field.

2. The Evolution of AI in 3D Bioprinting

AI has undergone substantial evolution since its initial concept in the 50s, with early developments in machine intelligence laying the groundwork for rule-based systems.[13] However, the limitations of these static systems spurred the emergence of ML, a subfield of AI that allows machines to learn and adapt from data, moving beyond fixed rules. Pioneering breakthroughs in artificial neural networks have driven significant advancements across multiple domains, including 3D bioprinting. A foundational framework for pattern storage and retrieval, inspired by human memory, was developed using energy minimization principles to address computational challenges, establishing the basis for neural networks in optimization and pattern recognition,[14] essential for achieving high precision in processes, such as 3D bioprinting. For example, AI-driven optimization algorithms now facilitate nozzle path planning, ensuring accurate deposition of bioinks and minimizing print errors during fabrication of complex tissue constructs.[15] The development of advanced neural networks, comprised of weighted-response neurons, mimics the behavior of biological neurons,[16] enhancing real-time decision-making in bioprinting systems.

Further, artificial neural networks (ANN), could efficiently solve complex optimization classic problems like the traveling salesman problem, outperforming traditional digital methods.[17] This capability to handle complex tasks has been adapted in 3D bioprinting, where it optimizes print-path planning, bioink distribution, and enhances the structural integrity of bioprinted tissues. The advancements in ANN, particularly with the development of Boltzmann machines, introduced unsupervised learning methods, allowing machines to learn from data without explicit labels.[18] These breakthroughs laid the foundation for modern DL techniques, which have been crucial in enhancing bioprinting.[19] Further progress in computer capabilities, backpropagation, and deep belief networks propelled AI forward, driving innovations in fields, such as CV and NLP.[20] The ability to effectively train deep neural networks transformed AI, making DL models indispensable across various fields, including bioprinting.[21]

AI-powered robots use ML and DL algorithms to learn from their environment, adapt to new situations, and autonomously execute tasks. In bioprinting, AI-enhanced robotics is used for precision manipulation, automation of intricate processes, and real-time quality control. These systems integrate AI functionalities to improve trajectory planning, navigation, and task execution, making them crucial for high-precision tasks in tissue engineering and other industrial applications.[20] As robots become more autonomous, their capacity to work alongside humans in dynamic environments continues to expand, addressing challenges posed by irregular and dynamic surfaces, which are crucial for in situ bioprinting. Similarly, ES, a branch of AI designed to emulate the decision-making capabilities of human experts, complement this autonomy by enabling robots to make precise, context-aware decisions in such complex environments.[22] ES typically employ "if-then" rules, using a knowledge base and inference engine to mimic expert-level reasoning. ES allows non-experts to make informed decisions based on predefined rules crafted by specialists, making them useful in fields such as diagnostics, bioprinting parameter control, and process optimization. However, ES face limitations when applied to highly complex problems, where creating an exhaustive rule-based system becomes impractical. Despite these challenges, ES remains valuable for tasks that require clear decision pathways, where data-driven ML models may not yet be applicable. Meanwhile, generative AI, such as NLP integrated with DL, is gaining importance through systems like ChatGPT, Copilot, and Gemini, offering complementary solutions for ES by handling more complex situations using artificial creativity.

The NLP branch focuses on creating new content, such as text, images, audio, videos, and soon, 3D models that resemble human-generated content. In bioprinting, generative AI provides promising tools to enhance the design and optimization of complex biological structures, such as tissues and organs. This technology leverages advanced models and algorithms to produce novel outputs based on training data, with applications like predicting tissue constructs, generating 3D models from patient data, and automating experiment documentation. It utilizes NLP, which enables computers to understand, interpret, and generate human language through various techniques, including DL and ML algorithms. Some types of AI models commonly used in bioprinting include generative adversarial networks (GANs), variational autoencoders (VAEs), and large language models (LLMs).[23] GANs are a type of AI that consists of two parts, one generates data and the other evaluates it by comparing the generated models with existing ones, improving the accuracy of the output over time. For example, GANs can

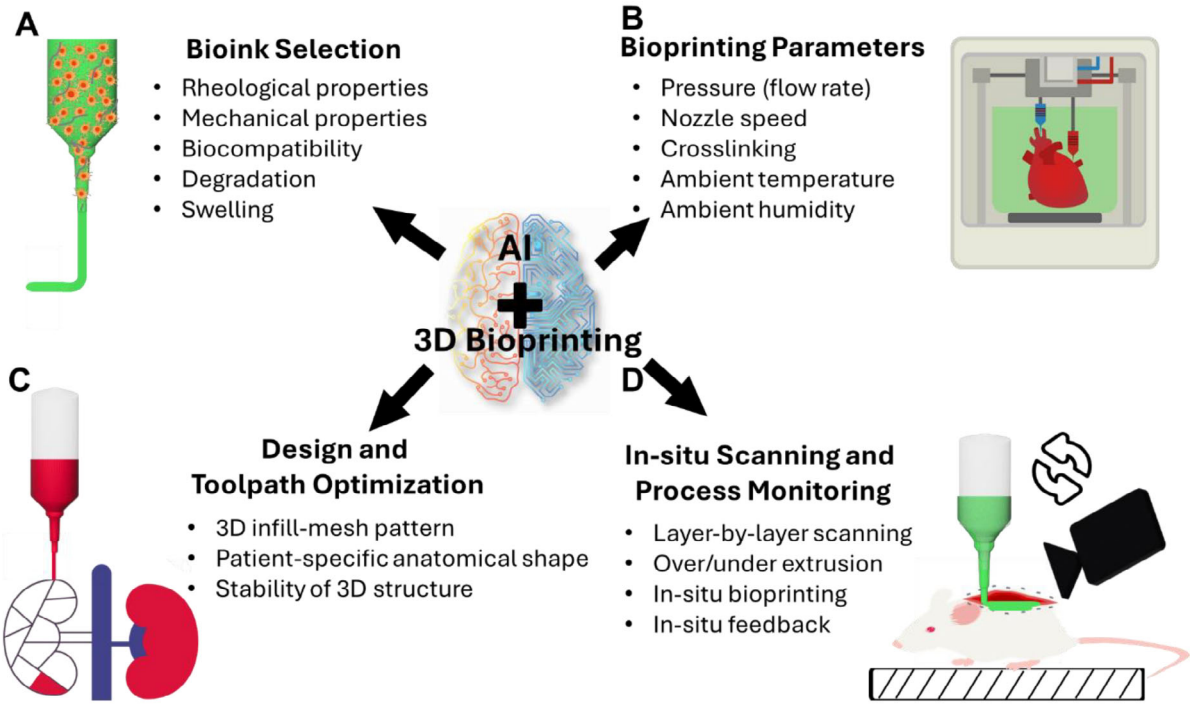

Figure 1. AI integration in bioprinting focuses on A) bioink selection, B) optimizing bioprinting parameters, C) design, and D) process monitoring through in situ scanning to enhance precision and cell viability and function for tissue engineering applications. This figure was produced with Adobe Inc., (2019), Adobe Illustrator.

process medical imaging data, like magnetic resonance imaging (MRI) or computed tomography (CT) data, to extract the detailed shapes and structures of patient-specific organs. By integrating additional patient-specific information as inputs, such as age, weight, and physiological characteristics, these models can generate customized 3D designs that match the patient's unique anatomy. This enables more precise bioprinting, with tailored tissue constructs with improved function and compatibility in medical applications.

2.1. Advancing 3D Bioprinting with AI

AI is transforming bioprinting by significantly enhancing precision, efficiency, and quality control throughout the entire process.[24] AI assists in selecting and fine-tuning bioinks.[25] Bioink selection is critical for successful bioprinting, especially when creating complex tissues, so the bioinks must have properties that support both printing and cell survival. Researchers have developed bioinks using natural and synthetic materials, each offering unique benefits.[26] Rheological properties of bioinks describe how they flow and deform. Key factors include viscosity and yield stress, supporting the structural property post-bioprinting. Balancing these factors ensures both printability and structural integrity. AI can analyze rheological data to predict optimal combinations of viscosity and yield stress[27] (Figure 1A). These properties help ensure the bioink can be printed smoothly and hold its shape. Moreover, mechanical properties, such as stiffness, elasticity, and strength, are also vital for the stability of bioprinted constructs.[28] AI can optimize these properties by learning from past data to adjust parameters like pressure, layer thickness, and crosslinking methods, leading to stronger and more consistent prints. Besides the structural properties, biocompatibility is critical for bioinks, as bioinks must support cell survival and growth without causing harm. Natural polymers like collagen and gelatin are often used, as they closely mimic natural tissues' extracellular matrix.[26] AI can understand how different bioink formulations interact with cells, optimizing parameters such as temperature and material composition to enhance biocompatibility. Degradation rates of bioinks are also crucial, as bioinks should break down in sync with tissue formation.[29] AI can help predict how bioinks degrade in biological environments, optimizing factors like crosslinking and biomaterial composition to achieve the desired degradation rate. Swelling is crucial for nutrient diffusion and waste removal in bioprinted constructs, which depend on factors like crosslinking density, polymer composition, and osmotic conditions. Excessive swelling can compromise constructs, while insufficient swelling hinders cell function.[30] AI optimizes swelling by analyzing the past data of material and environment, fine-tuning parameters like crosslinking intensity and polymer concentration to ensure functionality and support cell growth. Other bioprinting parameters, such as pressure (or flow rate), nozzle size, printing speed, ambient temperature, and humidity, can be optimized using AI (Figure 1B). By analyzing data from both successful and unsuccessful bioprinting attempts, AI can learn to predict the optimal parameters for future applications, tailored to specific tissue types.[7]

Another important role of AI is in design optimization, where algorithms analyze complex biological data, such as CT or MRI, to create precise 3D models that mimic the intricate internal

structure of native tissues, including porous structure, vasculature networks, and tissue interfaces.[31] These models ensure effective patterns and structures for bioprinting, which are crucial for the fabrication of scalable constructs, such as whole organs (Figure 1C). By integrating data from patient medical records and images, AI can design customized tissues and organs that precisely match the unique anatomical and physiological characteristics of each individual.[32,33] This level of personalization is essential for improving patient outcomes and advancing the field of regenerative medicine.[34] It enables the production of bioprinted tissues that are not only structurally accurate but also functionally viable, enhancing the likelihood of successful integration and performance in the patient's body.[35,36]

In addition, AI-powered CV and machine vision (MV) systems are integral to real-time process monitoring, capturing high-resolution images to verify that each layer of bioinks is accurately deposited[31] (Figure 1D). This real-time feedback mechanism allows for the immediate detection and correction of defects such as air bubbles, misaligned layers, and incomplete areas, thereby enhancing the precision and consistency of bioprinted constructs.[37] Furthermore, AI automates the calibration and alignment of bioprinters, significantly reducing the need for manual adjustments.[38] By utilizing visual markers and reference points, AI ensures that the print head and platform remain accurately positioned throughout bioprinting, resulting in faster and more efficient setups.[39] It predicts the optimal combinations of cells, growth factors, and biomaterials, and adjusts flow rates and viscosity in real-time to ensure smooth and accurate deposition.[25,38] This capability is crucial for maintaining the integrity and function of bioprinted tissues, particularly when dealing with complex and delicate structures. Avoiding faulty situations can be done using predictive maintenance, another area where AI proves invaluable.[40,41] By continuously monitoring the performance of bioprinting equipment, AI systems can predict maintenance needs through advanced analytics, ensuring consistent operation and minimizing downtime.[42,43] This proactive approach to maintenance helps to avoid unexpected equipment failures that could disrupt the bioprinting process and compromise the quality of bioprinted tissues. Post-processing analysis is also enhanced by AI, as tools can assess the structural integrity, geometric fidelity, and functional properties of bioprinted constructs, ensuring they meet required standards.[44] AI algorithms can analyze imaging data to detect any deviations from the intended design, allowing for quick adjustments and ensuring that the final constructs are of the highest quality.[45,46] This is particularly important for complex bioprinted tissues that require precise spatial organization of multiple cell types and bioinks.

Overall, AI's integration into bioprinting leads to enhanced precision and quality control, enabling real-time error detection and correction.[24,47] This reduces waste, lowers the risk of defects, and ensures that bioprinted tissues and organs are both functional and accurate in shape. By optimizing design, execution, and quality control, AI systems make the biofabrication of complex and high-quality tissues and organs more reliable and scalable, paving the way for significant advancements in regenerative medicine and personalized healthcare.[47,48] The use of AI in bioprinting not only accelerates the development of new medical treatments and technologies but also ensures that these innovations are effective and tailored to the needs of individual patients.

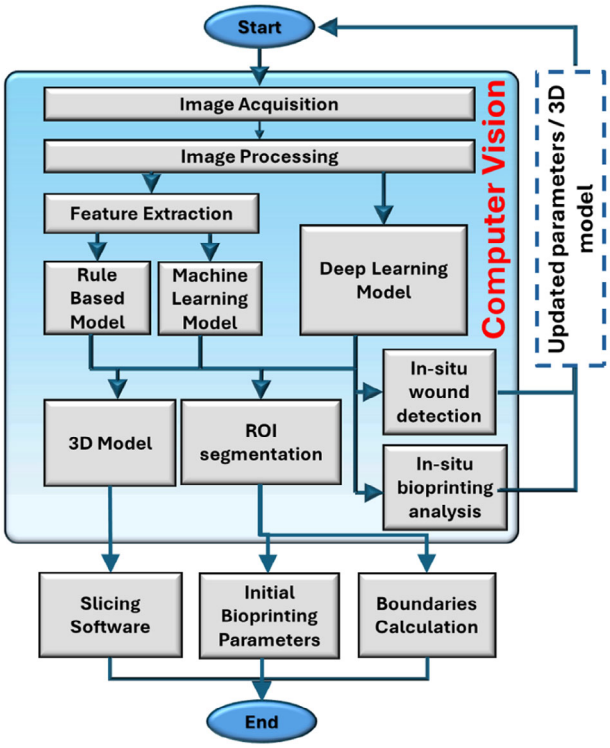

Figure 2. CV-based framework for 3D bioprinting and in situ analysis. The process begins with image acquisition and processing to extract key features. Rule-based, ML, or DL models analyze features for tasks such as wound detection and bioprinting analysis. ROI segmentation defines areas for further processing, including 3D model generation and boundary calculations. These outputs guide slicing, parameter optimization, and adaptive bioprinting with real-time feedback enabled by DL.

This transformative potential underscore the critical role of AI for the future of bioprinting.

3. AI Functions for 3D Bioprinting

As discussed in the previous sections, AI plays a key role in advancing bioprinting technologies. This section discusses various AI functions, such as CV, robotics, NLP, and ES. The discussion entails the methodology of associated algorithms and reviews their integration with bioprinting to enhance precision and adaptability.

3.1. Computer Vision

Computer vision (CV) is a branch of AI that enables computers to interpret the visual world in a way like human sight. While humans understand shapes, colors, textures, faces, and emotions, CV enables computers to visualize the outside world and perform specific tasks. The integration of CV with machines has revolutionized the interaction of machines with the world. The process involves multiple key steps, and **Figure 2** shows the flow of the basic functions of a CV system integrated with a bioprinter. The process begins with image acquisition, where images are captured using cameras or microscopes and converted into a digital form.

Then, image processing techniques, such as noise reduction and contrast enhancement, prepare the images for further analysis. Next, feature extraction identifies key characteristics like shape, size, and texture. These features can be processed by different approaches: rule-based models, ML models, or DL models. When there is enough data and a well-designed architecture, DL can automatically detect patterns in the images without the need for manual feature selection. All three methods can provide similar outputs, such as region of interest (ROI) segmentation or in situ bioprinting analysis to monitor the bioprinting process in real time. After analysis, the system generates 3D models of the bioprinted constructs, which are either prepared for bioprinting using slicing software or used to set the initial bioprinting parameters, like printing speed and bioink flow rate. Finally, boundary calculation ensures that the bioprinted constructs have the correct dimensions. This entire process operates as a feedback loop, constantly improving accuracy and reliability by monitoring and adjusting the bioprinting workflow.[49]

CV can use many algorithms to perform specific tasks. For example, medical imaging can be used in CV for tasks such as enhancing pre-operative and post-operative images.[50] Some algorithms, such as defect segmentation, are important to ensure that tissues are bioprinted with the precise placement of each layer according to the digital model.[51] These can monitor the process and respond in real time, verify that the final product matches the intended design, thus ensuring that bioprinted tissues are both accurate in shape and functionally viable (**Figure 3A**). High-resolution cameras integrated with software can identify defects like air bubbles, misaligned layers, or incomplete areas.[52] Early detection of these issues allows for instant corrections, reducing waste and ensuring the quality of bioprinted tissues or organs. Building on this, Rhee et al. explored bioprinting of collagen constructs for cartilage fabrication.[53] They utilized CV to ensure geometric fidelity, and they also showed high accuracy in the bioprinted constructs. This approach demonstrated that CV could improve the precision of bioprinted soft constructs. In another study, Schmieg et al. improved the quality control using MRI for non-destructive evaluation of hydrogel constructs.[54] They developed a protocol to measure repeatability and geometric fidelity of bioprinted hydrogel constructs, which related geometric errors to specific process parameters.

An important aspect of bioprinting involves scanning and analyzing medical data to reconstruct tissues or organs. However, processing these scanned data, which includes segmentation and reconstruction, can be hard and error-prone due to the limitation on 3D perceptions of 2D images. CV algorithms are capable of segmenting 3D images, such as those of the liver, heart, and brain, and enhancing the final resolution of scans[55,56] (Figure 3B). At this stage, CV and computer graphics are significant. While CV algorithms automate and improve the segmentation and identification of anatomical features from the scans, computer graphics techniques reconstruct these features into highly accurate 3D models. Advances in commercial software, like those equipped with ML and DL, have also been shown to improve the accuracy of organ segmentation and anomaly detection, providing automated solutions with a success rate of 98.8%.[57]

Kengla et al. integrated medical imaging with bioprinting to create patient-specific bone constructs.[58] They used CV to convert patient anatomy into bioprinted constructs, ensuring that shapes and architectures matched the individual's anatomy. Using 3D scanners, Borràs-Novell et al. enhanced precision in bioprinting on irregular surfaces.[59] They developed customized silicone masks for non-invasive ventilation by scanning the facial surface of a premature manikin and processing the data into a stereolithography (STL) file. The customized mask was printed with biocompatible silicone and showed a 14% reduction in air leaks compared to older model masks. Zhu et al. demonstrated that an integrated robotic system aided by CV can perceive changes in the 3D printing workspace, such as geometries and motions of target surfaces[60] (**Figure 4A**). They successfully printed functional electronic devices on a free-moving human hand and cell-laden hydrogels on live mice, creating models for future studies of wound-healing diseases and achieving up to 91% correction efficiency. Preprocessing of captured images includes binarization, noise removal, and edge detection using the Sobel operator for precision. A point cloud of the helix's centerline was generated and compared to the reference path, with deviations corrected using a compensation vector. This correction algorithm modified the reference path in real time to adjust the print head, minimizing errors and ensuring more accurate prints.[61] Another example of utilizing advanced imaging and bioprinting techniques for cartilage repair on irregular surfaces is demonstrated by Gatenholm et al.,[62] who analyzed large cartilage defects and osteoarthritis (OA) using computer-aided design (CAD) models generated from 3D imaging (Figure 4B). 3D Scanning provided the best results in terms of resolution, detecting precise OA defects. The results were used to generate G-code for in situ bioprinting directly into lesions.

Vascularization is one of the biggest challenges in bioprinting. Cadle et al. improved vascularization by creating anatomically realistic vascular patterns from CAD images of rodent mesentery and colon.[63] They used CV to bioprint these patterns, showing functional, anatomically accurate tissues for precision medicine. Bioprinting can also be used to construct phantoms, which are artificial models used for simulating human tissues for medical research and training. For example, Azizi et al. showed the use of bioprinted tissue-mimicking phantoms for studying diagnostic imaging techniques.[64] They created phantoms simulating benign and cancerous tissues, imaged with a clinical ultrasound scanner. CV analysis differentiated among tissue types, showing the ability of phantoms to mimic in vivo conditions closely. In terms of integration in AI functions, Bertelsen et al. used robotic arms with CV for knee cartilage lesion repair.[65] They developed an intra-operative scanner using photogrammetric pipelines to reconstruct cartilage surfaces from photographs taken by a robotic-handled endoscope.

By enabling real-time monitoring and error correction, CV technologies ensure the production of high-quality bioprinted tissues and organs, paving the way for more reliable and scalable bioprinting applications. MV, a subset of CV, is presenting essential advancements in the manufacturing industry, matching demands for quality control and product traceability.[66] MV systems, integrated into production lines, perform quality inspections to avoid defective products and control machines, such as guiding robots during assembly.[67] Key tasks include object identification, position detection, completeness checking, shape and dimensional inspection, and surface inspection. These ensure

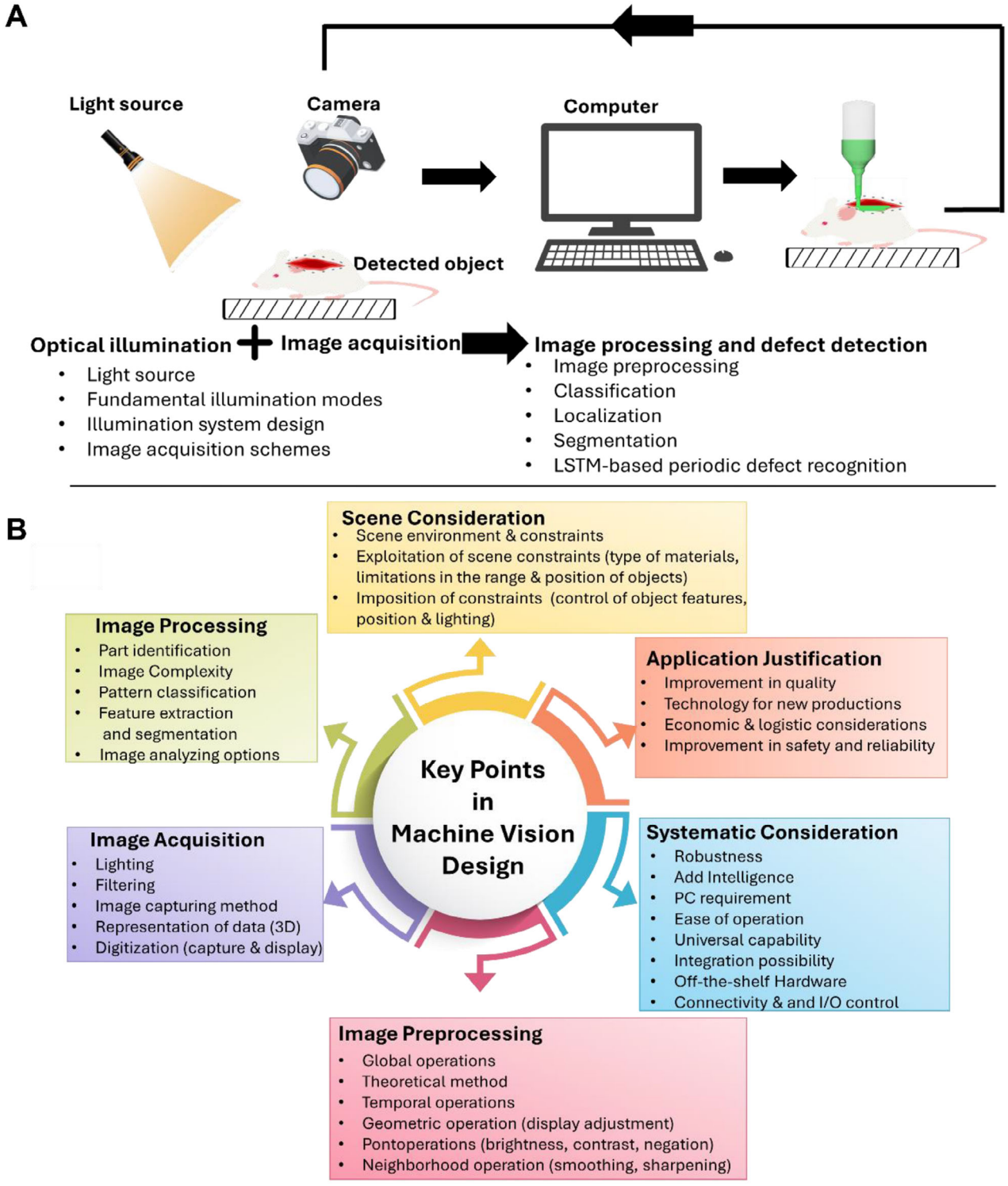

Figure 3. A) Overview of a standard industrial visual inspection system architecture, highlighting its key components and functional elements. Panel (A) is reproduced (adapted) with permission[45] Copyright 2021, Springer Nature. B) Essential aspects in the design and implementation of a machine vision system. Panel (B) is reproduced (adapted) with permission.[55] Copyright 2007, Elsevier B.V.

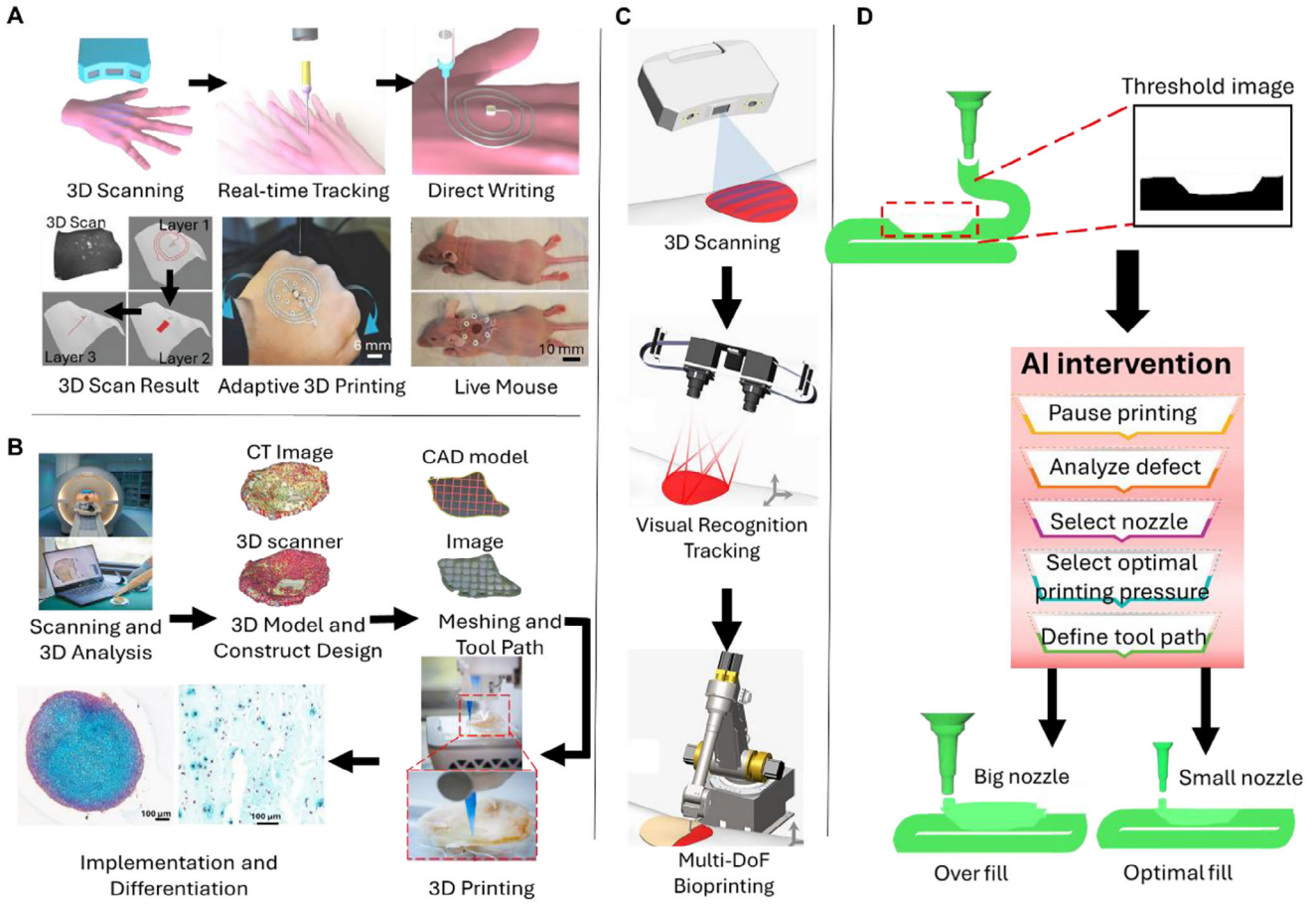

Figure 4. A) Adaptive 3D printing of multifunctional devices. The schematic illustrates 3D scanning of the target surface, real-time tracking of its motion, and direct writing of a conductive ink for precise and dynamic fabrication. Additional images show 3D scanning of a human hand with geometrically adaptive print-paths for each layer, along with a live mouse before and after the creation of an artificial wound with fiducial markers for alignment and monitoring. Panel (A) is reproduced (adapted) with permission.[60] Copyright 2018, John Wiley and Sons. B) Instrumental and experimental setup for analyzing the tibial plateau. The setup includes MRI and 3D scanning systems for data acquisition. Gaussian curvature analysis was performed on 3D models generated from CT and 3D scanning. CAD models with different infill patterns were developed for the construct evaluation. An in situ bioprinting setup was used to print directly into a cartilage defect in a tibial plateau obtained from an osteoarthritic patient following total knee arthroplasty. Histology sections show chondrocyte differentiation after 2 weeks, including bioprinted primary chondrocytes, demonstrating successful differentiation and matrix formation. Panel (B) is reproduced (adapted) with permission.[62] Copyright 2020, SAGE. C) A workflow schematic of the adaptive multi-degree-of-freedom robotic in situ bioprinter. Panel (C) is reproduced (adapted) with permission., [70] Copyright 2022, John Wiley and Sons. D) CV algorithms enable real-time monitoring, defect detection, and process optimization in bioprinting. High-resolution imaging systems identify issues such as overfilling, allowing AI to adjust bioprinting parameters and ensure precise, functional tissue fabrication. This figure was produced with Adobe Inc., (2019), Adobe Illustrator.

that products are correctly identified, accurately assembled, properly completed, within geometric tolerances, and free of surface defects. MV systems consist of cameras, illumination sources, image acquisition hardware, and software for processing and evaluating images.[68] Building on CV capabilities, although MV is specifically designed for industrial applications, it has the potential to advance bioprinting.[69] While CV focuses on understanding and extracting information from images, MV assists with automated calibration and alignment of a bioprinter. Utilizing visual markers and reference points, MV can automatically adjust the bioprinter and print-head, maintaining accurate positioning throughout the bioprinting process, reducing the need for manual adjustments, and making the setup faster and more efficient.

Algorithms, such as Simultaneous Localization and Mapping (SLAM), are valuable in bioprinting for real-time tracking and adjustment, especially for 6-axis robots that need to understand both their environment and their own position. This technology helps overcome current limitations in bioprinting hardware, such as inadequate process monitoring and quality control, thereby increasing the potential for industrial scale bioprinting applications.[69] An example of this application is automated calibration systems in high-end bioprinters, which use MV to detect and adjust the position of the print-head and platform, ensuring optimal alignment and reducing errors. Zakharova et al. proposed a novel method for 3D bioprinting on moving surfaces, addressing the challenge of maintaining accuracy and precision in dynamic environments.[69] Their approach involves real-time

video processing to analyze and adjust the bioprinting process, thereby improving tissue quality. Another study investigated bioprinting of tubular tissues, e.g., vascular tissues, using a custom 3D bioprinter with the MV technology,[11] where a quality inspection scheme was implemented utilizing advanced sensors for real-time measurement, establishing a relationship between tissue quality and factors like the angle and brightness of bioprinted constructs.

MV systems detect and correct errors immediately, enhancing the precision and consistency of bioprinted constructs, mainly in situ bioprinting, where the environment can change during the process. Factors such as nozzle alignment errors or non-linear behavior of bioinks can lead to discrepancies between designed and fabricated constructs. To address this, advanced scanning techniques, such as laser-based or interferometry methods, can be used to monitor bioink deposition in real time.[71–73]

Skin tissue engineering represents one of the most significant application areas for MV in 3D bioprinting. Effective clinical skin repair requires rapid healing, personalization, and functionality. MV can improve wound treatment, as shown by Gholami et al, who developed a tool for segmenting wounds, converting the data into instructions for a bioprinter robot.[74] This tool compared several segmentation methods, finding the Livewire method most effective. The segmented wound coordinates were used to generate G-codes, achieving high accuracy in bioprinted skin patches, enhancing clinicians' control over the bioprinting process. Similarly, Ding and Chang developed an in situ bioprinting workflow to fabricate skin grafts directly onto burn wound phantoms. Their method integrated contour extraction, calibration, and a novel printpath generation algorithm to achieve precise bioprinting of cell-laden constructs that promote cell viability and proliferation.[75] In another study, Zhao et al. introduced an adaptive bioprinting robot for in situ bioprinting (Figure 4C) on full-thickness excisional wounds in mice.[70] Equipped with a 3D scanning and closed-loop visual system, the robot offered precise wound coverage through stereotactic bioprinting. Using bioinks with epidermal stem cells and skin-derived precursors, bioprinted wounds exhibited complete wound healing. To advance personalized wound care, Jeong et al. developed INSIGHT (Intelligent in situ printing Guided by Eye-in-Hand robot Technology).[76] Using a depth camera and a robot arm, INSIGHT finds and prints on wounds at different angles, targeting multiple areas and applying various bioinks to create constructs and bandages quickly. On an *ex vivo* porcine model, INSIGHT's printing modes (extrusion or spray) reduced the time needed for large wounds. Its microgel-based bioink promoted cell growth and was effective for treating diabetic wounds.

Another critical application area of MV in bioprinting is addressing the lack of direct process control, which often leads to inaccuracies and design limitations in EBB.[77] Armstrong et al. tackled this issue by introducing an iteration-to-iteration process monitoring system that enhances bioink deposition accuracy.[77] This system uses a non-contact laser displacement scanner to measure bioink placement after the initial print. A custom image processing algorithm then compares the scanner data to the reference trajectory, generating an error vector that adjusts the reference trajectory for subsequent iterations. This method improves spatial bioink placement and reduces dimensional errors. Building on this, the same group developed a process monitoring and control strategy to improve bioink deposition accuracy a year later.[78] Using a non-contact laser displacement scanner and a custom image processing script, the system evaluates deposition errors and adjusts control inputs iteratively, reducing 1D and 2D errors significantly. This approach improves spatial material placement and width consistency, enhancing the precision of bioprinted constructs. In the future, the process can be further enhanced by integrating CV with multiple nozzles to improve the bioprinting accuracy. For example, upon identifying a defect layer through real-time scanning, the bioprinting could be paused to analyze the defect. Subsequently, an appropriate nozzle could be selected to precisely fill the cavity without over-filling, thereby ensuring higher precision and quality (Figure 4D).

Ensuring high quality during bioprinting remains a challenge, particularly for in situ and in-line monitoring. In this regard, Gugliandolo et al. proposed infrared (IR) imaging to monitor bioprinted geometries non-destructively.[79] This method addresses the limitations of visible-range imaging, particularly with transparent bioinks, and provides precise information on the latest bioprinted layer. IR imaging significantly enhances in-line monitoring of bioprinting ensuring construct quality. In another study, Zhang et al. developed a transformer-based neural network for real-time monitoring in top-down vat photopolymerization, an additive manufacturing method known for its low cost, high precision, and fast production.[80] This approach addresses the challenge of defect detection in large, segmented prints. Using a dataset of in situ images and the Swin Transformer model, they achieved a high mean intersection over union (a widely used metric for evaluating segmentation performance as it measures the overlap between predicted and ground truth regions, averaged across all classes) of 96.14% for accurate layer-by-layer monitoring. Additionally, a multi-quality monitoring indicator was created to detect common print issues, reducing waste and improving efficiency. This monitoring strategy holds significant potential for bioprinting applications, where precise control and defect detection are critical for maintaining cell viability and achieving high structural fidelity. Overall, MV systems bring substantial benefits to bioprinting by automating critical tasks, enhancing precision, and ensuring consistent quality. These advancements facilitate the industrial application of bioprinting technologies, making the processes more efficient and reliable for producing complex and high-quality biological constructs.

3.2. Robotics

Robotics is widely employed in in vitro and in vivo fabrication of 3D constructs with complex shapes, enhancing the precision and automation of bioprinting tasks.[81] Bioprinting with robots uses a predefined CAD model based on image reconstruction of defects, enabling the fabrication of complex tissues with the print path adjusted and monitored by the user. These devices can feature multiple print heads and bioink chambers. Key elements typically include a high-resolution 3D defect scanner, a bioprinting unit (e.g., EBB and DBB), a robotic manipulator (e.g., cartesian, parallel, or articulated) with three or more degrees of freedom, a control and monitoring cabinet, and occasionally a workbench.

Robots function by processing user commands and sensor signals, which are then sent to processing models, including

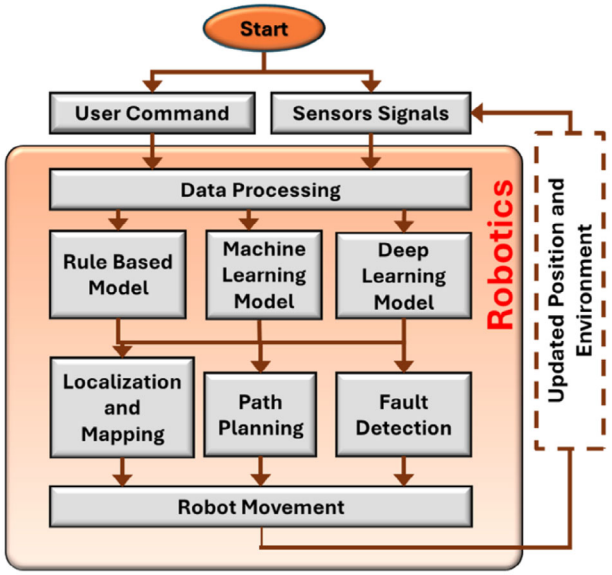

Figure 5. Schematic representation of the robotics framework for an autonomous process. The system starts with user commands and sensor inputs, which are processed through a data processing module. This module utilizes rule-based models for predefined actions, ML models for adaptive decision-making, and DL models for handling complex scenarios. The processed data drives three key robotic operations: localization and mapping for spatial awareness, path planning for navigation, and fault detection for reliability. These components work within a closed-loop system, where continuous sensor feedback optimizes robot movement and performance.

rule-based, ML, and DL approaches. This enables key tasks like localization, path planning, and fault detection. The processed data guide the robot, allowing autonomous movement and task execution with continuous feedback for real-time adjustments (**Figure 5**). The integration of robotics into a bioprinting setup allows for high accuracy and reduces the potential for operator fatigue. The configuration of these robots, whether Cartesian coordinate, articulated, or parallel, plays a crucial role in defining the working space, deposition flexibility, and operational precision required during bioprinting. Robots use sensors such as cameras, LiDAR, and tactile devices to analyze their environment and interpret events around them. Sensor data supports critical tasks like localization and mapping, path planning, and fault detection, enabling robots to plan their movements effectively. These calculations can use either rule-based models, which are fast but limited, or ML and DL algorithms, which are highly adaptive for tasks, such as object recognition and autonomous navigation in dynamic environments.

Cartesian coordinate bioprinting robots, or Cartesian bioprinters, are the most common bioprinters. Operating on the principles of Cartesian coordinates (x, y, and z axes), these bioprinters move print-heads along three linear axes, allowing precise positioning and layer-by-layer construction of 3D structures by depositing bioinks in a predefined pattern. This linear movement ensures high precision and accuracy, essential for creating detailed and complex biological structures. It offers a high degree of platform stiffness. Cartesian bioprinters are versatile, capable of handling a wide range of bioinks (e.g., hydrogels, and spheroids), making them suitable for various applications, such as tissue engineering, drug testing, and disease modeling.[3,82] However, challenges include non-uniform bioink viscosity, poor cell viability during bioprinting, anisotropic bioprinting, low resolution with speed, and the stair-step effect due to the restricted motion of the nozzle to a 2D plane. Technological advancements have enabled integration with imaging technologies, providing real-time feedback, improving cell viability, and ensuring accurate deposition by monitoring and adjusting parameters during the process. Additionally, enhanced automation and robotics mitigate anisotropic printing and the stair-step effect by enabling multi-axis motion, improving resolution without compromising speed, and ensuring greater reproducibility and efficiency in complex tissue fabrication. Examples of Cartesian bioprinters include the INKREDIBLE series by CELLINK, BioBot Basic by Advanced Solutions,[84] and R-GEN 100/200 by RegenHU,[85] each offering unique features for different research and medical applications. Innovations, like the biomimetic "tendon cable" soft robot arm, have been introduced to enhance printing flexibility by adding six degrees of freedom.[86] Moreover, the *xyz* gantry system has been employed for direct deposition on a moving human body, demonstrating the feasibility of robotic bioprinting on dynamic surfaces.

Parallel robots, or delta robots, have multiple arms connected to a single base, allowing for delicate and precise movement. Delta robots are known for their high efficiency and speed. For example, Zhu et al. introduced an adaptive 3D bioprinting technique on moving freeform surfaces using a Delta robot.[60] In another work, Zhao et al. developed a bioprinting platform integrated with advanced robotic technology for in situ bioprinting.[87] This platform employed a delta robot configuration for operations within the human body, using a printed circuit micro-electro-mechanical system to fit within a 30 mm diameter for endoscopic procedures. Articulated robots, equipped with 360° rotating joints, overcome the limitations of fixed-axis systems.[88] These robots feature rotary joints powered by servo motors, allowing precise placement of bioinks onto curved surfaces with sophisticated profiles. For example, the Da Vinci surgical system allows surgeons to perform delicate operations through small incisions.[89] In another study, Lipskas et al. used a robotic-assisted approach for repairing bone and cartilage defects through a minimally invasive procedure.[90] The system demonstrated high printing accuracy with an average error of 0.06 ± 0.14 mm, comparable to other bioprinting methods. Following this study, Ma et al. demonstrated an in situ bioprinting technology for cartilage regeneration, demonstrating its potential for clinical applications.[91] A six-degree-of-freedom robot was employed alongside a novel tool center point calibration method to enhance printing precision. The entire bioprinting process took ~60 sec, enabling rapid defect repair with the regenerated cartilage showing comparable biomechanical and biochemical properties with respect to the native cartilage. These robots allow precise placement of bioinks onto curved surfaces. For example, Zhao et al. developed an adaptive multi-degree-of-freedom in situ bioprinting robot for hair-follicle-inclusive skin repair.[70] This robot integrates 3D scanning and a closed-loop visual system with a six-degree-of-freedom manipulator, enabling precise wound coverage and functional skin repair. In a related study, Chen et al. developed a robot-assisted system for in situ bioprinting of skin using GelMA hydrogels.[92] This system

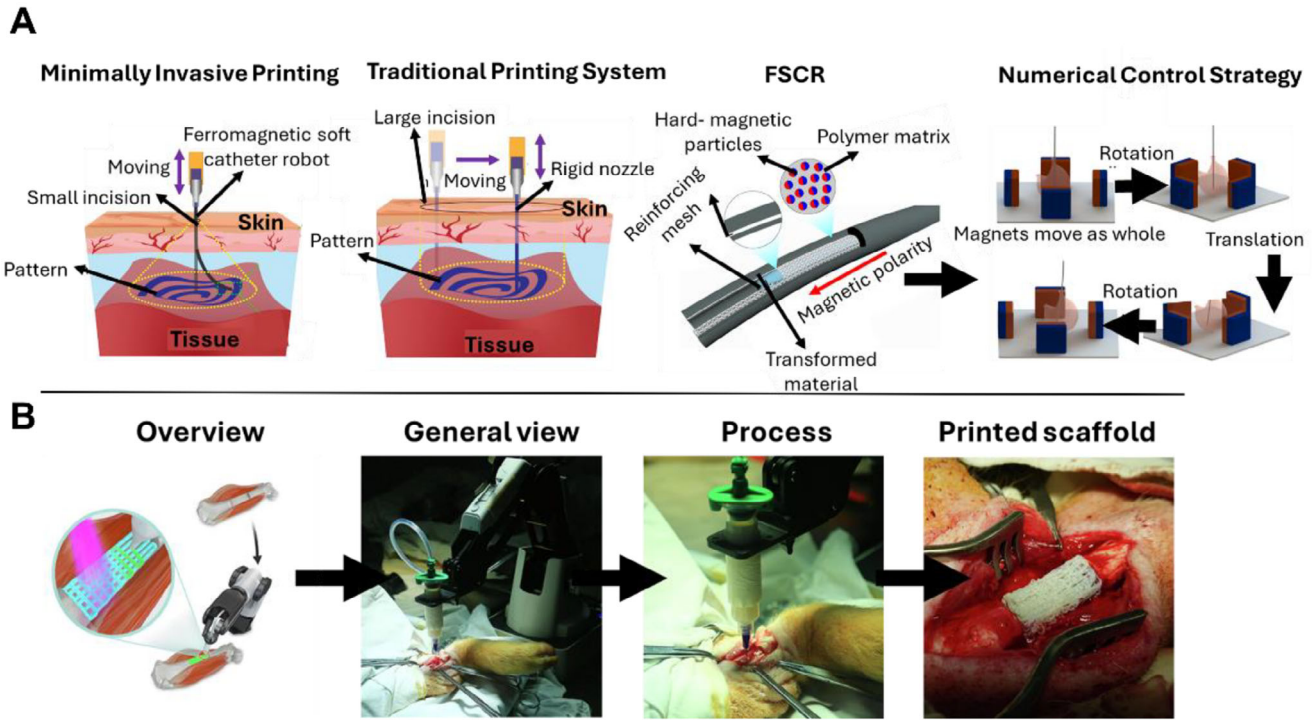

Figure 6. A) Schematic of minimally invasive bioprinting with functional inks through a small incision, compared to traditional bioprinting systems. The FSCR features a soft polymer matrix and operates via magnetic field-based control for precise maneuvering. Panel (A) is reproduced (adapted) with permission.[93] Copyright 2021, Springer Nature. B) Overview of the in situ bioprinting process and the in vivo study workflow. The figure includes a general view of the robotic manipulator-based bioprinter, demonstrating its capability for precise in situ bioprinting. Panel (B) is reproduced (adapted) with permission.[94] Copyright 2021, Elsevier B.V.

demonstrated complete wound healing and functional tissue regeneration, indicating potential clinical applications in skin repair. The robot-assisted bioprinting system, with its precise application capabilities, ensures efficient delivery of the bioink to wound sites, promoting skin regeneration that closely resembles native tissue. Concurrently, Zhou et al. developed a ferromagnetic soft catheter robot (**Figure 6A**) for minimally invasive bioprinting, using magnetic actuation for precise control.[93] Figure 6A also compares this system with a traditional bioprinting setup that uses a rigid nozzle and requires a larger incision, which may increase native tissue damage. The Flexible Soft Continuum Robot (FSCR) consists of a soft polymer matrix embedded with hard-magnetic particles and reinforced with a polylactide (PLA) mesh. Magnetic polarity is programmed along the FSCR's axial direction, enabling controlled movement. The numerical control strategy guides FSCR operations through digital data, allowing precise maneuvering via rotation and translation of four permanent magnets. Building on these advancements, Li et al. introduced an in situ bioprinting system (Figure 6B) for repairing large segmental bone defects, demonstrating improved accuracy and effectiveness in bone repair.[94] This advanced system integrates a robotic arm with a 3D bioprinter, facilitating precise deposition of bioinks directly at the defect site. The multi-material printhead can deposit various bioinks, including osteoinductive materials and cells, to enhance bone regeneration. In another study, Zhang et al. demonstrated a robotic bioprinter for cardiac tissue bioprinting, combining a six-degree-of-freedom robotic arm with an oil bath-based cell bioprinting method.[95] This system, combined with a custom bioreactor and a repeated print-and-culture strategy, successfully generated vascularized, contractile, and long-term viable cardiac tissues, thus offering a promising solution for in vitro fabrication of solid organs. Lastly, Zhao et al. developed a 7-axis robot-assisted minimally invasive surgery technique for fetal membrane repair, showing successful sealing of premature rupture of membranes in both in vitro and mid-gestational rabbit models, showing that the hydrogel patches could significantly prolong pregnancy by maintaining mechanical properties like native tissues.[96]

Overall, the integration of robotics with bioprinting represents a significant advancement. These robots, with their multiple degrees of freedom and precise control, allow for the accurate deposition of biomaterials onto complex and curved surfaces. The versatility and flexibility of these systems have been demonstrated in various applications, from repairing bone and cartilage defects to regenerating skin and cardiac tissues. As these technologies continue to evolve, they hold the promise of further enhancing the capabilities of bioprinting, paving the way for innovative treatments and breakthroughs toward clinical translations.

3.3. Natural Language Processing

Natural language processing (NLP) operates by breaking down human language into a machine-readable form, enabling computers to process, analyze, and even generate text or speech.[9,97] An NLP system processes text or speech input, transcribing

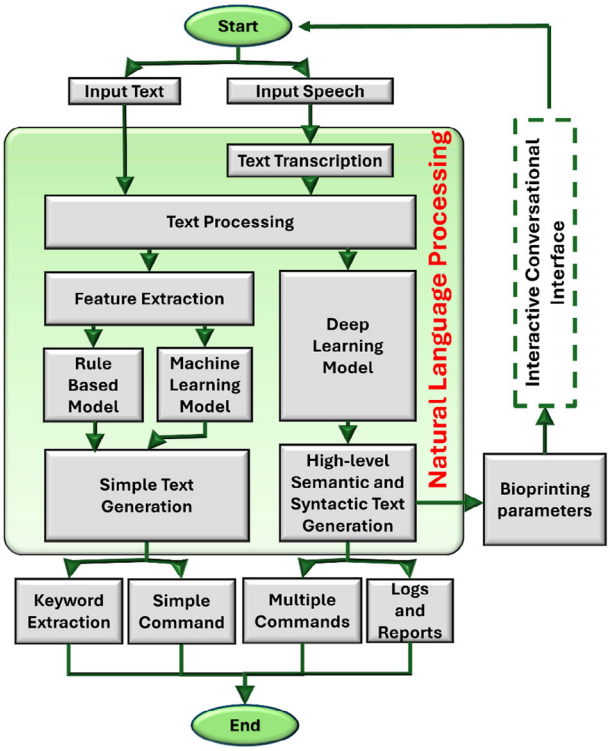

Figure 7. An NLP framework for bioprinting adjustments and command generation. The system processes input from text or speech, with speech input transcribed before entering the text processing module. Text processing involves feature extraction, enabling three pathways: rule-based models for predefined rules, ML models for adaptive text analysis, and DL models for advanced comprehension. Outputs include basic text generation for simple tasks and complex semantic and syntactic text generation for detailed command formation. These outputs support keyword extraction, command execution, and log/report generation. NLP-driven suggestions create a feedback loop to optimize bioprinting parameters in real time.

speech before text processing. Feature extraction enables two pathways: rule-based models for predefined rules and ML models for adaptive analysis. DL models, used for advanced comprehension, often bypass extensive feature extraction. Outputs include simple text generation for basic tasks and high-level semantic text generation for complex commands. These outputs support keyword extraction, command execution, and log/report generation. NLP-driven feedback optimizes bioprinting parameters in real time. **Figure 7** shows the basic flow of an NLP system in the context of bioprinting.

Text generation is achieved through advanced NLP models, particularly those based on DL, like transformers (e.g., Generative pretrained transformer (GPT)). These models are trained on vast amounts of text data, learning the underlying structure, grammar, and patterns of language. During text generation, the model uses this learned knowledge to predict the next word or sequence of words based on a given prompt. This allows for the creation of coherent and contextually relevant text, which is increasingly being used in applications such as chatbots, content creation, and automated reporting. In bioprinting, NLP can significantly enhance research and innovation by leveraging these principles to manage and interpret large volumes of scientific data and literature. For instance, NLP can automate the extraction of critical information, such as bioink compositions, cell viability, or printing parameters, from scientific papers, reports, and datasets. By applying NLP techniques to this data, researchers can quickly identify trends and insights, reducing the manual effort needed to collect vast amounts of literature.

However, it's important to remember that while NLP can make data analysis faster, it should not be the only method used, as it is still in the development stage. Manual supervision is advisable, especially during the initial stages of experimental planning to ensure accuracy and account for nuances that automated techniques may overlook. The algorithm then scans abstracts for these keywords, extracting insights on technological trends, emerging bioprinting technologies, and links between techniques, materials, and applications. For instance, Bonatti et al. showcased the application of NLP techniques to automatically extract and analyze knowledge from the bioprinting literature.[99] Their approach uses abstracts and author-provided keywords, which are automatically categorized into groups, such as manufacturing techniques, materials, and applications.

Moreover, NLP can streamline the operations of bioprinting systems by enabling natural language interfaces. Researchers could use voice commands or written inputs to control bioprinting parameters, making the process more intuitive and efficient. NLP can also assist in automatically generating research summaries and reports on bioprinting results, offering suggestions based on prior studies and experimental results for bioink changes and parameter tunning.[100,101] NLP techniques can convert textual descriptions of materials or shapes into CAD files or directly generate designs, as demonstrated by Khan et al. on text-to-3D model generation and Badagabettu et al. on the generation of the CAD model with the help of self-refinement loops.[102,103] This process bypasses manual coding by leveraging AI to understand natural language commands and generate specific geometries and properties required for bioprinting. Recent work by Kyaw et al. on "Speech to Reality" systems shows how NLP can drive on-demand production using generative AI for physical object creation, highlighting the efficiency of this approach in design and manufacturing. The system presented good results for slow operations; however, some instability was detected when the speed was increased.[104]

In bioprinting, robust quality control measures are essential across various stages of the workflow, including pre-process optimization, in-process monitoring, and post-process assessment, to ensure the final product is both functional and safe for clinical use.[48] NLP can play a pivotal role in this process by specifying the mechanical properties, cellular composition, and geometric features of tissue constructs. NLP algorithms can interpret user-defined input regarding mechanical properties (such as stiffness, elasticity, and compressive strength), cellular composition (such as the type and density of cells to be bioprinted), and geometric features of tissue constructs (such as shape, size, and porosity). By integrating NLP with bioprinting software, these inputs can be transformed into standardized design files (e.g., STL or G-code) and bioprinting parameters such as printing speed and layer thickness, which can be directly utilized by a bioprinter. Thus, the integration of NLP into bioprinting holds significant promise for advancing the field by enhancing user interactions,

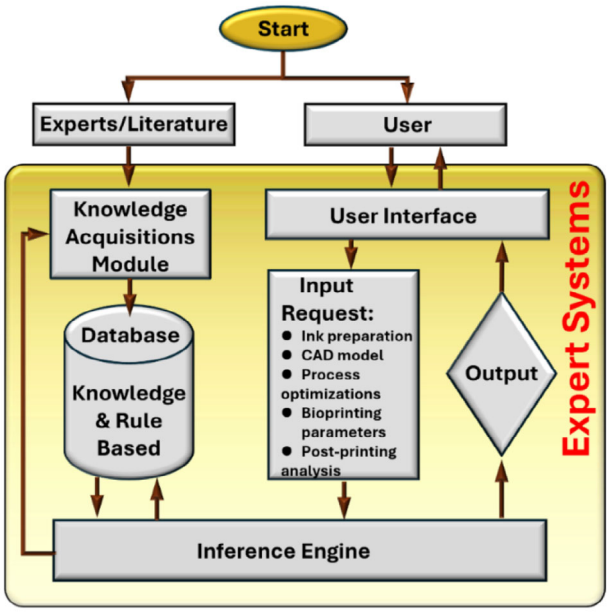

Figure 8. ES framework for bioprinting optimization and guidance. The framework combines input from experts, literature, and user interactions to support intelligent decision-making. A knowledge acquisition module collects and updates data, which is stored in a structured database and knowledge base. Users interact through a user interface to submit requests related to tasks such as bioink preparation, CAD modeling, process optimization, bioprinting parameters, and post-printing analysis. The inference engine processes these inputs using stored knowledge and rules to generate actionable recommendations, enabling precise and efficient bioprinting workflows.

improving design customization, and streamlining data analysis, thereby driving innovation and efficiency in bioprinting.

3.4. Expert Systems

Expert systems (ES) are intelligent software systems designed to replicate and apply the knowledge of human experts to solve complex problems within specific domains, such as multi-material bioprinting processes.[105,106] These systems use rules, knowledge bases, and reasoning mechanisms to provide insights, automate processes, and improve accuracy. ES are typically composed of three key components: 1) a knowledge base, which collects and store domain-specific knowledge, facts and rules; 2) an inference engine, which processes the information in the knowledge base by applying logical rules to draw conclusions and make decisions; and 3) a user interface, which allows users to interact with the system, input data, and receive advice or instructions based on the system's reasoning.[105] **Figure 8** shows how an ES works. ES in bioprinting leverages accumulated expert knowledge to apply well-established parameters, such as optimal pressure, temperature, and printing speed. By enforcing these boundaries, ES help predict and prevent failures and potential damage to both the bioink and bioprinter, ensuring smoother operations and maintaining the integrity of bioprinted constructs. As knowledge-based tools, ES offer significant advantages: they capture and reuse expert knowledge to ensure consistent decision-making, enhance efficiency by automating routine tasks, and swiftly process large datasets, ensuring accuracy while minimizing human errors, bias, and variability in decisions.[107,108] Thus, ES have been extensively adopted across various fields, including additive manufacturing, where their integration has ushered in a new era of possibilities, enabling enhanced design optimization, path planning, material selection, process control, and precision.[109]

Designing and reconstruction of 3D models serve as a fundamental and critical phase in 3D bioprinting, significantly influencing the successful fabrication of target constructs, particularly in the modeling of complex human tissues and organs.[110] ES can provide valuable design and modeling support by offering insights into optimal model geometry, orientation, supporting materials, and structural configurations, including filling density and structure. This assistance not only enhances the shape fidelity of bioprinted constructs and reduces material consumption but also contributes to the distribution of biomaterials and cells, mechanical properties, and the pore arrangement for exchange of nutrients, oxygen, and metabolites.[106,109] Moreover, an essential application of ES in bioprinting lies in process optimization. These systems analyze complex parameters of bioprinting, optimizing critical variables such as layer thickness, bioprinting speed, operating temperature, pneumatic pressure, biomaterial selection, and bioink formulations to enhance printing precision and efficiency.

Abdollahi et al. established an expert-guided optimization (EGO) system to optimize 3D printing of a polydimethylsiloxane elastomer resin.[12] This EGO strategy integrates expert knowledge with algorithmic optimization, using expert screening, hill-climbing search, and iterative decision-making to fine-tune the printing parameters. The developed EGO system was successfully applied to 3D printing of complex structures with unprecedented precision and shape fidelity, demonstrating its effectiveness in optimizing 3D printing processes. The EGO strategy is also well-suited for bioprinting applications, such as embedded bioprinting. EGO could enhance the ability of bioprinting functional tissues by incorporating parameters like cell type, growth factor levels, and other biological properties into the optimization process. For example, Yang et al. established a knowledge-based expert system, where a structured knowledge framework organizes and represents the geometry, materials, functions, and relationships of assembly components, and modified the RETE algorithm-based design decision-making, achieving the decision guidance for printability and integrity of target assembly in the additive manufacturing process.[111] Additionally, a prototype of ES was developed to detect polymer particles for 3D printing, analyzing key properties that influence the quality of selective laser sintering.[112] This ES can also be used for detecting the quality of preparing spheroids and cell-laden microgels, thereby enhancing the efficiency and stability of processes, such as aspiration-assisted bioprinting.[113]

The application of ES in manufacturing planning exhibited considerable potential for improvements in efficiency and decision-making. Effective bioprinting planning is crucial for creating complex multicellular tissues. A specialized expert system can optimize cell and material deposition, improving accuracy and mimicking native structures, enhancing tissue engineering for clinical use.[114,115] Likewise, Abdulwahab et al. reported a rule-based ES for the selection of additive manufacturing

systems, including common metal and non-metal printing, to streamline decision-making for manufacturers.[116] Given the variety of bioprinting techniques developed to date, establishing a similar ES for bioprinting selection is essential for adapting to the specific requirements of constructing different tissues or organs.[117,118] Moreover, quality assurance stands as a cornerstone of additive manufacturing, particularly in high-requirement sectors, such as aerospace and biomedicine. ES plays a crucial role in real-time monitoring and control of bioprinting processes, leveraging ML and image recognition technologies to promptly identify anomalies and deviations from established quality standards, thereby facilitating immediate adjustments to ensure optimal output quality and enhance the reliability of bioprinted constructs.[119] In the context of culturing and evaluating living tissue substitutes for bioprinting, the development of specialized ES grounded in biomedical knowledge and principles will be instrumental. This system can enhance functional tissue regeneration by dynamically adjusting growth factors and optimizing the tissue microenvironment, thus creating conditions conducive to effective tissue development.[120] Finally, maintaining bioprinting equipment is crucial for ensuring sustained productivity. ES plays a key role in predicting maintenance needs of machines or processes by analyzing machine data, historical maintenance records, and usage patterns, especially for automatic biofabrication processes in the future.[121] This predictive capability not only helps prevent costly downtime and bioink waste but also significantly enhances the reliability of bioprinting processes while extending their operational lifespans.[122]

Overall, ES significantly enhances additive manufacturing by supporting every stage of the processes, from design optimization and material selection to real-time monitoring, error detection, and even post-processing and quality assurance. By automating complex decision-making, these systems accelerate the development of bioprinting, addressing technical challenges, improving efficiency, and driving innovation in the field. While the integration of ES in additive manufacturing offers significant advantages, several challenges remain to be addressed, such as the need for more comprehensive databases, continuous refinement of AI algorithms, and standardized interfaces to ensure different systems work together. Particularly in the emerging field of bioprinting, establishing reliable and comprehensive databases for ES is a significant challenge, due to the complexity and variability of biological materials, cellular behavior, and tissue-specific requirements. However, with the rapid advancements and data accumulation in bioprinting, such as the establishment of an open source bioink database for EBB, along with the integration of ML and DL algorithms, empowers ES to enhance the efficiency and stability of bioprinting functional tissue analogs.[123] This progress is poised to significantly advance clinical transplantation efforts in biofabrication. Similarly, fuzzy logic, a mathematical approach used to model complex systems, offers a complementary tool for addressing the inherent uncertainties in bioprinting processes, where conventional models may fail due to their binary nature.[124]

Unlike traditional Boolean logic, which outputs values as either 0 or 1, fuzzy logic operates on a spectrum of truth values between 0 and 1.[125,126] This approach mirrors human reasoning more closely and is advantageous in various applications, including bioprinting. A fuzzy logic system comprises four key components: fuzzification, fuzzy inference, defuzzification, and a knowledge base.[124] Fuzzification is a process in fuzzy logic that transforms plain numbers into fuzzy values, which represent degrees of truth rather than absolute truths or falsehoods. These fuzzy values are generated using expert-set rules, which are graphically represented as shapes like triangles, trapezoids, or curves. These shapes help determine how much an input value, such as bioink temperature, fits into categories like "hot" or "cold." The range of fuzzy values between 0 and 1 allows for nuanced classifications, beyond just binary hot or cold, by indicating degrees of hotness or coldness. In more advanced fuzzy systems, these rules themselves can be fuzzy, introducing greater flexibility and capacity to handle uncertainties, though at the expense of more complex calculations.[127,128]

The knowledge base of fuzzy logic consists of rules expressed as IF-THEN statements. These rules relate input variables to output variables using linguistic terms. In bioprinting, one can consider the rule: IF extrusion speed is "very fast" and pressure is "very high," THEN bioprint quality is "very poor." The fuzzy logic system uses these terms to evaluate inputs against rules. In this scenario, the inference mechanism determines the relevance of each rule based on the given inputs: extrusion speed and pressure.[125] The output of this evaluation is a secondary fuzzy value, which is organized in a matrix format, showing the degree to which each rule, such as the one stated, applies. This matrix represents the fuzzy logic's intermediate step before final output generation. This fuzzy value is then processed in the defuzzification stage to transform it back into a clear and specific value.[125,127]

Fuzzy logic systems are particularly useful for optimizing bioprinting parameters. Given the often-vague nature of input data in bioprinting, fuzzy logic can enhance the resolution and quality of bioprinted constructs. For instance, Sedigh et al. used a fuzzy system to predict how printing parameters—speed, pressure, and bioink dilution—affect printed line width.[125] By printing squares with varying parameter combinations and measuring the line widths, they created a rule set for the fuzzy system. The system then predicted line widths for any combination of parameters within the tested range, resulting in significant precision improvements for bioinks. The researchers compared two fuzzy systems in predicting bone tissue mineralization based on cell culture duration and cell suspension density.[129] By feeding micro-CT data into both systems, they generated predictive models that accurately depicted how these parameters influence mineralization volume. The study highlighted the superior accuracy of type II fuzzy systems due to their ability to handle more complex uncertainties. Together, these studies demonstrate the benefits of fuzzy logic in optimizing bioprinting parameters. By reducing the need for extensive measurements and bioink usage, fuzzy logic systems can efficiently map how different parameter combinations affect bioprinting outcomes. This approach saves time and resources while providing highly accurate predictions, making it a valuable tool in bioprinting. Its ability to model systems with vague or imprecise information makes it ideal for optimizing bioprinting parameters, enhancing the quality and precision of bioprinted constructs, and contributing to advancements in bioprinting.

Table 1. AI functions integrated with bioprinting.

AI Technique	Working Mechanism	Key Strengths & Advantages	Major Limitations & Drawbacks	Applications
CV	Utilizes image data to identify defects, isolate areas of interest, reconstruct surfaces, and enhance automated quality control.[57,74]	• Enhances print fidelity and resolution, enabling real-time quality control and defect detection.[77] • Improves reproducibility by automating adjustments during bioprinting.[61]	• Processing speed and accuracy heavily reliant on high-quality imaging.[49]	Automated quality control, error detection, process optimization, surface reconstruction in complex applications.[60,66]
Robotics	Employs one or more multi-axis robotic arms for flexible, adaptable, and multi-material bioink deposition.[60,70]	• Automates bioink placement, reducing human error.[90] • Enhances real-time quality control and scalability.[130] • Ensures precise and repeatable manipulation of delicate tissues.[95]	• High setup and operational costs. • Complex AI and robotic integration required, challenging for smaller labs or teams.	Real-time process monitoring, high-precision manipulation of cells, automation of complex structures with a minimal error.[95]
NLP	Analyzes and interprets human language to facilitate user interaction, automate documentation, and extract insights from textual data.[98,99]	• Enhances user-machine communication. • Automates record-keeping and reporting processes.[100]	• May struggle with context-specific jargon or ambiguous language in technical settings. • Requires extensive training data.[97]	Improving usability in bioprinting software interfaces, automating process documentation, extracting data from scientific literature.[99,100]
ES	Utilizes a rule-based knowledge system to replicate human expert decision-making in controlling processes.[105]	• Provides domain-specific decisions quickly.[108] • Optimizes specific tasks with high precision.[109] • Reduces manual intervention by automating decision-making processes.[105,112]	• Rule-based systems are challenging to scale highly complex problems. • Difficult to adapt to new, unforeseen conditions.[105]	Diagnostic assistance, parameter control, and process optimization in bioprinting.[121,125] Applies during pre-bioprinting (bioink selection), post-bioprinting (quality control analysis), and active bioprinting processes.[105,125]

Table 1 summarizes the working mechanism, advantages, limitations, and applications of different AI functionalities in the context of bioprinting.

4. Optimizing Bioprinting Processes through ML

ML is a key branch of AI, and it is closely related to other branches such as CV, robotics, NLP, and ES. These branches can operate with an explicit set of rules, but adding ML improves their flexibility, accuracy, and effectiveness. ML helps them learn from data, adapt to new situations, and make smarter decisions. Nowadays, these areas often rely on ML techniques to improve their function and performance. These intelligent systems can adapt to new information and changing situations.[131] Much like humans and animals learn from their surroundings and experiences, ML systems in bioprinting use the data from previous experiments to improve future outcomes. In general, learning means adapting systems based on experience. For example, ML can refine print parameters after each experiment, optimizing future processes to achieve better quality and function.[20]

AI models that use ML are typically trained using large datasets, either from previous prints or from simulations (digital twins) of tissue growth and cell behavior, and are evaluated based on their ability to generalize to new scenarios. Metrics, such as accuracy, precision, recall, and mean squared error, are commonly used to assess performance of trained ML models.[8,9] ML algorithms are typically classified as supervised, unsupervised or RL, where supervised learning relies on labeled data employed to train the predictive models for pattern recognition and regression tasks, while unsupervised learning does not require labeled data, most suitable for clustering tasks,[132] which involve grouping similar data points based on their characteristics to identify patterns or relationships within the data. In bioprinting, supervised learning can help predict specific outcomes like cell survival, print quality, or bioink behavior using the data that are already labeled with known results. This allows researchers to adjust bioprinting settings like pressure, temperature, or bioink composition to achieve better results. Unsupervised learning, on the other hand, does not need labeled data. For example, it can group bioink types based on their properties or how well they print. This can reveal new insights that improve bioprinting without needing as much pre-labeled data. RL can optimize bioprinting parameters by learning from real-time feedback. For instance, a CV algorithm can monitor the process, assess layer precision and bioink deposition, and provide feedback to the RL system, assigning rewards for improved quality and penalties for defects, thereby optimizing the model in real time.

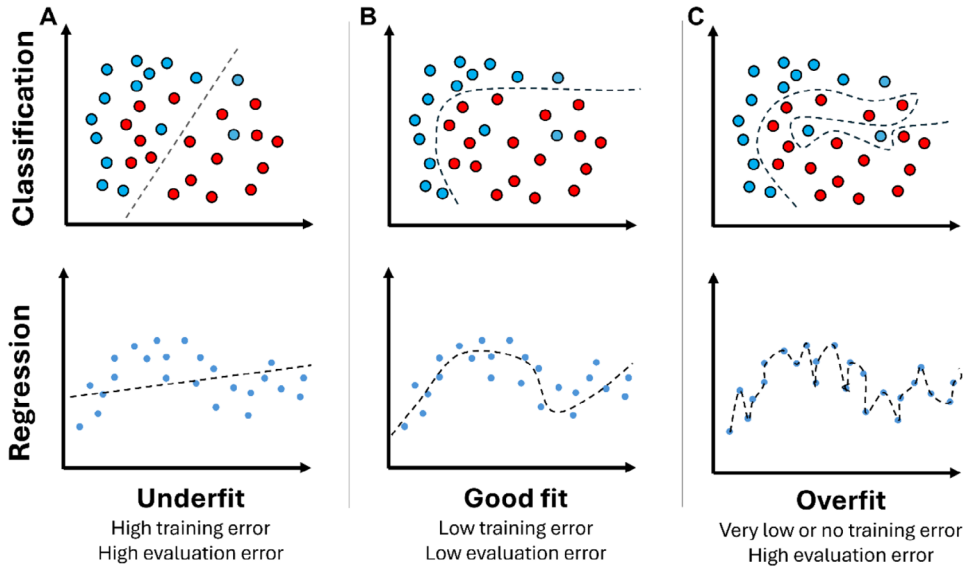

Figure 9. Illustration of model complexity and its impact on classification and regression in ML. Classification boundaries and regression models demonstrate different levels of fitting: A) underfitting: linear or simple models fail to capture the nonlinear separability or trend in the data, B) optimal fit: nonlinear models effectively balance bias and variance, accurately capturing the data structure or relationship, and C) overfitting: highly complex models fit noise, reducing generalization to unseen data.

A notable subfield of ML is DL, which automates the feature extraction process from raw data, leading to superior performance in various tasks. DL has shown remarkable success in applications such as image recognition, NLP, and generative models. In bioprinting, DL can be combined with CV for in situ scanning and real-time monitoring of bioprinting, ensuring print quality and layer precision.[133] Additionally, DL, alongside computer graphics, can analyze medical images like CT and MRI scans to generate detailed 3D models for personalized bioprinting. NLP can also be used to analyze medical records and generate diagnostics, further enhancing the accuracy of bioprinted constructs by tailoring them to specific patient needs based on medical data. Additionally, ML can facilitate real-time corrections during the bioprinting, enabling adjustments based on immediate feedback from sensors and monitoring systems.[61] This ensures that any deviations from desired parameters can be quickly addressed, leading to higher-quality output and reduced waste.

ML has two crucial aspects that are directly applicable in bioprinting. First are classification models, which focus on categorizing data into distinct groups. For instance, classification models can identify patterns or categories to determine the suitability of a bioink by analyzing specific properties of its formulations. This enables researchers to quickly assess which bioinks are viable for their applications.[48] These properties may include viscosity, cell concentration, gelation time, and mechanical strength, with the output classified as either suitable or not suitable. The second are regression models, which focus on predicting continuous numerical values. These models can predict and fine-tune outcomes, such as the precise pressure, printing speed, and temperature needed during extrusion, ensuring more accurate and consistent bioprinting results.[26]

Data representation is crucial for effective ML in bioprinting. Input data must be organized to capture the critical features that determine successful bioprinting. Key parameters such as rheological and mechanical properties, biocompatibility, degradation rate, swelling behavior, environmental conditions, and the specific cell types used all play a critical role in influencing bioprinting quality and ensuring cell viability. Properly organizing this input data ensures that ML models can efficiently learn and make accurate predictions. For example, if the data captures how bioink viscosity affects printability, the model can predict bioprinting results for bioinks having different viscosities, provided other parameters are maintained the same.[134] Additionally, data quality directly affects the performance of the ML model. High-quality data that accurately reflects the properties of bioinks leads to better predictions. This requires precise and reliable instruments for data collection. If the data is biased or incomplete, the model's predictions will be unreliable, leading to suboptimal results. Therefore, the calibration and accuracy of data acquisition tools, such as sensors or other hardware, are vital for the successful implementation of ML in bioprinting.[135]

A crucial concept in ML is generalization, which ensures that models not only perform well on training data but also on new, unseen data. In bioprinting, where bioinks and processes can vary significantly, generalization is especially important. ML models must capture the underlying patterns in the data rather than memorizing specific details from the training set. One common challenge in ML is underfitting (**Figure 9**A), where a model is too simple to capture the underlying patterns in the data, resulting in poor performance on both the training and new data. To achieve optimal fitting, it is essential to strike a balance between underfitting and overfitting by ensuring that the model captures the underlying patterns in the data without becoming overly specialized to the training set (Figure 9B). This requires a combination of robust model design, appropriate data preprocessing, and effective training strategies. Achieving sufficient generalization, meaning the model performs well on both training and new data, requires careful design of the model architecture and

tuning of hyperparameters. For example, selecting the right neural network architecture is crucial for optimal performance. CNNs are well-suited for tasks involving image data, such as real-time defect detection, while recurrent neural networks (RNN) are ideal for sequential data, like monitoring cell behavior over time. Hyperparameters, which are model configurations set before training, play a significant role in balancing accuracy and avoiding overfitting. Key hyperparameters include the learning rate, batch size, and the number of hidden layers, each of which directly influences the model's learning dynamics and performance.[136] On the other hand, overfitting (Figure 9C) occurs when a model becomes overly specialized to the training data, leading to poor performance on the new data.[137] The learning rate controls how quickly the model updates in response to data. A high learning rate can cause abrupt shifts, leading to unstable predictions and issues like uneven layer deposition or cell damage due to poorly tuned parameters. Conversely, a low learning rate slows down learning, prolonging training times and delaying results. The batch size affects the amount of data processed at once. While smaller batches require less computational power, excessively small batch sizes may impair generalization, resulting in lower accuracy on new data. The number of hidden layers determines the network's depth and its capacity to learn complex patterns. Deeper networks are beneficial for capturing intricate relationships, particularly with large datasets. However, too many hidden layers can cause overfitting, as the model becomes overly tailored to the training data and struggles to generalize new examples.[136]

Furthermore, the adaptability of ML models is essential in the fast-evolving field of bioprinting. As new bioinks and techniques are developed, ML models can be updated to incorporate new knowledge, ensuring that bioprinting processes remain efficient and cutting-edge. Overall, ML is more than just a tool for analyzing data; it is a driving force of innovation in bioprinting and related fields. Its ability to learn, adapt, and optimize processes is key to pushing the boundaries of what bioprinting can achieve, making it an indispensable part of the future of tissue engineering.[138]

Table 2 provides an overview of various ML algorithms utilized in bioprinting. Several key subfields of ML that contribute significantly to advancing AI-driven applications in this domain are highlighted below.

4.1. Supervised Learning

In supervised learning, models are trained on labeled datasets to recognize patterns and make predictions based on input-output pairs. In other words, the models depend on data with known input and output to perform two major tasks: classification and regression. This approach is foundational in ML and bioprinting, allowing for precision and adaptability in various tasks. Supervised learning techniques such as artificial neural networks, deep learning, and convolutional neural networks are widely utilized due to their ability to learn complex relationships and improve decision-making.[132] These models enhance the accuracy of bioprinting processes by optimizing parameters and predicting outcomes with high reliability. In the following sections, supervised learning methods are explored, highlighting their structure, functionality, and applications in bioprinting.

4.1.1. Artificial Neural Networks (ANNs)

ANNs are predictive models inspired by the structure and function of the human nervous system. These models can learn system behavior from data and apply it to a wide range of problems, including pattern recognition, regression, control, time series forecasting, and optimization.[155–157] ANNs consist of artificial neurons, which are interconnected and perform computations analogous to synaptic connections in biological neurons (**Figure 10A-i**). The concept of artificial neurons can be described as a model with multiple inputs, like a neuron's dendrites, represented by variables (x_1, x_2, ..., x_n), and a single output, akin to a neuron's axon, represented by a variable (y).[158] During the training process, the synaptic weights (w_n, w_1, w_2, ..., w_n) are adjusted based on the training data. An activation function is then used to produce the output of the neuron, based on the input values and their corresponding synaptic weights. Figure 10A-ii illustrates the schematic of an artificial neuron. The simplest form of an ANN is a single artificial neuron, also known as a "perceptron." However, in practical applications, multiple neurons are often combined into more complex architectures. One of the most widely used architectures is the Multilayer Perceptron (MLP), which consists of multiple layers of neurons. MLPs typically have an input layer that receives the inputs, one or more hidden layers containing neurons, and an output layer.[159–161]

The training process for ANNs, known as backpropagation, involves two phases.[41] The first phase is the feed-forward phase, where inputs are propagated through the network layer by layer, and the final output (y) is computed based on the current synaptic weights. This output is then compared to the target value ($\hat{y}$) to calculate the error ($\mathcal{E}$). In the second phase, known as the backward phase, this error is propagated back through the network to update the synaptic weights. The two phases are repeated iteratively to minimize the difference between the predicted output (y) and the target value ($\hat{y}$) (Figure 10B).

In pattern recognition tasks, the perceptron is effective when the data are linearly separable. For instance, in a 2D graph with the blue and the red dots, if a straight line can separate blue from red, the data are linearly separable. Figure 10C shows an example of how separation hyperplanes can be used with two inputs in a perceptron network. However, when the data are not linearly separable, more complex architectures like MLPs are required, where the hyperplanes in MLPs handle more complex decision boundaries. For challenging problems, using an MLP with one or more hidden layers is necessary. In a study by Mohammadrezaei et al., ANNs were applied in EBB.[139] They built a comprehensive dataset of bioprinting parameters for gelatin and alginate bioinks, and developed regression and classification neural network models to predict cell viability (Figure 10D). This approach allowed the identification of optimal bioprinting parameters to maximize cell, significantly reducing the need for laborious trial-and-error experiments. The neural network-based Bayesian optimization model proved highly effective in predicting cell viability with high accuracy and optimizing the bioprinting

Table 2. ML algorithms in 3D bioprinting.

Supervised Learning				
ML algorithms	Primary functions	Major advantages	Limitations	Applications in bioprinting
ANN	Model non-linear relationships, optimize printing processes, predict outcomes, and adapt based on historical data for improved performance.	• Capable of modeling complex, non-linear relationships and solving diverse problem types across various domains.	• High computational demands. • Reliance on large datasets • Risk of overfitting and limited interpretability.	• Predict cell viability;[139] develop DMSO-free bioinks for cryo-bioprinting.[140]
DL and DNN	Learns complex patterns from large datasets through multiple layers of neural networks. An advanced version of ANNs with many hidden layers, used for complex pattern recognition.	• High flexibility for complex, non-linear datasets. • Can handle highly complex problems. • Very high flexibility in applications. • Performs well with large datasets.	• Require very extensive computational resources. • Large, labeled datasets are prone to overfitting. • Have limited interpretability. •	• Parameter optimization in DLP bioprinting.[141]
CNN	Specializes in image and pattern recognition, often used in visual data analysis and CV tasks. Modified version of ANN with convolutional and pooling layers.	• Great for image data and real-time monitoring. • Automatically extracts features from visual data.	• Perform optimally only with image data, require extensive labeled datasets, are computationally demanding, and offer limited interpretability. • Raw data requires preprocessing strategies.	• Real-time quality control and parameter optimization;[47] image segmentation and organoid analysis in high-throughput drug screening.[142]
RNN	Processes sequential data by remembering information from previous inputs. Modified version of ANN in which the previous outputs are used as inputs for the next inference.	• Ideal for handling time-series data. • Useful in modeling sequential processes in bioprinting.	• It can struggle with long-term information. • Requires high computing power. • Sometimes they are slow to train and can struggle with finding optimal network parameters.	• No relevant applications found.
Decision trees, RF, gradient boosting, and extreme gradient boosting (XGBoost)	Splits data into branches based on features to guide decisions.	• Easy to interpret and visualize. • Works well with both categorical and numerical data. • Handles non-linear relationships. • Advanced versions handle overfitting and perform well in complex scenarios.	• Decision Trees are prone to overfitting and sensitive to data changes. • Ensemble methods like RFs, Gradient Boosting, and XGBoost require significant computational resources. • These methods need careful hyperparameter tuning. • They can struggle with imbalanced or noisy datasets. • As complexity increases, interpretability may decrease. • Without proper regularization, they risk overfitting.	• Accurate pathogen classification in bioprinted constructs;[143] predict scaffold quality and cell response.[144]

(*Continued*)

Table 2. (Continued)

Supervised Learning				
ML algorithms	Primary functions	Major advantages	Limitations	Applications in bioprinting
SVM	Strong classification model.	• High accuracy in classification tasks. • Effective in cases where the data has a clear margin of separation. • No need for large datasets if the margin is clear.	• Require significant computational resources for large datasets. • Struggle with noisy data and overlapping classes. • They are less effective for high-dimensional data without careful hyperparameters selection.	• Optimize printing parameters for Pluronic in EBB.[145]
BO and GP	Efficiently searches for optimal parameters by balancing exploration and refinement based on data. It uses a probabilistic model to predict outcomes by treating input-output relationships as a continuous function and guides the next experiments to refine the system.	• Reduces the number of experiments required. • Efficiently handles small datasets. • Efficient in high-dimensional spaces. • Balances exploration and exploitation. • Works well for complex, non-linear processes.	• Computationally demanding for high-dimensional problems. • Do not scale well with large datasets.	• Optimize EBB parameters for GelMA and GelMA/HAMA bioinks.[146] Optimize nozzle geometry and material properties for improved cell viability in EBB.[147]
Linear regression and logistic regression	Predict continuous outcomes by modeling relationships between dependent and independent variables. Classifies binary outcomes (e.g., success vs failure) based on input parameters.	• Simple and interpretable. • Effective when relationships between variables are linear. • Good for binary classification problems. • Easy to implement.	• May underperform with complex or non-linear data. • Sensitive to outliers and multicollinearity in predictors.	• Develop DMSO-free bioinks for cryo-bioprinting.[140]
k-NN	Predicts print outcomes by finding the closest data points in previous bioprinting experiments.	• Simple and easy to implement. • Requires no assumptions about the data distribution. • Effective with small datasets.	• It can be slow with large datasets. • Relies on the proper choice of the number of neighbors and distance metric. • Struggles with high-dimensional data. • Sensitive to noise and irrelevant features, which can reduce accuracy.	• Predict cell viability based on printing conditions in SLA bioprinting.[148]
Ensemble learning and hML	Combines multiple algorithms or layers hierarchically to improve decision-making accuracy.	• Increases model robustness. • Reduces overfitting. • Highly adaptable to complex processes in bioprinting.	• It can be computationally intensive. • Require careful model tuning. • Often lacks interpretability due to complexity. • Rely heavily on the hierarchy's structure. • May propagate errors across levels, affecting overall performance.	• Predict cell numbers and monitor droplets in DBB;[149] improve glioma treatment prediction and analyze tumor microenvironments[150]; optimize alginate bioprinting with minimal experimentation[151]; predict printing resolution in EBB.[152]

(*Continued*)

Table 2. (Continued)

Supervised Learning				
ML algorithms	Primary functions	Major advantages	Limitations	Applications in bioprinting
Unsupervised Learning				
ML Algorithms	Primary Functions	Major Advantages	Limitations	Applications in Bioprinting
Kmeans	Cluster data categorizes them into groups.	• Split data into categories, making it easier to understand.	• An expert is required for cluster interpretation. • Requires a predefined number of clusters	Classify 3D-printed scaffolds based on biomaterial compositions and printing conditions.[144]
GANs	Generates new data. It can be used for data augmentation.	• Replace expensive experiments with data collection. • Feasible digital twin option.	• Require large datasets.	3D Nuclei segmentation in CLSM images to analyze cell behaviors in 3D models[153]
Reinforcement Learning				
ML algorithms	Primary functions	Major advantages	Limitations	Applications in bioprinting
Q-Learning	Learns through trial-and-error feedback from real-time bioprinting environments.	• Adaptable to dynamic environments. • Continually improves performance with more iterations. • Minimizes human intervention. • Low or no training required.	• Requires a precise reward system.	Generate a 3D vascular network in a bone model based on a medical image dataset.[154]

Abbreviations: ANNs, Artificial neural networks; DL, Deep learning; DNN, Deep neural networks; CNNs, Convolutional neural networks; RNNs, Recurrent neural networks; CV, Computer vision; RF, Random forest; SVM, Support vector machine; BO, Bayesian optimization; GP, Gaussian processes; EBB, Extrusion-based bioprinting; DLP, Digital light processing; SLA, Stereolithography; DBB, Droplet-based bioprinting; GelMA, gelatin methacryloyl; HAMA, hyaluronic acid methacrylate; DMSO, dimethyl sulfoxide; k-NN, k-nearest neighbors; hML, hierarchical machine learning; GANs, generative adversarial networks; CLSM, confocal laser scanning microscopy.

process, offering a powerful tool for more efficient and precise bioprinting techniques.[139] In cryo-bioprinting, Qiao et al. applied ML to predict the effects of different cryoprotective agents (CPAs) on GelMA bioinks. The study compared four ML models: multiple linear regression, decision trees, random forest, and ANN, to determine their predictive accuracy. The ANNs model outperformed the others, proving especially effective in predicting the cryopreservation efficiency of bioinks composed of various CPAs. These findings highlight the potential of ML, particularly neural networks, in accelerating the development of dimethyl sulfoxide-free (DMSO-free) cryoprotective bioinks, which are crucial for maintaining cell viability during cryo-bioprinting. This approach represents a significant advancement in the long-term preservation of artificial tissues and organs, offering an efficient pathway for bioink development.[140] In another study, a neural network was used to optimize bioprinting parameters for fabricating personalized gingival grafts. By applying second-order quadratic regression, the system identified ideal printing conditions with minimal experiments. The resulting constructs maintained high shape fidelity and cellular viability over 18 days.[162]

4.1.2. Deep Learning and Deep Neural Network

Deep learning (DL) is a subset of ML that uses neural networks with multiple layers, known as deep neural networks (DNNs), to model complex patterns in data. **Figure 11** shows an example of a deep DNN. Unlike traditional ML algorithms, which typically require manual feature extraction and simpler architectures, DL automates the identification of relevant features directly from raw data.[163] This capability makes DL particularly effective for working with large and complex datasets, such as those encountered in fields like computer vision, robotics, NLP, ES, and bioprinting.

In bioprinting, preferring DL over traditional ML methods depends on several important factors. DL is especially advantageous when dealing with complex, high-dimensional, or unstructured data, such as images or sensor readings, because it can automatically detect patterns without the need for extensive manual work.[19] It excels when applied to large or non-structured datasets, often yielding better accuracy by identifying intricate, non-linear relationships. DL is also suitable for tasks that involve predicting multiple outcomes simultaneously, making it a valuable tool for modeling complex bioprinting processes. For

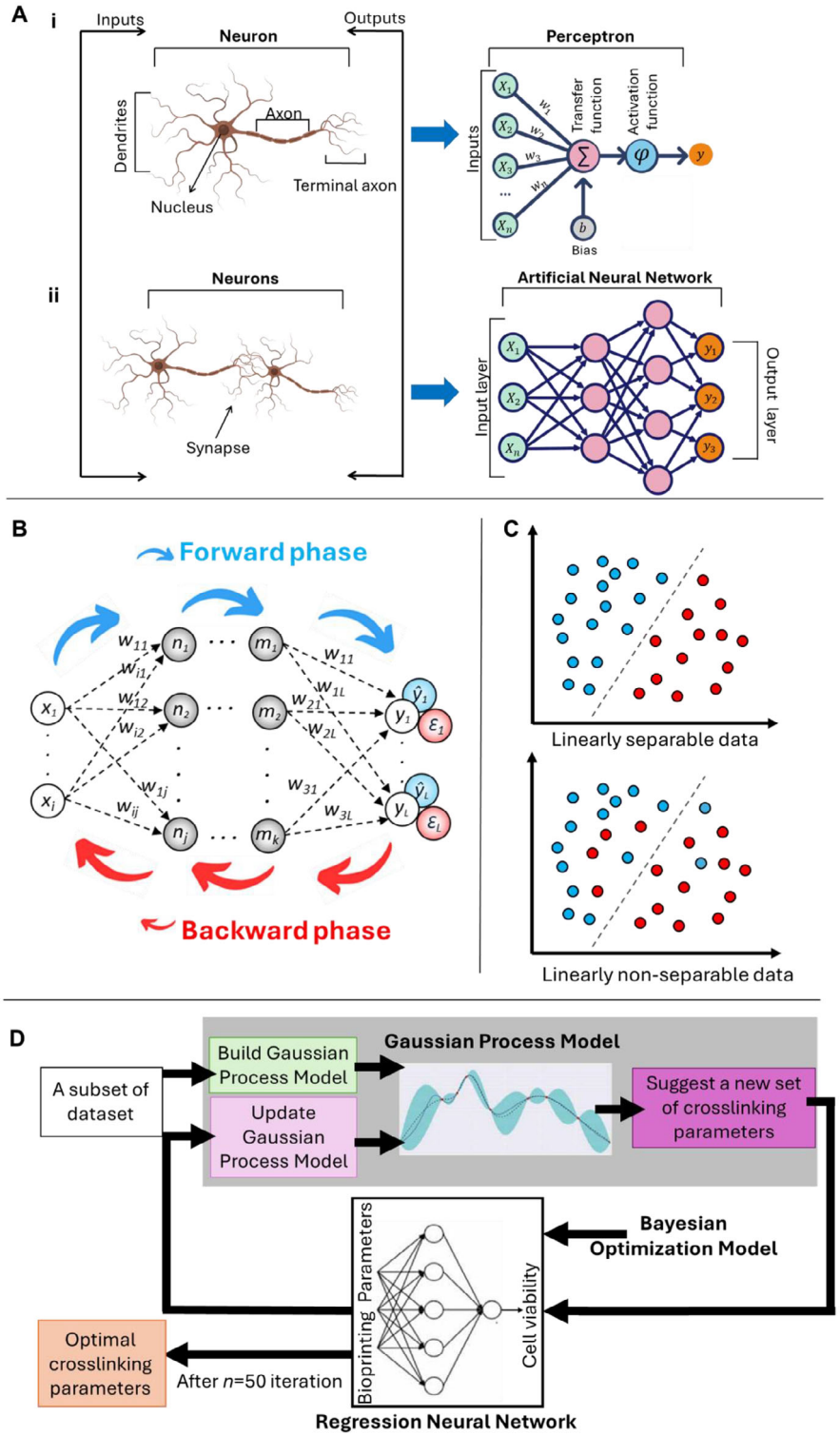

Figure 10. A) i) Illustration of a neuron structure, highlighting its anatomical features, ii) schematic representation of a perceptron and ANN, showing neurons' interconnections within a neural network architecture (produced with Adobe Inc., (2019), Adobe Illustrator). B) Simplified representation of forward and backward propagation in a neural network. During the forward phase (blue arrows), predictions ($\hat{y}$) are computed from input data (x) by passing information through network layers using weights (w) and neurons. In the backward phase (red arrows), errors ($\mathcal{E}$) are calculated by comparing predictions ($\hat{y}$) with true values (y) and propagated backward to adjust weights (w). This iterative process trains the neural network to minimize errors and enhance prediction accuracy. C) Perceptron behavior on linearly separable and non-separable data. For linearly separable data, the perceptron finds a decision boundary. For non-separable data, it fails to converge due to the lack of a linear solution. D) Algorithm of a Bayesian optimization model utilizing a regression neural network for optimizing bioprinting. Panel (D) is reproduced (adapted) with permission.[139] Copyright 2024, IOP Publishing Ltd.

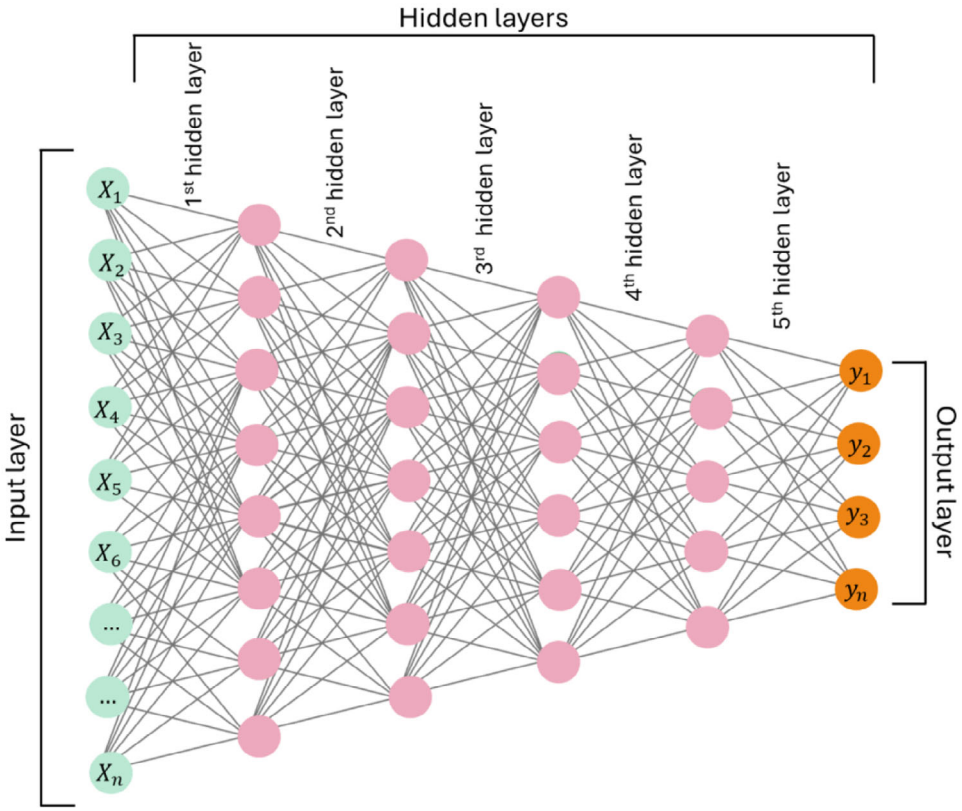

Figure 11. Schematic representation of a deep neural network (DNN) architecture, illustrating input, hidden, and output layers. This figure was produced with Adobe Inc., (2019), Adobe Illustrator.

example, the system can take input from various sensors, such as cameras, accelerometers, and thermometers in a DBB setup, to monitor important factors like droplet size and stability, temperature, and vibration.

Using this data, it can automatically adjust the voltage of a droplet actuator, control the temperature, and fine-tune the printing speed to prevent errors and ensure a stable DBB process all at once. However, DL comes with higher computational demands and often requires more specialized expertise. When computational resources or expertise are limited, traditional ML methods may be more appropriate for simpler tasks. For example, Guan et al. applied DL techniques to address the challenges of cell-induced light scattering in DLP bioprinting.[141] They used a DNN model (**Figure** 12A) with multiple layers to automatically generate optimized bioprinting parameters, improving printing fidelity. The model's hierarchical feature learning compensated for complex scattering effects, which would be difficult for even experienced operators to manually adjust. Despite training the model on a small dataset of only 32 samples, it demonstrated generalization capabilities, significantly enhancing print quality across a range of designs and biomaterials (Figure 12B). That study highlights the potential of DL in bioprinting, particularly in situations where data are limited, and manual parameter adjustments fall short.

4.1.3. Convolution Neural Network

Convolution Neural Networks (CNNs) are one of the most well-known and widely used algorithms in DL.[133] They are similar to MLPs, but they offer the distinct advantage of automatically extracting relevant features from raw data, eliminating the need for manual feature extraction typically required in MLPs, where specialists apply statistical strategies to preprocess data. CNNs have become popular across various domains, including speech recognition, image analysis, and fault detection.[164,165] CNN's architecture can include several layers, with convolutional, pooling, and flattening layers being the most common. These layers play crucial roles in processing input data and optimizing model performance. Convolutional layers use filters to scan the input data, automatically learning important patterns and features, while pooling layers simplify the data by reducing its size, which helps lower the complexity of the network and makes it easier for the model to process without losing key information. This reduction decreases the number of training parameters, helping to prevent overfitting. At the end of the network, the flattened layer shapes the data to fit a fully connected layer's neural network, which maps the information from the previous layers into the final output.[41] **Figure** 13A shows the flow of a CNN with two convolutional layers and two pooling layers.

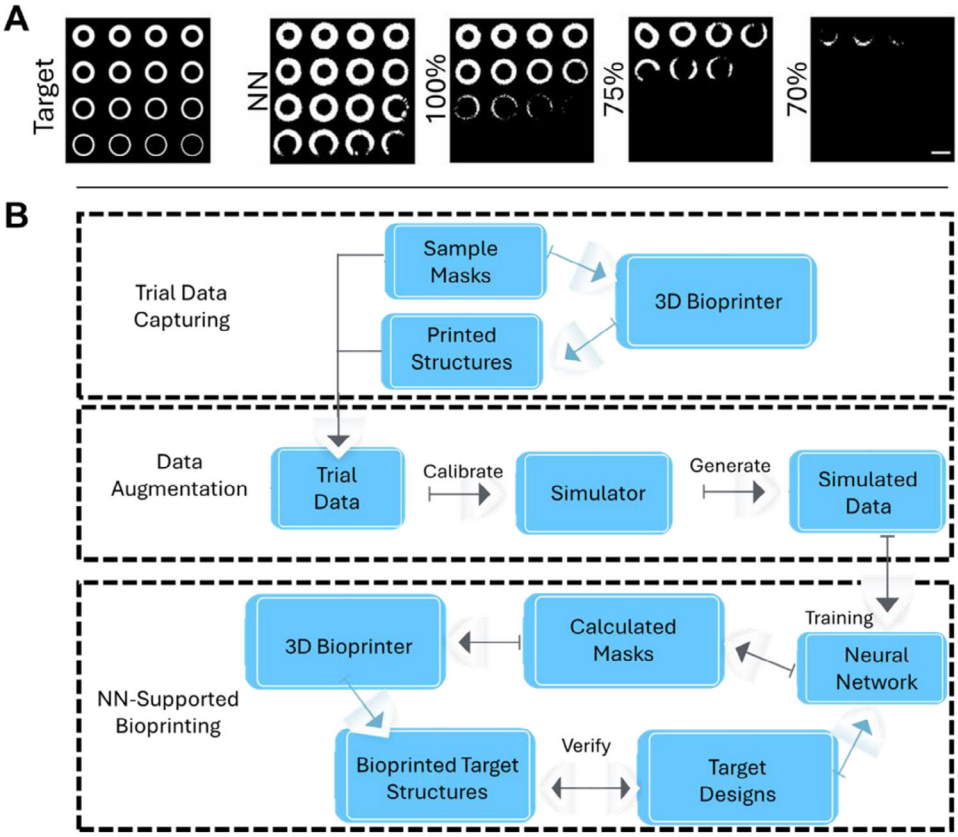

Figure 12. A) Schematic of the learning process: 32 sample masks are bioprinted as single-layer trials to calibrate a bioprinter simulator. The calibrated simulator generates extensive training data, which, along with bioprinted samples, trains the neural network. The network then calculates optimized masks to compensate for cell scattering, with final quality tested on predefined target designs. B) Post-processed microscopic images of test prints. The first column displays the designed target structures, while the second column shows bioprinted structures using neural network (NN)-calculated masks. The third, fourth, and fifth columns present the printing results with identical masks at exposure doses of 100%, 75%, and 70%, respectively. Scale bar: 200 µm. Panels (A) and (B) are reproduced (adapted) with permission.[141] Copyright 2021, IOP Publishing.

Recent advancements in CNN and DL have significantly impacted the field of bioprinting, offering new approaches for optimizing and automating various stages of bioprinting processes. One notable example is the work by Bonatti et al., who developed a DL-based CNN quality control system for EBB.[47] By leveraging CNNs, their system was able to optimize bioprinting parameters and monitor the process using machine vision in real time. High-resolution video data of different bioprinting outcomes, such as under-extrusion or over-extrusion, were recorded and used to train the CNN model. This allowed the system to predict print quality as "ok," "under extrusion," or "over extrusion," reaching above 90% of accuracy, and make automatic adjustments to bioprinting parameters, which significantly reduced bioink waste and improved overall print fidelity. This innovative integration of machine vision with CNNs sets the stage for a fully automated quality control loop, ensuring consistent and reliable bioprinting outcomes.

Tebon et al. introduced a novel pipeline combining bioprinting, high-speed live cell interferometry (HSLCI), and ML for high-throughput drug screening at the single-organoid level.[142] Their bioprinting process maintained the native characteristics of tumor cells using a Matrigel bioink with precise temperature control to ensure consistent extrusion. This setup allowed for accurate control of the size and shape of bioprinted constructs, which were then analyzed using HSLCI to monitor mass changes over time. ML algorithms, including CNNs (with U-Net architecture and ResNet-34 encoder) for image segmentation and XGBoost for track classification, were applied to analyze large datasets generated during this process (Figure 13B). This approach enabled accurate tracking and analysis of individual organoids, offering critical insights into drug resistance and sensitivity, and potentially informing personalized cancer treatment strategies. Sokmen et al. employed a CNN-based deep learning approach for the segmentation of coronary arteries from Computed Tomography Angiography images, using the nnU-Net architecture enhanced by transfer learning to overcome dataset limitations. By leveraging pre-trained weights from a liver vessel segmentation network, the model outperformed two other CNN-based architectures, U-Net and MultiResU-Net, in terms of accuracy. The AI-generated segmentations were used to reconstruct 3D models of patient-specific coronary arteries, which were successfully bioprinted using hydrogel.[166] Collectively, these studies demonstrate the transformative potential of integrating DL and ML techniques into bioprinting. From real-time process optimization and quality control to advanced applications in tissue maturation and drug screening, integration of these technologies is driving

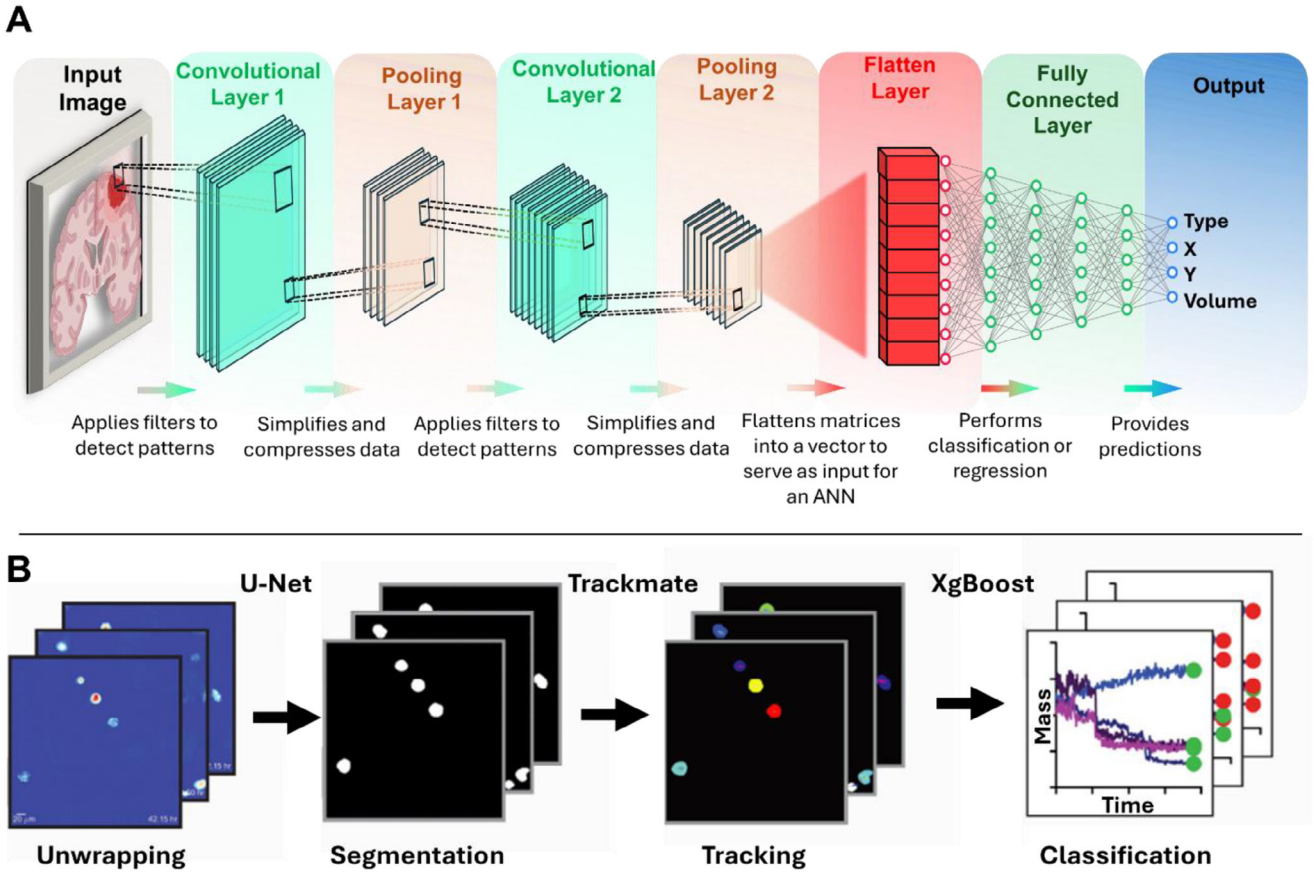

Figure 13. A) Architecture of a CNN for image analysis and feature extraction. The network processes an input image through two convolutional layers for feature detection, each followed by a pooling layer to reduce spatial dimensions. The features are then flattened into a 1D vector and passed through a fully connected layer for classification and regression tasks. The output includes type classification and coordinate predictions (*x*, *y*, and volume), showcasing the network's ability to perform object recognition and spatial localization. This figure was produced with BioRender.com and Microsoft PowerPoint. B) General schematic of the pipeline for cell cluster identification. Image segmentation was performed using a U-Net architecture with a ResNet-34 backbone. The U-Net's encoder extracts features, while the decoder restores resolution, aided by skip connections that retain pixel-level contextual information. This approach produces detailed segmentation masks, even with small training datasets, enabling accurate identification despite background noise and debris. Panel (B) is reproduced (adapted) with permission.[142] Copyright 2023, Springer Nature.

innovations in the field. DL models are proving instrumental in overcoming challenges related to print fidelity, tissue development, and organoid analysis, setting the stage for future advancements in personalized medicine and bioprinting technologies.

4.1.4. Recurrent Neural Network

Recurrent neural networks (RNNs) are a class of ML algorithms designed for tasks involving sequential or time-dependent data.[167,168] Their architecture enables them to capture and utilize information from previous inputs through a dynamic hidden state, making them particularly effective for modeling temporal patterns (**Figure 14**A). This ability is vital for optimizing computationally intensive simulations, as RNNs can capture complex dynamic behaviors, minimizing the need for resource-heavy simulations that often slow research and development. In the realm of bioprinting, for example, RNNs can simulate bioink flow behavior, reducing reliance on finite element simulations, which require significant computational power. By learning from data and approximating system behavior, RNNs provide a more computationally efficient alternative to traditional modeling approaches, accelerating optimization while maintaining accuracy. RNNs can also be employed to predict the behavior of cells and tissues in response to various bioprinting conditions, environmental factors, and biological stimuli. For example, they can be used to forecast how cellular structures respond to growth factors or mechanical stresses over time, significantly reducing the need for repeated physical trials and simulations.[169] However, despite their potential, no significant studies have yet been published that combine RNNs with bioprinting, indicating an area ripe for exploration and innovation.[170]

4.1.5. Decision Trees, Random Forest, Gradient Boosting (GBoost), and Extreme Gradient Boosting (XGBoost)

A foundational component of ML, decision trees (DTs) are nonparametric, supervised learning models used for classification and regression tasks.[171,172] In bioprinting, decision trees can

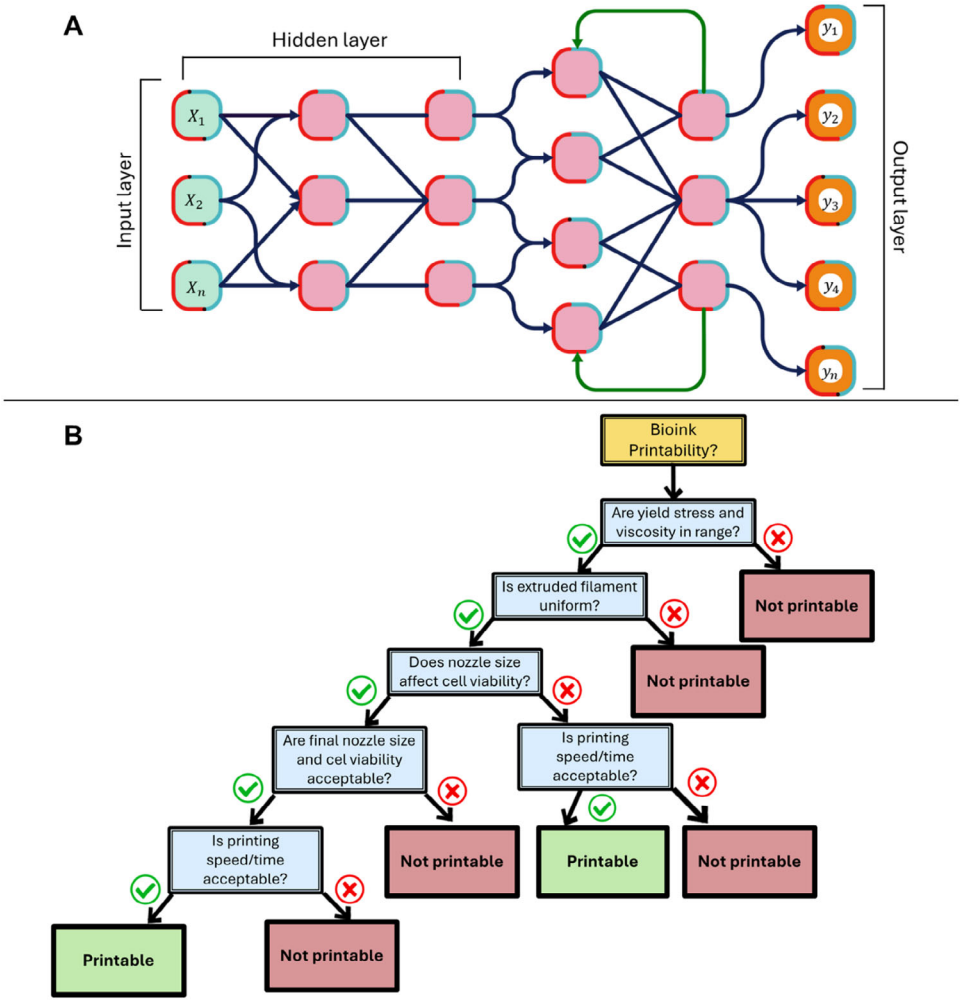

Figure 14. A) Architecture of RNNs. The diagram illustrates the structure of RNNs, which consist of input, hidden, and output layers. Unlike traditional neural networks, RNNs have recurrent connections that enable them to maintain a memory of previous inputs by passing information through hidden states. This figure was produced with Adobe Inc., (2019), Adobe Illustrator. B) Example of a DT for evaluating bioink printability based on key parameters, including yield stress, viscosity, nozzle size, cell viability, and printing time. The assessment begins by verifying if the bioink's yield stress and viscosity are within an acceptable range. If acceptable, it is followed by checking the uniformity of the extruded filament. Next, the impact of nozzle size on cell viability is evaluated. The next step is to assess whether the final cell viability and nozzle size fall within the required range. Finally, printing speed and time are evaluated to ensure that they fall within acceptable limits. Bioinks that satisfy all criteria are classified as printable, ensuring optimal performance and cell integrity during bioprinting. This figure was produced with BioRender.com and Microsoft PowerPoint.

streamline processes like evaluating bioink printability by guiding decision-making based on key parameters, like viscosity or cell viability, making them powerful tools for improving bioprinting outcomes.[173,174] For example, a decision tree evaluating bioink printability might start with the question of viscosity, followed by assessments of shear stress stability, bioactivity, and extrusion capability. They operate by starting with a primary question, such as "Is this bioink printable for 3D bioprinting?" and branching out through a series of feature-based queries, creating decision nodes that segment the data into subsets. Each path from root (initial node) to leaf (final decision node) node represents a classification or prediction, with leaf nodes indicating the outcome (e.g., printable or not printable). The decision tree progresses by comparing values against thresholds defined during the training phase. For example, a question like "Is cell viability greater than 80%?" guides the flow: if the answer is yes, the process continues to the next node. If not, the flow either terminates or redirects to a more appropriate set of questions for further evaluation (Figure 14B). DTs are simple to understand, interpret, and visualize, making them useful for both technical and non-technical stakeholders. They require minimal data preparation and can handle both categorical and numerical data, although they are prone to overfitting, where the model becomes too complex and captures noise in the data. Techniques such as pruning, limiting tree depth, or setting minimum sample sizes at nodes are used to prevent overfitting.[171] DTs employ the classification and regression tree (CART) algorithm, utilizing metrics such as Gini impurity or mean squared error to evaluate the efficacy of splits and optimize data partitioning.[175] There are several types of DTs used in ML as discussed in the following paragraphs.

Random forest (RF) is a powerful and robust ensemble learning algorithm that leverages the combined output of multiple

decision trees to improve predictive accuracy and reduce the risk of overfitting. Known for its flexibility, RF is effective for both classification and regression tasks. It uses a method called bagging, where it randomly selects samples of data (bootstrap sampling) and features to build many decision trees. By choosing different features at each split, RF ensures that trees are less similar to each other, which helps reduce the risk of overfitting, a common problem with single decision trees. This makes RF more accurate and reliable in its predictions.[176,177] The core strength of RF lies in aggregating predictions from multiple DTs, using averaging for regression tasks and majority voting for classification tasks. This approach allows the algorithm to capitalize on the strengths of individual trees, resulting in more accurate and stable predictions.

In the context of bioprinting, Safir et al. employed an RF classifier to analyze Raman spectra for classifying bacterial and blood cell types within droplets bioprinted using an acoustic bioprinter.[143] Their study aimed to rapidly analyze cellular components in complex samples by integrating surface-enhanced Raman spectroscopy (SERS) with ML. Given the high-dimensional nature of the spectral data, researchers utilized principal component analysis (PCA) for dimensionality reduction and t-distributed Stochastic Neighbor Embedding (t-SNE) for visualization. These techniques enabled efficient data processing, allowing the RF algorithm to achieve more than 99% classification accuracy for single-cell-line droplets and over 87% accuracy for mixed-pathogen samples. Beyond pathogen identification, this approach demonstrates broader applicability in bioprinting applications, including the evaluation of cell viability. By enabling high-throughput screening of biological constructs, this methodology supports advancements in tissue engineering and regenerative medicine, providing tools for quality control and optimization of bioprinted constructs.

Gradient boosting is a powerful ensemble learning technique that builds predictive models sequentially, where each new model is trained to correct errors of previous ones.[178,179] It works by converting weak learners, typically decision trees, into a strong learner by combining their outputs to reduce bias and variance. At each iteration, the algorithm computes the negative gradient of the loss function, which represents the direction and magnitude of the steepest reduction in error. A new decision tree is then trained to predict this negative gradient, effectively focusing on the new model in correcting the most significant mistakes of the previous models. After the new model is fitted, predictions are updated by adding the predictions of the newly trained tree to the existing model. This process continues until the model converges or reaches a predefined stopping criterion, such as the number of iterations or a performance threshold. XGBoost's ability to handle structured data with superior accuracy and speed has made it a popular choice in ML, outperforming other gradient and boosting implementations in many real-world applications.[180] By combining weak learners, typically DTs, gradient boosting produces highly accurate models for both classification and regression tasks. Extreme gradient boosting (XGBoost), a highly optimized version of gradient boosting, adds features like regularization and parallelization, making it faster and more accurate for large datasets.[180,181]

In bioprinting, these techniques can be used to optimize complex parameters like printability and scaffold quality. For example, Rafieyan et al. employed both gradient boosting (GBoost) and XGBoost, along with other ML algorithms, to analyze one of the most extensive open-source datasets on printed scaffolds.[144] Their dataset included detailed information on 1171 scaffolds, covering over 60 biomaterials, 49 cell lines, and various printing conditions. Their model, tuned for optimal performance, demonstrated superior accuracy for XGBoost in predicting scaffold quality and cell response over other algorithms.

4.1.6. Support Vector Machine

Support vector machine (SVM) is a supervised learning algorithm originally designed for binary classification tasks. The objective of SVM is to maximize the margin of the decision boundary, which separates samples of different classes. The decision boundary is defined by focusing on the samples that are closest to the line separating different classes. These key samples, which have similar features but belong to different classes, are called support vectors. In its original strategy, SVM is capable of separating linearly separable samples, for instance, in a 2D scenario, samples could be separated into distinct classes using a straight line. This approach aims to enhance the generalization capability of the model while addressing overfitting issues. SVM was originally designed to separate data into distinct categories with a clear boundary. Over time, they have been improved to handle more complex data that does not have a simple dividing line, thanks to methods like "soft margins."[182] A soft margin allows the model to make a few classification errors, making it more flexible when dealing with messy data or outliers (unusual data points). The flexibility is controlled by a setting called the "box constraint" (C). A smaller value for C creates a wider margin, which makes the model more tolerant to errors, while a higher value of C makes the model focus more on precision, which can be less tolerant to noisy data.

Another improvement is the use of "kernel functions," which help separate data that cannot be divided by a straight line by transforming the data into a higher-dimensional space. This transformation makes it easier for SVM to find a dividing boundary. Common kernels include "polynomial," "RBF" (Radial Basis Function), and "sigmoid". RBF kernel, widely used for its simplicity, requires only one setting to adjust, making it easier to optimize compared to more complex kernels.[183,184] **Figure 15**A shows how a linear kernel hyperplane would be fit to two separate 2D classes.

An example of SVM's application in bioprinting is illustrated in the work by Fu et al., where the researchers developed an ML model using SVM to optimize bioprinting parameters for Pluronic.[145] The SVM model was trained on the data related to material properties and print quality, enabling it to identify the best combinations of printing parameters (Figure 15B). This approach led to the creation of a process map that guided the selection of optimal settings, resulting in a success rate of over 75%. The study demonstrates how SVM can significantly reduce the need for extensive trial-and-error experiments by providing data-driven recommendations, making it easier to optimize printing conditions for new bioinks.

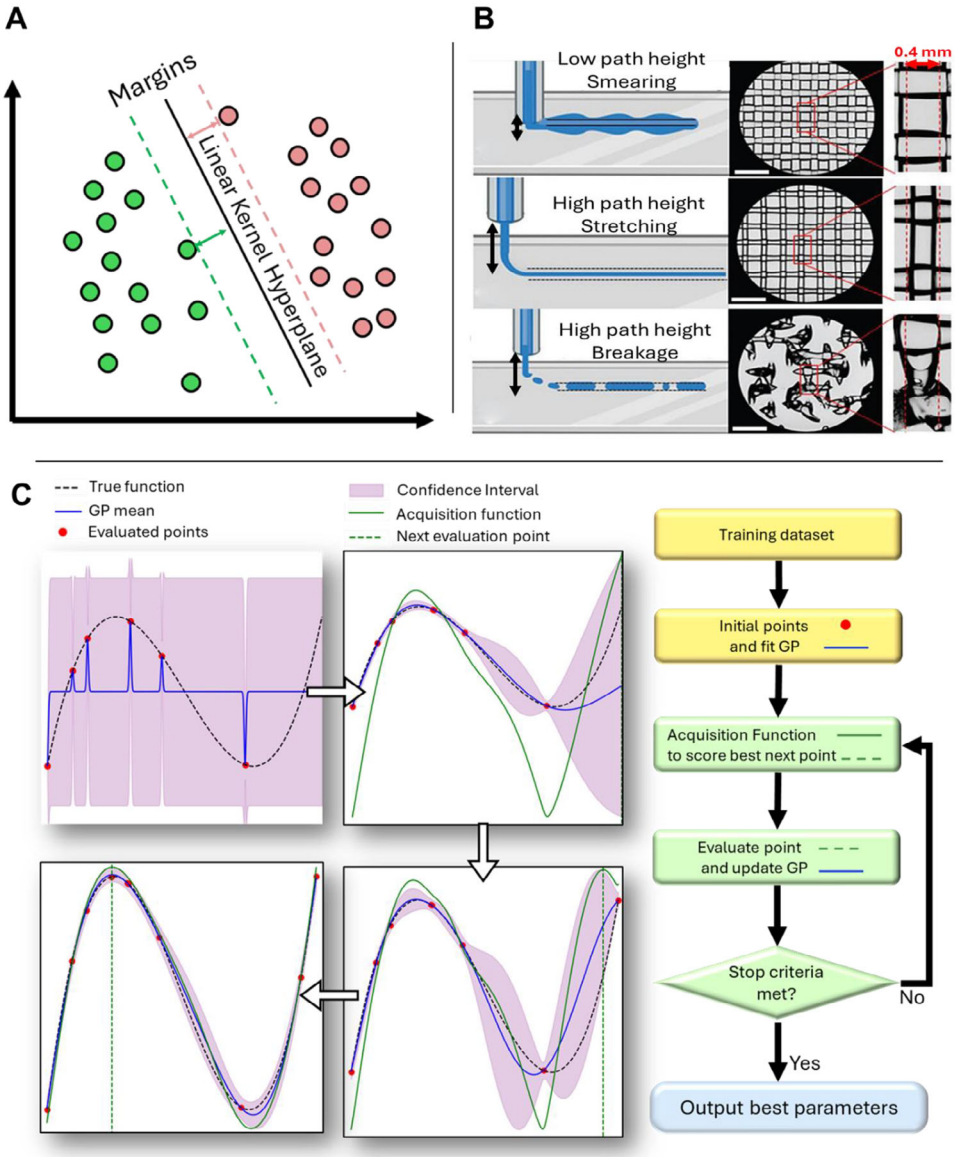

Figure 15. A) SVM decision boundary and margin. The diagram illustrates an SVM separating two classes (green and pink) using a linear decision boundary (solid line). The margin, defined as the distance between the boundary and the nearest data points (support vectors), is maximized to enhance classification robustness. Support vectors play a crucial role in defining the boundary, while other data points do not directly affect their placement. B) Effect of path height on printing outcomes with experimental examples. The correct path height is shown with the stress region highlighted. Low path height results in interference and smearing, while high path height leads to stretching, thin lines, or breakage. The correct line width is indicated by the dashed line. Scale bar: 1.87 mm. Reproduced (adapted) with permission.[145] Copyright 2021, AccScience Publishing. C) BO process using a GP model. The figure illustrates the iterative steps of BO. The initial GP model is built with a few evaluated points (red dots), and the acquisition function (green line) identifies the next point for evaluation. Sequential updates refine the GP model, improving its approximation of the true function (dashed line) and reducing uncertainty (shaded region). The acquisition function dynamically adjusts to suggest the next optimal evaluation point. The flowchart on the right outlines the process: starting with a training dataset, fitting a GP model, selecting the next point using the acquisition function, updating the GP, and iterating until the stopping criteria are satisfied. The process outputs the parameters corresponding to the optimal function value. This figure was produced with BioRender.com and Microsoft PowerPoint.

4.1.7. Bayesian Optimization with Gaussian Process Modeling

Bayesian optimization (BO) and Gaussian process (GP) modeling have become essential tools in optimizing the complex and resource-demanding process of bioprinting. In EBB, where precise control over parameters like bioink composition, nozzle geometry, and extrusion pressure is crucial, traditional trial-and-error methods can be inefficient and time-consuming. BO starts by testing a few initial parameter combinations and using a GP to create a model that predicts the system's behavior. It then uses an acquisition function to decide the next parameters to test, searching for a balance between exploring new possibilities and refining

the most promising ones. Each new result updates the GP model, making predictions more accurate. The process repeats until a stopping condition is met, such as reaching a set number of iterations or finding a sufficient result. Finally, the approach identifies the best solution found[185] as shown in Figure 15C.

GP modeling, often used within BO, creates a probabilistic model of the system by predicting the outcomes of experiments based on limited data. It treats the relationship between input parameters and outputs as a continuous function, allowing for predictions about how changes in bioprinting conditions, such as bioink properties or nozzle geometry, will affect outcomes like shear stress or cell viability. Overall, while BO refers to the optimization framework that searches for the best parameters, GP is the statistical model used within that framework to predict the system's behavior. For example, in bioprinting, BO may be used to find the optimal bioink composition and extrusion speed, while GP models identify how these parameters affect outcomes like shear stress or cell viability. The GP model helps BO choose the next experiments to refine the search for optimal conditions. As new data are collected, the model is updated, improving its accuracy over time.

In a study by Ruberu et al., BO was employed to optimize EBB parameters for GelMA and GelMA/HAMA bioinks.[146] The researchers devised a scoring system to evaluate filament formation and pore architecture during extrusion. BO enabled them to significantly reduce the number of experiments required to identify optimal bioprinting parameters, conducting as few as 4 to 47 experiments instead of thousands typically needed in traditional trial-and-error approaches. This study highlights the potential of BO to accelerate the bioprinting process by efficiently narrowing down parameter sets, offering a quantitative and robust method for evaluating printability in EBB. Similarly, Reina-Romo et al. applied GP modeling to explore how nozzle geometry and bioink properties affect shear stress and cell viability in EBB of shear-thinning hydrogels.[147] Using in-silico modeling techniques, such as computational fluid dynamics, the study analyzed the impact of different nozzle designs (conical versus blunted) and hydrogels (alginate–gelatin, alginate, and pluronic) on shear stress, a key factor influencing cell survival during bioprinting. The GP model successfully captured the complex relationships between nozzle geometry, bioink properties, and shear stress, providing valuable insights into optimizing nozzle design to improve cell viability. By integrating a design of experiments approach, this study demonstrated how GP modeling can reduce experimental workload and improve the precision of the bioprinting process. Together, these studies illustrate the significant advantages of BO and GP modeling in bioprinting. Both methods streamline parameter optimization, reduce experimental overhead, and enhance the understanding of key bioprinting factors, such as filament formation, shear stress, and cell viability. These approaches offer efficient, data-driven solutions for refining bioprinting processes and improving their outcomes.

4.1.8. Linear Regression and Logistic Regression

Linear regression is a straightforward ML algorithm used to predict continuous outcomes by modeling the relationship between a dependent variable and one or more independent variables[186,187] (**Figure 16A**). Linear regression can help optimize key parameters like extrusion pressure, bioink viscosity, or nozzle speed to predict outcomes such as print resolution or bioink strength. For example, it can be used to determine how adjustments in bioink composition affect the tensile strength of printed constructs, enabling researchers to fine-tune the process for better structural integrity. However, it is best suited for simpler problems, where the relationship between variables is relatively linear. Logistic regression, on the other hand, is a classification algorithm used to predict categorical outcomes[188,189] (Figure 16B). In bioprinting, it can be applied to classify whether a set of bioprinting parameters, such as temperature, bioink composition, or printing speed, will lead to either optimal or poor cell viability. Logistic regression models the probability of success or failure by analyzing how these variables influence cell survival. Like linear regression, logistic regression is effective for problems, where the relationships between variables are not too complex or nonlinear. Overall, the main difference between linear and logistic regression is what they predict. Linear regression predicts continuous numbers, like the strength of a material, while logistic regression predicts categories, like whether a process will succeed or fail.

A model was proposed by Huang et al. that employed ML to predict printability in bioprinting.[149] In cryo-bioprinting, where developing DMSO-free bioinks for safe cell cryopreservation is a major challenge, predictive models like linear regression are invaluable. As demonstrated in a study by Qiao et al., ML models, including linear regression, can be used to predict cell viability in cryoprotective bioinks.[140] This accelerates the bioink formulation process by providing data-driven predictions on how different bioink compositions will impact cell survival during freezing and thawing. Such predictive models streamline bioink development, reducing the time and resources needed for experimental testing and enabling more efficient advancements in cryo-bioprinting.

4.1.9. K-Nearest Neighborhood

The K-nearest neighborhood (k-NN) algorithm is a simple yet effective ML technique used for both classification and regression tasks. It works by identifying the *k* closest data points in the training set to a given input, typically using Euclidean distance as the metric, where *k* is an integer arbitrarily chosen by the programmer. In classification tasks, the algorithm assigns the most frequent label among the neighbors (Figure 16C), while in regression tasks, it predicts the value by averaging the neighboring points[190,191] (Figure 16D). In bioprinting, k-NN can be particularly useful for predicting outcomes based on historical data. For example, if researchers have a dataset containing successful bioprinting conditions for different bioinks, k-NN can predict the optimal printing parameters for a new bioink by comparing it to previously successful cases. For instance, in SLA bioprinting, Xu et al. developed a predictive model that incorporated k-NN alongside other ML algorithms to forecast cell viability under varying bioprinting conditions.[148] They used experimental data as inputs, including UV intensity and exposure time, GelMA concentration, and layer thickness, to predict cell viability. By applying k-NN to analyze similarities between bioprinting parameters and

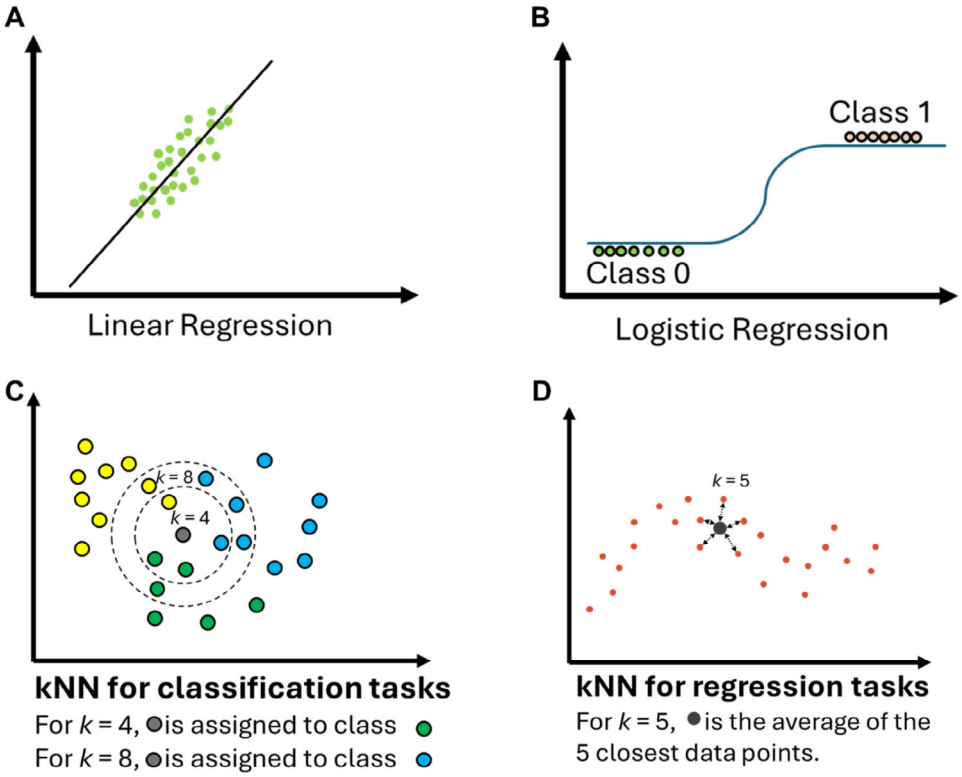

Figure 16. Comparison of linear versus logistic regression. A) The plot illustrates linear regression, where a line is fit to model the trend continuously. B) The plot demonstrates logistic regression, which uses a logistic (sigmoid) function to map the linear combination of inputs to probabilities between 0 and 1. By applying a threshold (e.g., 0.5), data points are classified into two distinct classes: those below the threshold are assigned to the green class and those above it to the orange class. Illustration of kNN classification and regression. C) The plot demonstrates kNN classification, where a new gray point is classified based on its nearest neighbors. With $k = 4$, it is classified as green due to the majority class among its 4 nearest neighbors. When $k = 8$, it is classified as blue, emphasizing the impact of hyperparameter selection on classification accuracy. D) The plot illustrates kNN regression, where the black point represents the average value of its 5 nearest red neighbors ($k = 5$), highlighting how kNN predicts continuous outputs by averaging values from nearby data points.

previous results, the model achieved a high predictive accuracy of 0.953, a relative error of 0.013, and a root mean squared error of 0.015. Their study found that UV exposure time was the most significant factor affecting cell viability, while UV intensity had the least effect. The combination of multiple models, including k-NN, enabled highly accurate predictions of bioprinting outcomes, demonstrating the potential of k-NN in optimizing bioprinting conditions and improving cell viability.

4.1.10. Ensemble Learning and Hierarchical Machine Learning

Ensemble learning and hierarchical machine learning (HML) are both advanced techniques that enhance decision-making by leveraging multiple models, though they operate in different ways. Ensemble learning combines the predictions of several ML algorithms in parallel to improve accuracy and robustness, and reduces bias and variance.[192] Models such as neural networks, decision trees, or regressors are trained independently, and their outputs are aggregated using methods like averaging for regression or voting for classification. The strength of ensemble learning lies in utilizing the advantages of different models to compensate for individual weaknesses, leading to a more accurate overall prediction. Bagging, boosting, and stacking are techniques used to improve the accuracy of prediction models.[192] Bagging involves training multiple models on different subsets of data and averaging their predictions (**Figure** 17A). Stacking uses multiple models for the same data set to make predictions, and then a final model combines these into one optimal prediction by learning the best way to blend them[193] (Figure 17B). Boosting sequentially trains models, each focusing on correcting errors made by the previous one, to improve accuracy (Figure 17C). In bioprinting, ensemble learning can, for instance, enhance the accuracy of predicting a bioink's printability by aggregating the outcomes from multiple predictive models. This approach leverages a voting system among models to determine the most likely classification, effectively utilizing collective insights of various algorithms to improve decision-making.

HML structures the decision-making process sequentially, with each layer refining the predictions from the previous one while incorporating domain-specific knowledge. In HML, middle layers act as a bridge between input parameters and the final output, using known physical or chemical laws to simplify the data-driven process.[194] In bioprinting, for example, insights into the rheological behavior of bioinks can be integrated into these middle layers, allowing the model to focus on improving

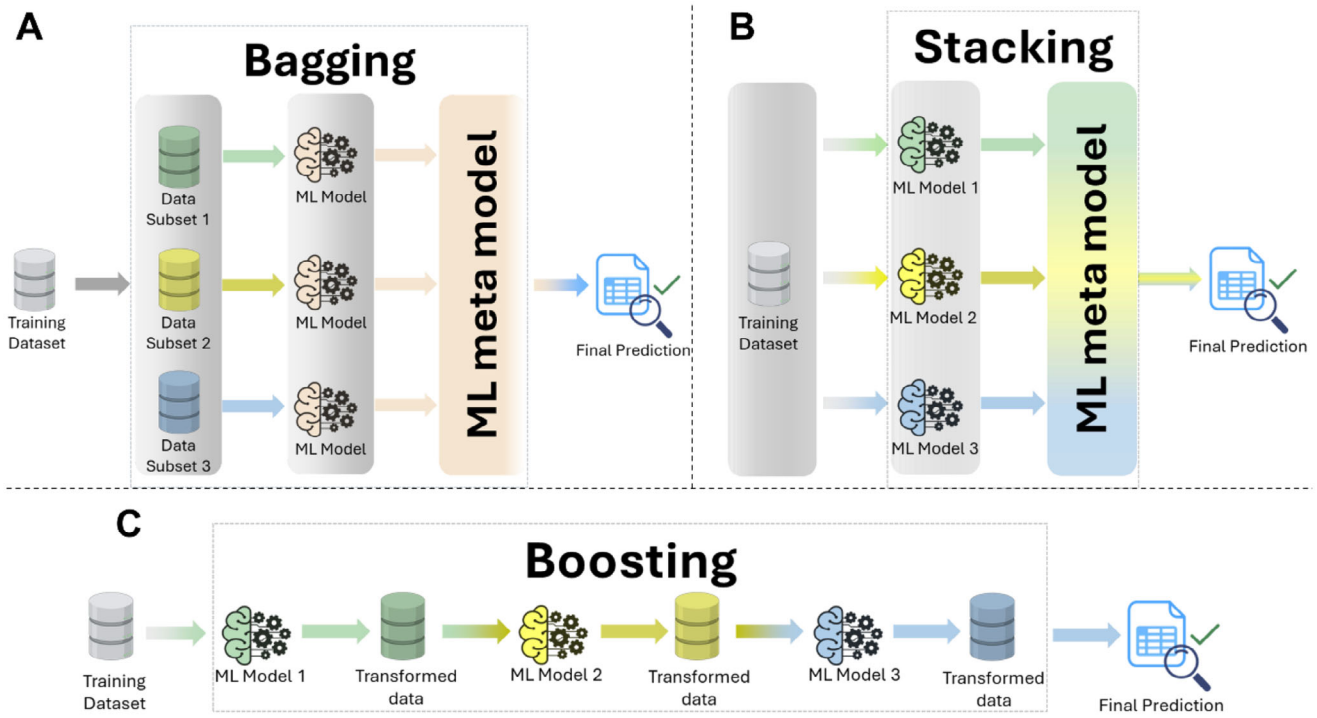

Figure 17. Ensemble learning techniques for enhanced model performance. A) Bagging, where the dataset is randomly sampled with replacement to create subsets. Each subset trains a separate model, and the final prediction is made by averaging (for regression) or voting (for classification) the outputs of all models, reducing variance and improving stability. B) Stacking, where predictions from multiple models are used as inputs for a meta-model, which learns to generate the final prediction. This method leverages the strengths of diverse models for better performance. C) Boosting, where models are trained sequentially on the entire dataset. Each subsequent model focuses on correcting errors made by its predecessor, and predictions are combined using a weighted average or voting to improve accuracy. This figure was produced with BioRender.com and Microsoft PowerPoint.

predictions related to print fidelity and structural accuracy. By embedding this expert knowledge, HML can optimize bioprinting processes more efficiently with fewer data points, reducing the need for extensive trial-and-error experimentation.[151]

In a proof-of-concept study, Huang et al. explored the use of ensemble learning to predict the number of cells in droplets during DBB by analyzing droplet velocity at two points along the nozzle-substrate trajectory.[149] They employed an ensemble of ML algorithms, including linear regression, support vector regression, decision tree regressor, random forest regression, and extra tree regression. These algorithms were used to detect the presence of cells in single droplets and predict the total number of cells in multiple droplets. The RF regressor achieved 80% accuracy in detecting cells within single droplets, while the extra tree regressor exhibited a low mean error of 12% when predicting the number of bioprinted cells in multiple droplets. This study underscores the potential of ensemble learning in droplet monitoring systems for real-time cell count assessment, enhancing the precision and control of cell distribution in bioprinted constructs. In another study, Tang et al. integrated 3D bioprinting with a multi-algorithm ML approach to enhance the understanding of glioma treatment responses and tumor microenvironment characteristics.[150] The researchers developed Glio Machine Learning, a workflow incorporating nine distinct ML algorithms and a weighted ensemble model to generate robust gene expression-based predictors. The ensemble model outperformed individual algorithms across various in vitro systems, including bioprinted patient-derived tissues. The integration of bioprinting and ML expanded treatment evaluation, particularly in *T*-cell-related and anti-angiogenesis therapies, revealing immunosuppressive and angiogenic microenvironments within glioma. The success of the ensemble model demonstrates its potential to improve treatment prediction accuracy and advance personalized cancer therapeutics.

Bone et al. developed an HML framework to optimize the bioprinting of alginate using a small dataset of 48 prints.[151] The model employed LASSO (Least Absolute Shrinkage and Selection Operator) regression for feature selection and incorporated a middle layer of physical variables, such as shear rate, viscosity, and flow rate, achieving an R^2 value of 0.643 for print prediction accuracy. The HML framework optimized print parameters, enabling high-fidelity features like 80 μm linewidths and sharp corners (0 mm radius) with less than 10% error, critical for complex tissue constructs. It identified trade-offs between optimizing line morphology and corner sharpness, emphasizing the need for multi-objective optimization in bioprinting. This approach offers a scalable and data-efficient method for optimizing print quality and can be extended to evaluate cell viability, density distribution, and live/dead cell ratios. In another study, Oh et al. compared different models, including an SVM and RF, with their new rheology-informed hierarchical ML (RIHML) model[152] to predict printing resolution. The SVM model showed good predictive abilities, but the RIHML model performed the best, with the lowest error rates when predicting outcomes across different

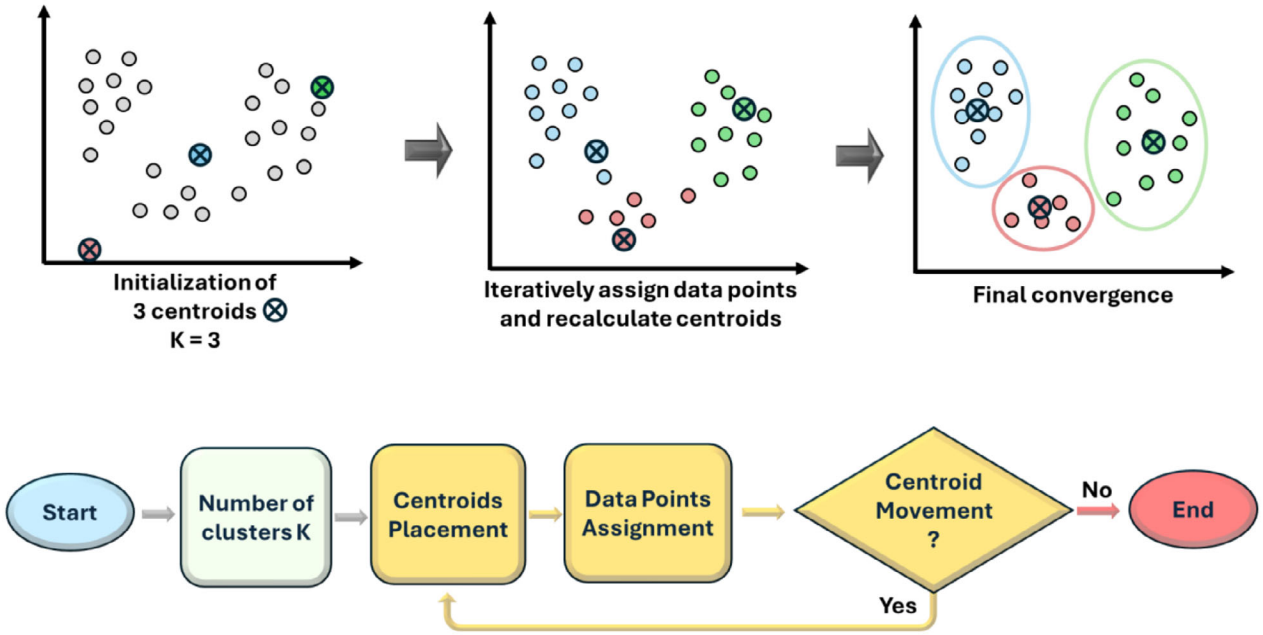

Figure 18. K-Means clustering process. The figure illustrates the K-Means algorithm, beginning with the random initialization of centroids. Data points are assigned to the nearest centroid based on the Euclidean distance. The centroids are updated iteratively by calculating the mean position of the assigned points. This process repeats until the centroids stabilize, forming distinct clusters, as shown in the top sequence. The flowchart below outlines the steps: selecting the number of clusters (K), initializing centroids, assigning data points, recalculating centroids, and iterating until centroids no longer change. The algorithm optimizes clustering by maximizing intra-cluster similarity and minimizing inter-cluster similarity.

printing conditions, like nozzle speed and extrusion pressure. The RF model also did well but was not as accurate as the RIHML model, especially when new components were added to the bioink. This study shows that while SVM is effective, the RIHML model is even more accurate and adaptable, making it better suited for complex bioprinting tasks.

4.2. Unsupervised Learning

Unsupervised learning is a branch of ML that identifies patterns in data without the need for labeled examples. Unlike supervised learning, which relies on predefined labels to guide the algorithm, unsupervised learning autonomously explores data to find underlying structures, relationships, and groupings. Common techniques include clustering algorithms, such as KMeans, which group the data based on similarity, and generative models, such as GANs, which learn to create new data samples resembling the original dataset.[195] For instance, clustering algorithms like KMeans can reveal hidden groupings in scaffold compositions or printing settings, helping to classify scaffold designs based on their quality and cell compatibility. GANs, on the other hand, can generate synthetic data or enhance existing images, which is valuable in scenarios where real experimental data are limited or costly to obtain, which are discussed in detail in the following sections.

4.2.1. KMeans

The KMeans algorithm works by initially assigning data points to random clusters and then iteratively updating these clusters to minimize the distance between each point and the cluster's centroid (the average position of points in that cluster). Through this process, KMeans aims to find clusters that group similar data points together while maximizing the differences between clusters[196] (**Figure 18**). In bioprinting, KMeans can be particularly useful for categorizing complex datasets generated from different biomaterials, printing conditions, or scaffold designs. For instance, Rafieyan et al. applied KMeans clustering to classify printed scaffolds by analyzing various printing conditions and biomaterial compositions.[144] By clustering a large dataset of over 1000 scaffolds, they identified five distinct groups that revealed key differences in factors like crosslinking methods, nozzle size, cell density, and syringe temperature. For instance, Cluster 4 included scaffolds printed under high pressure and temperature with larger nozzles, while Cluster 2 featured primarily photocrosslinked scaffolds. This clustering approach allowed pinpointing optimal material and cell combinations for improved scaffold quality and cellular responses, enhancing the performance of supervised methods later applied in the study.

4.2.2. Generative Adversarial Networks

Generative adversarial networks (GANs) are a type of model that consists of two neural networks, the generator and discriminator, competing against each other. The generator creates synthetic data samples, while the discriminator evaluates these samples against real data, trying to distinguish between genuine and generated data. Through this adversarial process, the generator learns to produce highly realistic samples that closely resemble the original data, making GANs particularly useful for data

augmentation and image enhancement in cases, where labeled data is limited.[197] When the discriminator evaluates a sample incorrectly, its weights are adjusted. Conversely, if it evaluates the sample correctly, the generator's weights are adjusted, as shown in **Figure** 19A.

In bioprinting, GANs can be applied to enhance or generate synthetic biological data, which is valuable for training models in cases where real data are scarce, difficult to obtain, or expensive to produce. For example, Yao et al. present the Aligned Disentangled Generative Adversarial Network (AD-GAN), a variation of GAN for 3D nuclei segmentation in Confocal Laser Scanning Microscopy (CLSM) images that offers a faster, cost-effective way to assess 3D cell culture models.[153] By disentangling and mapping real nuclei images to synthetic masks, AD-GAN more accurately captures nuclei shape and position compared to tools like CellProfiler and Squassh. This model enables detailed insights into cell behaviors within fibrous scaffolds, such as adhesion, migration, and proliferation, key for improving scaffold design (Figure 19B). Future applications of AD-GAN could extend to complex structures like spheroids and organoids, providing insights into tissue-like architectures. Additionally, adapting AD-GAN to other imaging techniques, such as electron or X-ray microscopy, could deepen our understanding of cell behavior and interactions in disease and drug testing models.

4.3. Reinforcement Learning

Reinforcement learning (RL), a subset of ML, combines methods of both supervised and unsupervised learning.[198,199] In RL, the agent interacts dynamically with its environment through a continuous loop of perception and action without explicit instructions on which actions are correct.[199] Instead, the agent receives rewards or punishments upon task completion, which serve as feedback to guide its learning process.[7] Through repeated interactions, the algorithm learns to optimize its path to maximize rewards, balancing exploration of new paths with exploitation of known paths to develop the most efficient route to reward. This learning paradigm allows RL agents to autonomously improve their performance on complex tasks, making RL a powerful tool for various applications such as robotics, energy, finance, healthcare, transportation, and bioprinting.[200]

In the context of bioprinting, the agent may begin in a specific state, defined by initial settings such as bioink composition, nozzle speed, or layer thickness. The agent then takes an action, for example, adjusting one of these parameters, which causes the environment (bioprinter) to respond by transitioning to a new state. This new state could involve the bioprinted layer, with its characteristics such as shape accuracy or cell viability. After each action, the agent receives either a reward or a penalty based on how well the bioprinted layer aligns with the desired outcome. For instance, a camera or sensor evaluates the bioprinted layer in real-time. If the layer meets predefined target points such as dimensional accuracy or cell distribution, the agent is rewarded. If the printed layer deviates from the target design, the agent is penalized. Based on this feedback, the agent refines its decision-making process, learning to associate certain settings (such as bioink viscosity or nozzle speed) with better results. This process is iterative, with the agent continually adjusting parameters and improving its strategy. Over time, the agent learns to balance exploration (trying new settings to discover better outcomes) and exploitation (using known successful actions). Through repeated iterations, the agent converges on an optimal policy, learning the best set of actions to consistently produce high-quality, accurate prints.[201] Figure 19C illustrates the process, where an agent interacts with an environment to optimize its actions. The agent begins by observing the environment's state and processing it into relevant features. Based on this observation, the agent uses its rules to decide an action, which is executed in the environment. The environment responds by transitioning to a new state and providing feedback in the form of a reward, indicating the effectiveness of the action. The agent then updates its rules, neuron weights, or value function using this reward and the next observation to improve future decisions.

In bioprinting, RL can be used to optimize properties of bioprinted constructs, such as microstructure, possibly for diffusion coefficient and cell viability, as well as tissue-specific mechanical properties like viscosity and yield stress.[202] RL can also be employed for scaffold design, bioreactor conditions, or experiment setups, enhancing the overall efficiency and effectiveness of bioprinting processes. By continuously adapting to their environment, RL agents progressively enhance their decision-making capabilities, demonstrating increasing efficiency and effectiveness over time. For instance, Dharmadhikari et al. used Q-learning, a common RL algorithm, to optimize parameters such as laser power and scan velocity for achieving the desired melt pool depth in 3D printing.[202] They found the optimal combination of laser power and scan velocity and analyzed the effects of various hyperparameters on the results. This study demonstrates the potential of RL to fine-tune bioprinting parameters, leading to more precise and reliable outputs.

One notable application of RL in bioprinting is the design of patient-specific bone tissue containing complex vasculature. Creating a viable vascular structure to accurately mimic that of native human tissue is one of the most significant challenges in regenerative medicine. Current bone-engineered tissue in vitro often lacks the spatial complexity required for cell viability, creating a disconnect between research and clinical needs. Sedigh et al. were able to generate a 3D vascular network inside a bone model using CT and MRI scans as cross-sections.[154] These cross-sections were turned into a grid that acted as the state map with inlets, outlets, and avascular regions that the RL algorithm, Q-learning, had to navigate. Results from experiments showed that the RL algorithm could create vasculature through a patient's bone with minimal computational cost. Despite the promising potential of RL in bioprinting, there are relatively few studies exploring its applications compared to traditional ML methods. This is partly due to the high cost of biomaterials and the large number of iterations required for RL training.[7] To make it feasible, RL can optimize the creation of customized tissue scaffolds. Imagine a bioprinter making a patient-specific heart valve, with an RL system adjusting parameters like bioink viscosity, nozzle path, and nozzle speed. A camera monitors each printed layer, comparing the result to the intended design. If the print matches well, the RL system gets a reward; if not, it receives a penalty. Over time, the RL system learns to fine-tune the process, improving print quality and accuracy.

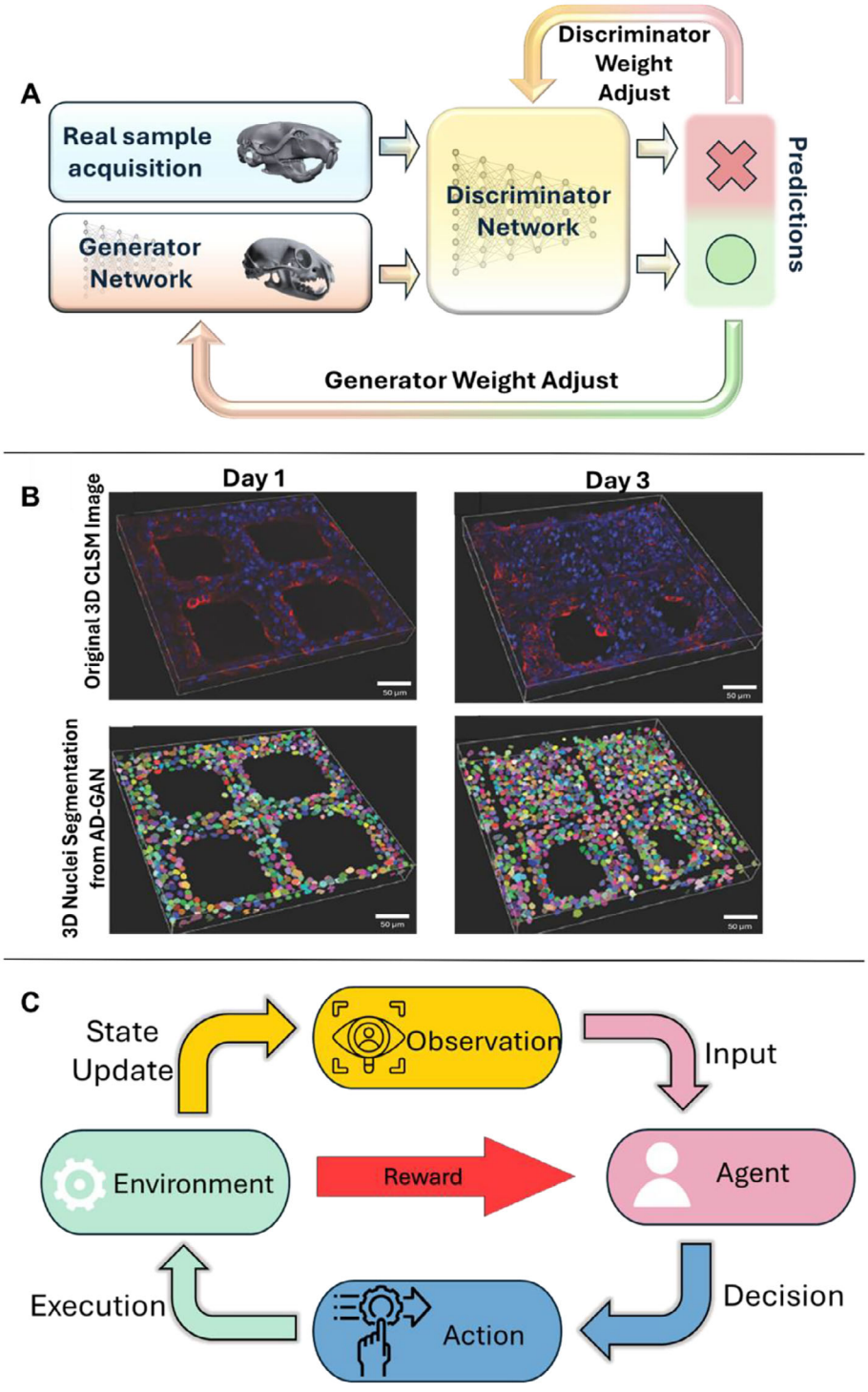

Figure 19. A) Architecture of a GAN. The framework consists of two competing networks, the generator and discriminator. The generator produces synthetic samples, while the discriminator evaluates whether the inputs are real or generated. Real samples are sourced from a dataset and compared against the generator's outputs. The discriminator provides feedback to the generator, enabling iterative improvements in output realism. Through this adversarial process, the generator learns to produce highly realistic samples, while the discriminator refines its ability to distinguish between real and generated data. This figure was produced with BioRender.com and Microsoft PowerPoint. B) Confocal laser scanning microscopy images and 3D nuclei segmentation of A549 cells cultured at low density on Days 1 and 3. Panel (B) is reproduced (adapted) with permission.[153] Copyright 2021, AccScience Publishing. C) RL framework illustrating the interaction between an agent and its environment in an RL setup. The agent observes the environment, processes inputs, and takes actions that influence the environment's state. These actions result in feedback in the form of a reward signal, guiding the agent's learning process. By optimizing decisions to maximize cumulative rewards, the agent continuously improves its performance through this iterative cycle. This figure was produced with Adobe Inc., (2019), Adobe Illustrator.

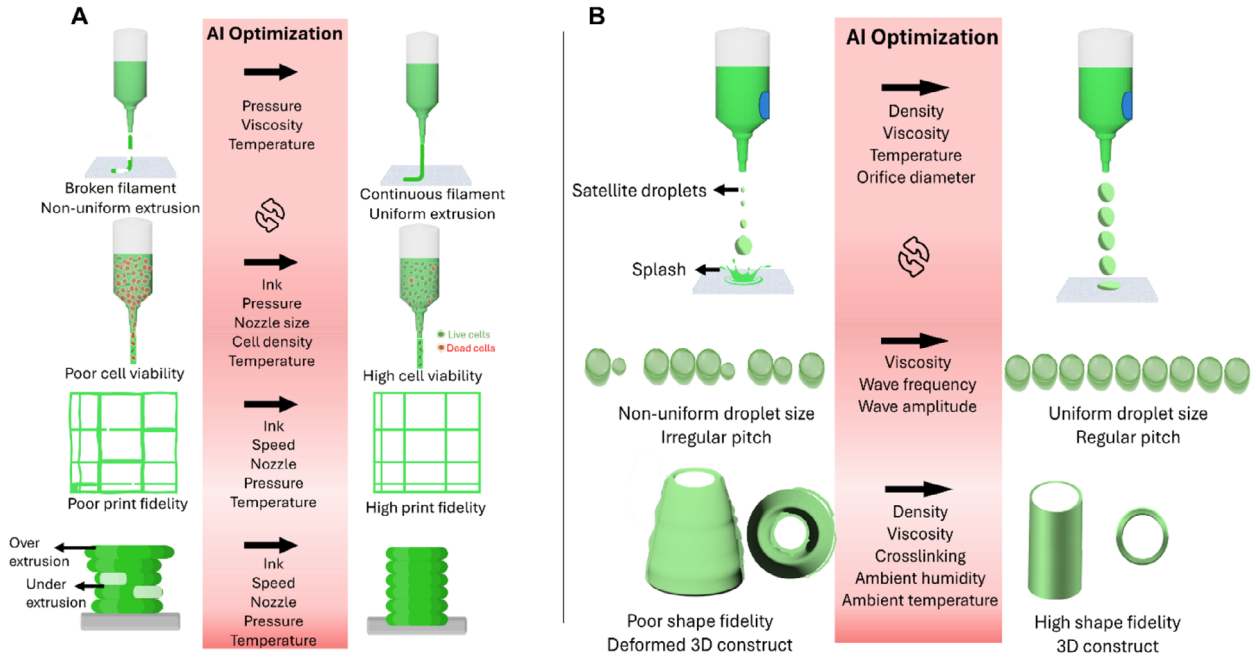

Figure 20. A) Utilization of AI in EBB to optimize ink properties, such as pressure, viscosity, and temperature, ensuring high print quality and cell viability. AI systems dynamically adjust parameters to enhance structural fidelity and biological function. B) DBB benefits from AI integration for optimizing droplet formation by controlling density, viscosity, temperature, and crosslinking. AI algorithms improve droplet consistency, enabling precise deposition and reducing errors during bioprinting. This figure was produced with Adobe Inc., (2019), Adobe Illustrator.

Going forward, RL could be utilized to optimize printing conditions, scaffold design, material selection, waste reduction, and patient-specific parameter selection for in situ bioprinting.[203] The integration of RL into bioprinting could lead to significant advancements in precision and function of bioprinted tissues and organs, ultimately enhancing the capabilities of 3D bioprinting in clinical applications. RL offers a powerful approach to optimizing bioprinting processes by dynamically adjusting parameters to achieve desired outcomes. Its ability to learn from interactions with the environment and continuously improve decision-making enables RL to be a valuable tool in advancing bioprinting technologies.

4.4. ML Algorithm Selection Criteria

Here, we provide a selection criterion for the ML algorithms discussed before. We present **Table 3** as a guide to assist in selecting the most appropriate algorithm based on key factors such as data type, the amount of data available for training, computational power available, input-output structure, specific objectives, and the required tuning and preprocessing steps. It is important to remember that this table is merely a suggestion, and the algorithms can be adapted or combined to suit different situations and specific project needs. This structured approach aims to simplify the decision-making process by aligning algorithm characteristics with the project's requirements.

5. AI integration with bioprinting modalities

Recently, advancements have been observed in the application of ML to bioprinting-related needs such as medical imaging, bioink optimization, and bioprinting process refinement, all of which are enhancing the effectiveness of bioprinting. The most common 3D bioprinting techniques include EBB, DBB, laser-assisted bioprinting (LaBB) and light-assisted bioprinting (LiBB), with newer techniques like aspiration-assisted and magnetic-assisted bioprinting also emerging. **Table 4** highlights these different bioprinting techniques, listing out their working mechanism, advantages, limitations, applications, and potential integration with AI.

5.1. Extrusion-Based Bioprinting

Extrusion-based bioprinting (EBB) is the most common bioprinting technique that involves the continuous deposition of bioinks through a nozzle.[204–206] With the integration of AI, EBB is emerging as a powerful tool for enhancing precision, automating process optimization, and reducing errors in bioprinting (**Figure 20A**). AI technologies provide dynamic solutions to the challenges in EBB, such as optimizing print quality and maintaining cell viability.[145,207] In recent years, researchers have integrated ML algorithms to develop quality control loops for EBB, thereby reducing the trial-and-error approach traditionally associated with parameter optimization. For example, Bonatti et al. applied DL in a closed-loop control system for EBB, where a CNN was used to monitor and classify printing outcomes in real-time.[47] This model was trained on high-resolution videos of the EBB process and could automatically detect anomalies, such as under-extrusion or over-extrusion, providing immediate feedback to adjust printing parameters. In another study, Tian et al. successfully applied RF regression models to predict cell

Table 3. Guide to the best algorithm for ML applications.

Group	ML Situation	ANN	DNN	CNN	RNN	DT, RF, GBoost, XGBoost	SVM	BO and GP	Linear regression	Logistic regression	kNN	Ensemble	Kmeans	GAN	Q-Learning
Data amount available for training	Big data amount?	✓	✓	✓	✓	✓	✓	×	×	×	×	✓	×	✓	✓
	Low data amount?	●	×	●	●	✓	✓	✓	✓	✓	✓	✓	✓	×	✓
	Scalability Need?	✓	✓	✓	✓	✓	✓	×	×	×	✓	✓	✓	✓	✓
	Handle high-dimensional data?	✓	✓	×	×	✓	✓	×	×	×	×	✓	●	×	●
Data Type	Numeric?	✓	✓	×	✓	✓	✓	✓	✓	✓	✓	✓	×	✓	✓
	Image?	×	×	✓	×	×	×	×	×	×	×	✓	×	✓	×
	Time-dependent Data	×	×	×	✓	×	×	×	×	×	×	✓	×	●	✓
Computer power available	Limited computer power?	×	×	×	×	✓	×	×	✓	✓	✓	×	✓	×	×
	High computer power?	✓	✓	✓	✓	×	✓	✓	×	×	×	✓	×	✓	✓
	Training time?	×	×	×	×	✓	●	●	✓	✓	✓	●	✓	×	×
	Inference time?	●	●	●	●	✓	●	●	✓	✓	✓	●	✓	●	●
Input and output	Labeled data?	✓	✓	✓	✓	✓	✓	✓	✓	✓	✓	✓	×	✓	✓
	Unlabeled data?	×	×	×	×	×	×	×	×	×	×	×	✓	✓	×
Objective	Regression?	✓	✓	×	✓	✓	×	✓	✓	×	✓	✓	×	×	×
	Classification?	✓	✓	✓	×	✓	✓	×	×	✓	✓	✓	×	×	×
	Clustering?	×	×	×	×	×	×	×	×	×	×	×	✓	×	×
	Data augmentation?	●	●	●	●	×	×	×	×	×	×	●	×	✓	×
Tuning and preprocessing	Outlier sensitivity?	×	×	✓	●	✓	×	×	×	×	×	✓	×	✓	●
	Noise sensitivity?	●	●	✓	✓	●	●	×	×	×	×	✓	×	✓	●
	Hyperparameter tuning?	×	×	×	×	●	●	×	✓	✓	✓	●	✓	×	×

✓ indicates that the method is well-suited for the given condition. ● suggests that its applicability depends on data size, hyperparameters, or requires modifications for optimal performance. × denotes that the method is not suitable or ineffective for the specified condition. For sensitivity, ✓ represents low sensitivity, ● indicates moderate sensitivity, and × signifies high sensitivity to variations in data or conditions.

Table 4. Bioprinting modalities and their features.

Modality	Working mechanism	Strengths	Limitations	Applications	AI Integration	Refs.
EBB	• The most common and affordable bioprinting modality. • Employs pneumatic, mechanical, or screw-driven systems to extrude bioink through a nozzle in a continuous filament.	• Versatile with a wide range of bioink viscosities. • Enables scaffold-free printing with tissue spheroids. • Supports high cell densities. • Facilitates vascularization.	• Shear stress can damage cells. • Limited resolution. • Nozzle clogging. • Slower printing speeds for complex structures.	Used for creating large tissue constructs, organoids, and organ-on-a-chip models.	AI can optimize bioink flow rates and viscosity in real-time, minimizing nozzle clogging and shear stress. CV systems ensure precise layer deposition and detect misalignments during bioprinting. Predictive algorithms improve resolution by dynamically adjusting extrusion parameters, enhancing print quality and reliability.	[77, 204, 208]
DBB	• Inkjet printers are the most commonly used type. • Utilizes thermal, piezoelectric, or acoustic forces to eject tiny droplets of bioink from a nozzle.	• High precision, high speed, and high resolution. • Suitable for low-viscosity bioinks. • Suitable for high-throughput bioprinting.	• Nozzle clogging. • Inconsistency in droplet size • Difficulty in supporting spheroid bioprinting. • Potential for cross-contamination with multiple bioinks	Ideal for high-throughput screening, creating microarrays.	AI can ensure consistent droplet size and monitor for nozzle clogging through real-time image analysis. Automated calibration of droplet ejection improves bioprinting efficiency, while predictive maintenance avoids disruptions.	[228, 229, 230]
LaBB	• Less popular than DBB or EBB. • Involves using laser pulses to generate a shock wave that deposits bioink onto a substrate.	• High resolution. • Minimal cell damage. • No nozzle clogging. • Capable of precise placement of individual cells.	• Labor-intensive setup. • High cost. • Difficulty in accurately targeting spheroids. • Not yet widely commercially available.	Suitable for applications requiring high precision at the single-cell level.	AI-powered systems can control laser precision and alignment, ensuring minimal cell damage. Automated calibration and feedback mechanisms improve accuracy and reduce setup time.	[214, 231, 232, 233]
LiBB	• Utilizes light sources for polymerization of photosensitive hydrogels/bioinks, allowing high precision bioprinting. • Utilizes light sources (e.g., UV) to polymerize photosensitive hydrogels at specific locations.	• High accuracy. • No nozzle-related issues. • Suitable for creating complex. • Rapid bioprinting speed in the case of volumetric bioprinting.	• Limited choice of biocompatible hydrogels. • Potential UV toxicity to cells (affecting cell viability) and potential damage from residual curing agents • Challenges with multi-cell bioprinting • Expensive equipment and materials.	Ideal for detailed tissue constructs, complex scaffold structures with embedded vascular networks.	AI can enhance biomaterial selection, optimizing hydrogel formulations to balance UV toxicity and biocompatibility. Real-time monitoring ensures layer consistency and quality control during polymerization.	[148, 234, 235, 236]
AAB	• Uses aspiration to pick up and deposit cell aggregates, including spheroids and organoids.	• High Precision and accuracy. • Flexibility in handling different sizes and types of cell aggregates. • Suitable for high-throughput bioprinting.	• Requires fine control of aspiration forces to avoid cell damage • May require frequent calibration to maintain high precision	Ideal for highly precise tissue constructs. Beneficial for studies requiring the controlled placement of spheroids for in vitro modeling.	AI-driven control systems can optimize aspiration forces, ensuring cell viability and precise spheroid placement. Automated calibration improves reproducibility, while real-time monitoring prevents handling errors.	[113, 225]

viability and filament diameter based on data from multiple studies using alginate and gelatin bioinks.[207] These models enable researchers to optimize conditions, such as extrusion pressure, in real time by analyzing large datasets and predicting outcomes based on bioink and bioprinter settings. They also minimize the need for manual interventions and allow for continuous adjustments throughout bioprinting, ensuring higher precision and consistency in final constructs.

One of the challenges in EBB is maintaining cell viability during the extrusion process, as cells can be damaged due to shear stress.[208] AI models have been used to predict the impact of different extrusion pressures, nozzle geometries, and bioink compositions on cell viability.[209,210] These models analyze historical data and use predictive algorithms to identify conditions that maximize cell survival while maintaining structural fidelity. The integration of AI in this context enables the creation of more viable constructs, particularly for applications in regenerative medicine. The integration of AI technologies is transforming EBB by enhancing the precision, efficiency, and scalability of the process. AI-driven systems offer real-time monitoring, automatic parameter optimization, and improved quality control, significantly reducing the manual labor and time required for successful bioprinting. As AI continues to evolve, its role in EBB will expand, enabling the creation of more complex, functional tissues.

5.2. Droplet-Based Bioprinting

Droplet-based bioprinting (DBB) enables precise deposition of droplets of hydrogels loaded with cells onto a substrate as building blocks. DBB shows great potential for enabling high-throughput fabrication of tissue models; however, there are other factors, which should be optimized, such as droplet velocity, bioink rheology, and droplet volume. That is where AI could play a crucial role in optimizing and getting a precise bioprinted structure with high cell viability. AI technologies, such as ML algorithms, can be used to optimize droplet formation, ensuring even deposition of bioinks and minimizing errors in the printing process (Figure 20B). For example, Shi et al. demonstrated the elimination of satellite droplets using learning-based cell injection control to simulate the piezoelectric DBB head, replacing experimental trials, and an MLP, to optimize printing parameters.[211] This was required because satellite droplets may form during DBB, which are unwanted smaller droplets that deviate from the mainstream of bioink and affect printing position accuracy.

In another study, electrohydrodynamic (EHD) printing was used as an alternative to conventional inkjet bioprinting for generating ultra-high-resolution droplets, where key process parameters like applied voltage, back pressure, and nozzle standoff height were optimized using desirability function analysis. This methodology was integrated with multi-objective optimization to achieve precise control over droplet size and printing frequency for better functionality.[212] Furthermore, AI-driven systems can also be used to predict the volume of the droplet for precise cell deposition that gives a reliable and replicable 3D microenvironment. For instance, Shin et al. used an ML approach to predict cell-laden droplet volumes for precise 3D microtissue and organoid reconstruction.[213] Here, the bioprinting platform generated a high-throughput dataset, comparing three ML and two DL algorithms. It used bioprinting parameters like bioink viscosity, nozzle size, and pressure, and controlled droplet sizes from 0.1 to 50 µL. Using 5% GelMA and alginate with GFP-tagged 3T3 fibroblasts, the models achieved high predictive accuracy, optimizing volume control and enhancing the scalability of organoid production.[213] Despite these efforts, integrating AI into DBB presents challenges that must be addressed to optimize its effectiveness, such as the need for large and high-quality datasets for training ML models, as limited or biased data can hinder performance.

5.3. Laser-Assisted Bioprinting

Laser-assisted bioprinting (LaBB) is a sophisticated technique that uses laser pulses to accurately deposit cells and biomaterials. The process involves focusing a laser beam on a ribbon coated with a bioink, causing a droplet to form and precisely deposit onto a substrate.[214–216] LaBB is renowned for its high precision, which includes single-cell bioprinting per droplet to high cell density, making it ideal for applications requiring excellent spatial resolution and complex tissues. In terms of AI integration, LaBB can benefit significantly from advancements in AI and ML. AI algorithms can optimize laser parameters, such as pulse duration, energy, and focus, to ensure that the jet formation process is consistent and tailored to the specific needs of different bioinks or cell types (**Figure 21A**). In LaBB, jet flow transfers the bioink to the substrate via bubble generation, and printing quality mainly depends on jet flow regime, which could be stable or unstable. AI can help to predict the best parameters for each situation to get better printability by monitoring flow in real-time, predicting instability, optimizing parameters (such as laser power, focus, and pulse time), and simulating fluid dynamics to maintain stability. In the literature, Qu et. al used a computational-fluid-dynamics (CFD)-based model to predict the static balance between jet and substrate along with jet size and achieved less than 14% similarity as compared to experiments.[217] AI can enhance the precision and accuracy of jet deposition by continuously monitoring and adjusting the printing process in real-time.[218] ML models trained on data from previous prints could predict optimal conditions for various bioinks, improving reproducibility and reducing trial-and-error efforts in biofabrication.

5.4. Light-Based Bioprinting

Light-based bioprinting (LiBB) fabricates tissue and artificial organs by selectively using UV light and sometimes near UV (405 nm) light to crosslink a bioink, fabricating complex structures. This technique relies on key chemical components, such as photocrosslinkable hydrogels and photoinitiators.[219] The photocrosslinking process is finely controlled by factors including polymer selection, functional group modifications, and the choice of the photoinitiator. These elements enable precise modulation of mechanical properties and degradation rates, allowing for tailored fabrication of 3D bioprinted structures. By doing so, it provides resolution around 20–50 um and with detailed complex structure, even it can fabricate microchannels which are challenging to achieve with other bioprinting techniques.[220]

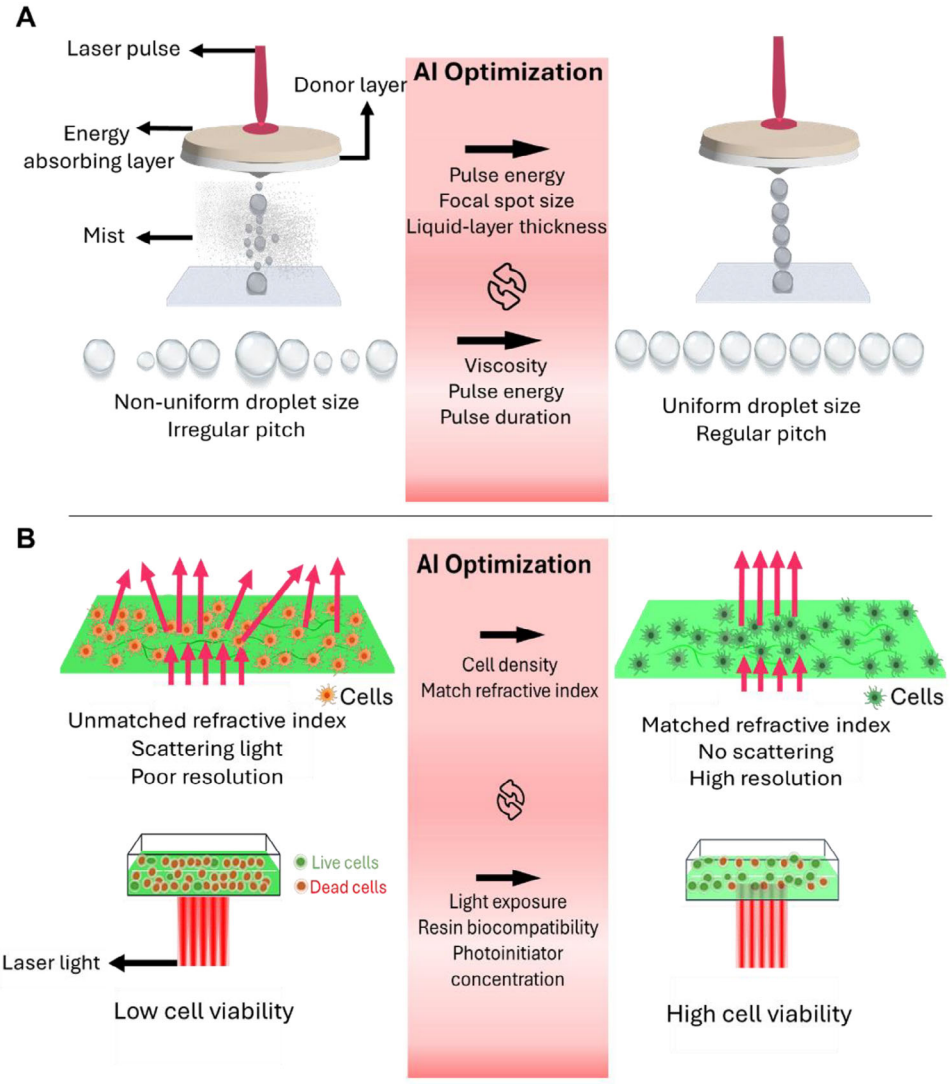

Figure 21. A) In LaBB, AI algorithms optimize laser parameters, including pulse duration, energy, and focal spot size, to achieve consistent, droplet formation. AI-driven adjustments ensure compatibility with various bioinks and cell types, improving precision and cell viability. B) LiBB benefits from AI integration to enhance process efficiency and resolution. AI optimizes parameters such as light exposure, resin biocompatibility, and photoinitiator concentration, enabling higher cell viability and structural fidelity. This figure was rproduced with Adobe Inc., (2019), Adobe Illustrator.

The integration of AI with LiBB can significantly enhance the precision and efficiency of the process (Figure 21B). For instance, ML algorithms have been integrated to optimize grayscale design, enhancing the resolution and accuracy of printed microstructures. One study applied evolutionary algorithms and ML to optimize the grayscale of DLP bioprinting blocks, achieving high-precision structures that could not be easily fabricated by traditional methods.[221] Similarly, another study integrates RF models with DLP bioprinting to enhance precision and reduce print errors. By analyzing 690 experimental datasets from commercial resin prints, the researchers developed a predictive model for print errors, achieving remarkable control over feature sizes.[222] In LiBB, which relies on light sources, such as UV light, to pattern and crosslink bioinks, AI can optimize crucial parameters such as light intensity, exposure time, and wavelength to ensure better control over the printed structure. For instance, optical projection stereolithography, which is similar to DLP, ML models have been used to predict cell viability during bioprinting.[148] These models take parameters such as light intensity, exposure time, and bioink properties to optimize cell survival rates. Moreover, studies have explored using ANNs to tailor drug release rates from 3D-printed tablets, showcasing how AI-driven optimization can improve not only structural integrity but also functional performance, like in drug delivery.[148] Despite these advancements, challenges remain in integrating AI with LiBB, primarily due to the requirement of large, high-quality datasets for model training. Biases or insufficient data can limit the accuracy and effectiveness of these ML systems, but ongoing research continues to refine these techniques for improved precision and cell viability in bioprinting.

5.5. Nonconventional Bioprinting Techniques

Aspiration-assisted bioprinting (AAB) is a relatively new technique that uses aspiration forces to pick and precisely place cell aggregates, such as spheroids, onto a substrate.[113,223] AAB enhances positional accuracy and precision while minimizing the risks of cell or tissue damage seen in other spheroid bioprinting approaches.[223,224] AAB can be used with either scaffold-based or scaffold-free approaches, depending on whether spheroids are printed into a functional gel or a sacrificial gel.[225] AAB relies on careful pressure optimization to avoid spheroids during pickup and transfer.[226] Despite several advantages, it faces limitations when applied to spheroids with larger diameters or very low stiffness, such as tumor spheroids, hepatic spheroids, brain, lung, and renal organoids. To address this, a new magnetic-assisted bioprinting approach called Spatially Patterned Organoid Transfer (SPOT) has been reported.[227] SPOT uses magnetic nanoparticles and 3D printing to precisely control the spatial arrangement of organoids, enabling accurate modeling of neurodevelopmental phenomena and disease progression, including brain tumor integration.

Although there is no literature available on AI integration with aspiration and magnetic-assisted bioprinting, AI can detect positional inaccuracy of spheroids, occasional dropping of spheroids before bioprinting, and breakage of spheroids during their pickup. Consequently, it can optimize key parameters in the bioprinting process, such as aspiration pressure, nozzle movement, precise placement, and magnetic fields for magnet-assisted printing. By analyzing large datasets from previous sessions, AI can predict the optimal conditions for the size of spheroids, minimizing the need for manual adjustments and trial-and-errors that can lead to better control and accuracy.

6. Challenges and Opportunities in Clinical Translation of AI-integrated Bioprinting

The clinical translation of AI-integrated bioprinting presents several challenges, despite its vast potential to revolutionize healthcare. One significant challenge lies in ethical concerns, as AI models depend on large datasets that can raise privacy and bias issues, if not properly managed.[237–240] Ensuring that these AI-driven bioprinting systems are safe and reliable for clinical use is also a key obstacle.[241] Data limitations further complicate AI's implementation, as bioprinting often lacks the large and diverse datasets required for training effective models, leading to potential generalization problems across diverse populations, ethnicities, and ages. Additionally, integrating AI tools with existing medical systems remains difficult due to the lack of interoperability and traditional infrastructure not being designed for seamless AI adoption.[242–244] Gaining the trust of medical professionals is another hurdle, with many skeptical of AI decision-making due to concerns about the "black box" nature of AI and its potential for errors.[245–247] Furthermore, the high cost and scalability issues associated with AI-driven bioprinting technologies create barriers to widespread clinical use, especially in resource-constrained healthcare systems.[248–250]

Regulatory hurdles also exist, as AI in healthcare requires compliance with evolving frameworks to ensure safety and efficacy. The US Food and Drug Administration (FDA)'s "Artificial Intelligence/Machine Learning (AI/ML) Software as a Medical Device (SaMD) Action Plan" outlines the regulatory framework for AI/ML-based medical devices.[251] It emphasizes a risk-based approach to premarket review, ensuring that AI/ML technologies meet safety and effectiveness standards before reaching the market. The plan also promotes good machine learning practices (GMLP) to encourage transparency, reproducibility, and real-world performance monitoring. This initiative supports continuous learning AI systems and ensures that devices can adapt safely to new data after deployment.

Despite these challenges, AI offers substantial opportunities to improve bioprinting processes and outcomes. By enhancing precision in cell placement, tissue architecture, and bioink selection, AI allows for highly customized bioprinted tissues, enabling personalized treatments tailored to individual patients.[54,72,253] AI can also improve predictive modeling, helping clinicians forecast how bioprinted tissues will behave in vivo, thus increasing the success rate of bioprinted implants and reducing the need for extensive clinical trials. Another major opportunity is the automation of quality control, where AI can continuously monitor and correct printing errors, ensuring higher consistency and reliability.[254,256] Moreover, AI-augmented bioprinting can accelerate drug discovery and development by creating realistic tissue models for high-throughput pharmaceutical screening, bridging the gap between traditional cell cultures and animal models. Finally, AI's ability to manage complex bioprinting processes could advance regenerative medicine, particularly in the fabrication of vascularized tissues and organs, addressing the global shortage of transplantable organs and reducing reliance on donors. Overall, while challenges in clinical translation exist, the opportunities for AI-enhanced bioprinting to improve personalized medicine and regenerative therapies are immense.

7. Summary and Future Perspectives

The integration of AI into bioprinting holds transformative potential for advancing precision, functionality, and scalability in regenerative medicine. AI technologies significantly improve bioprinting processes by enhancing predictive modeling, optimizing cell placement, and enabling real-time quality control. These advancements open the door to more personalized treatments, higher success rates for bioprinted tissues, and the potential to accelerate drug development through realistic tissue models.

The branches of AI hold significant potential to advance bioprinting technologies. CV can enhance quality control, facilitate model generation, and enable fault detection. When combined with robotics, it can create bioprinting systems that are more autonomous, precise, and less prone to errors. Additionally, the integration of robotics and CV can adapt to dynamic surfaces, enabling in situ bioprinting, a critical capability for regenerative medicine. By incorporating rule-based or ES, these technologies can make precise decisions and minimize critical errors. While this integration would render the system largely autonomous, human supervision would still be essential to ensure smooth and safe operations. NLP further improves human-machine interaction by suggesting adjustments, generating reports, and providing recommendations for future procedures. ML acts as a powerful tool to optimize all these features, making the system more adaptable and precise across various aspects of the bioprinting

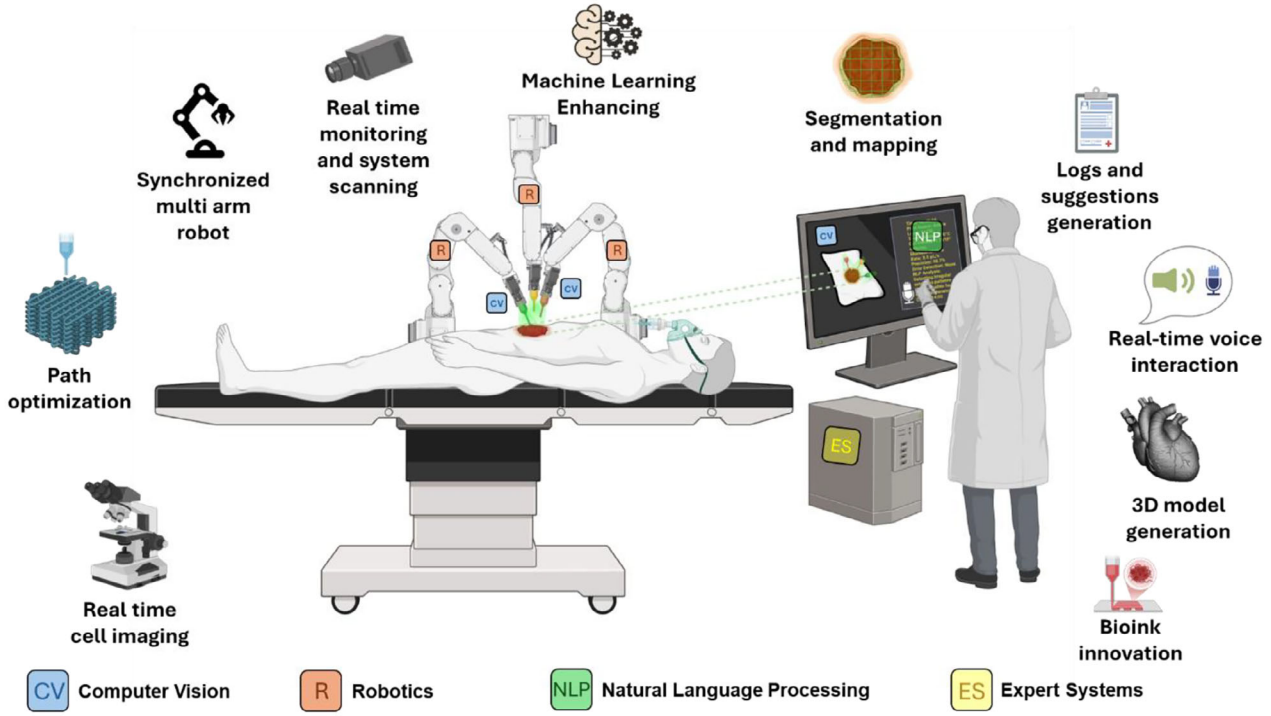

Figure 22. AI integrated in situ 3D bioprinting set-up. CV enhances quality control, facilitates model generation, and enables fault detection. When combined with robotics, it allows for the development of bioprinting systems that are more autonomous, precise, and less prone to errors. The integration of robotics and CV also enables adaptation to dynamic surfaces, a crucial capability for bioprinting intraoperatively. Rule-based or ES further refine the process by enabling precise decision-making and reducing critical errors, while maintaining the necessity of human supervision for safe operations. NLP improves human-machine interactions by suggesting adjustments, generating reports, and providing recommendations for future procedures. ML optimizes these functionalities, enhancing system adaptability and precision across various aspects of bioprinting. This figure was produced with BioRender.com and Microsoft PowerPoint.

process. **Figure** 22 envisions how a fully AI-integrated in situ bioprinting system would function.

Looking ahead, the future of AI-enhanced bioprinting is poised for rapid expansion and clinical adoption.[256,257] As AI technologies continue to evolve, they will likely enable more autonomous bioprinting systems capable of making real-time decisions with minimal human intervention. In the coming years, improvements in ML algorithms and the availability of larger, more diverse datasets will help mitigate current data limitations, allowing AI models to better generalize across different patient populations and biological environments. Additionally, AI-driven innovations will likely play a critical role in refining tissue fabrication, bringing the goal of creating fully functional, transplantable organs closer to reality. Ethical and regulatory frameworks need to be adopted to ensure patient safety and equitable access to these cutting-edge treatments. As AI continues to bridge the gap between technological capabilities and clinical needs, the integration of AI with bioprinting could transform healthcare by enabling personalized, on-demand tissue engineering solutions and advancing the field of regenerative medicine to unprecedented levels.

Acknowledgements

J.V.S.R. and I.D.D. contributed equally to this work. This work has been supported by the National Institute of Allergy and Infectious Diseases Award U19AI142733, National Institute of Biomedical Imaging and Bioengineering Awards R01EB034566 and R01EB036245, and National Institute of Dental and Craniofacial Research R01DE028614.

Conflict of Interest

ITO has an equity stake in Biolife4D and is a member of the scientific advisory board for Biolife4D and Healshape. Other authors confirm that there are no known conflicts of interest associated with this publication, and there has been no significant financial support for this work that could have influenced its outcome.

Keywords

3d bioprinting, artificial intelligence, computer vision, expert systems, machine learning, natural language processing, robotics

Received: April 15, 2025
Revised: June 19, 2025
Published online:

[1] G. Saini, N. Segaran, J. L. Mayer, A. Saini, H. Albadawi, R. Oklu, *J. Clin. Med.* **2021**, *10*, 4966.
[2] Y. Wang, M. Gao, D. Wang, L. Sun, T. J. Webster, *Int. J. Nanomed.* **2020**, *15*, 215.

[3] H. Lee, *CBS* **2023**, *4*, 0018.
[4] J. M. Tien, *Annal. Data Sci.* **2017**, *4*, 149.
[5] Y. Duan, J. S. Edwards, Y. K. Dwivedi, *Int. J. Inf. Manage.* **2019**, *48*, 63.
[6] L. Wu, H. Li, Y. Liu, Z. Fan, J. Xu, N. Li, X. Qian, Z. Lin, X. Li, J. Yan, *Int. J. Bioprint.* **2023**, *10*, 1256.
[7] J. Shin, Y. Lee, Z. Li, J. Hu, S. S. Park, K. Kim, *Micromachines (Basel)* **2022**, *13*, 363.
[8] N. Japkowicz, in *Imbalanced Learning: Foundations, Algorithms, and Applications*, Wiley, New York **2013, pp**. 187-206.
[9] J. Dessain, *Expert Syst. Appl.* **2022**, *199*, 116970.
[10] H. Moussaoui, N. E. Akkad, M. Benslimane, *Int. J. Comp.. Digit. Syst.* **2023**, *13*, 1465.
[11] X. Wu, S. Wang, *Intern. J. Pattern Recognit. Artif. Intell.* **2023**, *37*, 1.
[12] S. Abdollahi, A. Davis, J. H. Miller, A. W. Feinberg, *PLoS One* **2018**, *13*, 0194890.
[13] A. Turing, in *The Essential Turing*, Oxford University Press, Oxford, **2004**, pp. 433–464.
[14] J. J. Hopfield, *Proc. Natl. Acad. Sci.* **1982**, *79*, 2554.
[15] S. J. Lee, W. Jeong, A. Atala, *Adv. Mater.* **2024**, *36*, 2408032.
[16] J. J. Hopfield, *Proc Natl Acad Sci* **1984**, *81*, 3088.
[17] J. J. Hopfield, D. W. Tank, *Biol. Cybern.* **1985**, *52*, 141.
[18] D. H. Ackley, G. E. Hinton, T. J. Sejnowski, *Cogn. Sci.* **1985**, *9*, 147.
[19] W. L. Ng, A. Chan, Y. S. Ong, C. K. Chua, *Virtual Phys. Prototyp* **2020**, *15*, 340.
[20] S. Russell, P. Norvig, in *Artificial Intelligence: A Modern Approach*, 4th ed, Pearson Education **2021**, pp. 669–1031.
[21] G. E. Hinton, S. Osindero, Y. W. Teh, *Neural Comput.* **2006**, *18*, 1527.
[22] B. K. Chakrabarty, *Trans. Indian Ceram. Soc.* **2002**, *61*, 118.
[23] A. Bandi, P. V. Adapa, Y. E. Kuchi, *Future Int.* **2023**, *15*, 260.
[24] A. Kathirvel, V. M. Gobinath, In *Biosensors: Developments, Challenges and Perspectives*, Springer, Berlin, **2024**, pp. 303–320.
[25] D. Verma, Y. Dong, M. Sharma, A. K. Chaudhary, *Mater. Manuf. Processes* **2022**, *37*, 518.
[26] S. Freeman, S. Calabro, R. Williams, S. Jin, K. Ye, *Front. Bioeng. Biotechnol.* **2022**, *10*, 913579.
[27] J. Lee, S. J. Oh, S. H. An, W. D. Kim, S. H. Kim, S. H. Kim, *Biofabrication* **2020**, *12*, 035018.
[28] A. Skardal, M. Devarasetty, H. W. Kang, I. Mead, C. Bishop, T. Shupe, S. J. Lee, J. Jackson, J. Yoo, S. Soker, A. Atala, *Acta Biomater.* **2015**, *25*, 22.
[29] M. Hospodiuk, M. Dey, D. Sosnoski, I. T. Ozbolat, *Biotechnol. Adv.* **2017**, *35*, 217.
[30] K. Hölzl, S. Lin, L. Tytgat, S. Van Vlierberghe, L. Gu, A. Ovsianikov, *Biofabrication* **2016**, *8*, 032002.
[31] J. S. Dhatterwal, K. S. Kaswan, A. Tiwari, B. Balusamy, R. Gopal, in *Computational Intelligence in Bioprinting*, Wiley Online Library **2024, pp. 239-257**.
[32] S. K. Zhou, H. Greenspan, C. Davatzikos, J. S. Duncan, B. Van Ginneken, A. Madabhushi, J. L. Prince, D. Rueckert, R. M. Summers, *Proc. IEEE* **2021**, *109*, 820.
[33] A. S. Panayides, A. Amini, N. D. Filipovic, A. Sharma, S. A. Tsaftaris, A. Young, D. Foran, N. Do, S. Golemati, T. Kurc, K. Huang, K. S. Nikita, B. P. Veasey, M. Zervakis, J. H. Saltz, C. S. Pattichis, *IEEE J. Biomed. Health Inform.* **2020**, *24*, 1837.
[34] B. Arjmand, P. Goodarzi, F. Mohamadi-Jahani, K. Falahzadeh, B. Larijani, *Acta Med.* **2017**, *55*, 144.
[35] S. Vijayavenkataraman, W. C. Yan, W. F. Lu, C. H. Wang, J. Y. H. Fuh, *Adv. Drug Deliv. Rev.* **2018**, *132*, 296.
[36] A. N. Leberfinger, S. Dinda, Y. Wu, S. V. Koduru, V. Ozbolat, D. J. Ravnic, I. T. Ozbolat, *Acta Biomater.* **2019**, *95*, 32.
[37] E. S. Barjuei, J. Shin, K. Kim, J. Lee, *Sci. Rep.* **2024**, *14*, 17764.
[38] A. Zijl, In *Printing the Future: On the Enhancement of Bioprinting Techniques Through Artificial Intelligence*, Utrecht University, Utrecht **2024**.
[39] Z. Zhu, D. W. Ng, H. S. Park, M. C. McAlpine, *Nat. Rev. Mater.* **2021**, *6*, 27.
[40] G. A. Susto, A. Schirru, S. Pampuri, S. McLoone, A. Beghi, *IEEE Trans Industr Inform* **2015**, *11*, 812.
[41] Y. Lei, B. Yang, X. Jiang, F. Jia, N. Li, A. K. Nandi, *Mech. Syst. Signal Process* **2020**, *138*, 106587.
[42] CP. Sharma, T. Chandy, V. Thomas, in *Artificial Intelligence in Tissue and Organ Regeneration*, Elsevier, Amsterdam **2023**, pp. 267–288.
[43] E. C. Adeniyi Kehinde Adeleke, K. Ani, O. Andrew Olu-lawal, D. Kayode Olajiga, J. P. Montero, *Int. J. Sci. Res. Arch.* **2024**, *11*, 2346.
[44] W.-C. Yan, P. Davoodi, S. Vijayavenkataraman, Y. Tian, W. C. Ng, J. Y. H. Fuh, K. S. Robinson, C.-H. Wang, *Adv. Drug Deliv. Rev.* **2018**, *132*, 270.
[45] S. P. Leo Kumar, *Eng Appl Artif. Intell.* **2017**, *65*, 294.
[46] M. Javaid, A. Haleem, R. P. Singh, R. Suman, *J. Industr. Integrat. Manag.* **2022**, *7*, 83.
[47] A. F. Bonatti, G. Vozzi, C. K. Chua, C. De Maria, *Int. J. Bioprint.* **2022**, *8*, 620.
[48] A. F. Bonatti, G. Vozzi, C. De Maria, *Biofabrication* **2024**, *16*, 022001.
[49] R. Szeliski, in *Computer Vision: Algorithms and Applications*, Springer Nature, **2022**, pp. 1–26.
[50] Q. Tang, Y. Lee, H. Jung, *Sustainability* **2024**, *16*, 2161.
[51] C. Liu, L. Wang, W. Lu, J. Liu, C. Yang, C. Fan, Q. Li, Y. Tang, *Bone Res.* **2022**, *10*, 21.
[52] Z. Jin, Z. Zhang, X. Shao, G. X. Gu, *ACS Biomater. Sci. Eng.* **2023**, *9*, 3945.
[53] S. Rhee, J. L. Puetzer, B. N. Mason, C. A. Reinhart-King, L. J. Bonassar, *ACS Biomater. Sci. Eng.* **2016**, *2*, 1800.
[54] B. Schmieg, S. Gretzinger, S. Schuhmann, G. Guthausen, J. Hubbuch, *Biotechnol. J.* **2022**, *17*, 2100336.
[55] H. Golnabi, A. Asadpour, *Robot Comput Integr Manuf* **2007**, *23*, 630.
[56] E. R. Davies, In *Computer and Machine Vision: Theory, Algorithms*, Academic Press, 4th ed., Cambridge **2012, pp. 82-148**.
[57] S. Singh, D. Choudhury, F. Yu, V. Mironov, M. W. Naing, *Acta Biomater.* **2020**, *101*, 14.
[58] C. Kengla, E. Renteria, C. Wivell, A. Atala, J. J. Yoo, S. J. Lee, *3D Print. Addit. Manuf.* **2017**, *4*, 239.
[59] C. Borràs-Novell, M. G. Causapié, M. Murcia, D. Djian, Ó. García-Algar, *Int J Bioprint* **2022**, *8*, 516.
[60] Z. Zhu, S. Z. Guo, T. Hirdler, C. Eide, X. Fan, J. Tolar, M. C. McAlpine, *Adv. Mater.* **2018**, *30*, 1870165.
[61] W. Sun, V. Webster-Wood, *Mater. Today Proc.* **2022**, *70*, 376.
[62] B. Gatenholm, C. Lindahl, M. Brittberg, S. Simonsson, *Cartilage* **2021**, *13*, 1755S.
[63] R. Cadle, D. Rogozea, L. Moldovan, N. I. Moldovan, *Appl. Sci.* **2022**, *12*, 4430.
[64] S. Azizi, S. Bayat, A. Rajaram, E. M. Anas, T. Mohamed, K. Walus, P. Abolmaesumi, P. Mousavi, *Proc. SPIE* **2018**, *10576*, 430.
[65] Á. Bertelsen, A. Iribar-Zabala, E. Otegi-Alvaro, R. Benito, K. López-Linares, I. Macía, *Healthc. Technol. Lett.* **2024**, *11*, 59.
[66] V. Sergis, D. Kelly, G. Britchfield, A. Pramanick, K. Mason, A. Daly, *Biofab.* **2025**, *17*, 025004.
[67] C. Liu, C. Yang, J. Liu, Y. Tang, Z. Lin, L. Li, H. Liang, W. Lu, L. Wang, *Int. J. Bioprint.* **2022**, *9*, 644.
[68] Z. Ren, F. Fang, N. Yan, Y. Wu, *IJPEM-GT* **2022**, *9*, 661.
[69] K. Zakharova, A. Czekanski, *Prog. Can. Mech. Eng.* **2023**, *6*, 20720.
[70] W. Zhao, H. Chen, Y. Zhang, D. Zhou, L. Liang, B. Liu, T. Xu, *Bioeng. Transl. Med.* **2022**, *7*, e10303.
[71] P. Sitthi-Amorn, J. E. Ramos, Y. Wang, J. Kwan, J. Lan, W. Wang, W. Matusik, *ACM Trans. Graph* **2015, 34, 1**.

[72] M. S. Chaudhry, A. Czekanski, *Bioprinting* **2023**, *31*, 00271.
[73] X. Zhao, Y. Pan, C. Zhou, Y. Chen, C. C. Wang, *J. Manuf. Process* **2013**, *15*, 432.
[74] P. Gholami, M. A. Ahmadi-Pajouh, N. Abolftahi, G. Hamarneh, M. Kayvanrad, *IEEE J. Biomed. Health Inform.* **2018**, *22*, 1269.
[75] H. Ding, R. C. Chang, *Addit. Manuf.* **2018**, *22*, 708.
[76] S. H. Jeong, J. Kim, B. C. Thibault, J. A. L. Soto, F. Tourk, J. Steakelum, D. Azuela, V. Carvalho, G. Quiroga-Ocaña, W. Zhuang, M. L. L. Cham-Pérez, L. L. Huang, Z. Li, E. A. Valsami, E. Wang, N. Rodrigues, S. F. Teixeira, Y. Lee, J. Seo, A. Veves, S. Hassan, G. Theocharidis, L. Fiondella, S. R. Shin, *Adv. Mater. Technol.* **2024**, *9*, 2400060.
[77] A. A. Armstrong, J. Norato, A. G. Alleyne, A. J. Wagoner Johnson, *Biofabrication* **2020**, *12*, 045023.
[78] A. A. Armstrong, A. G. Alleyne, A. J. Wagoner Johnson, *Biofabrication* **2020**, *12*, 045023.
[79] S. Giovanni Gugliandolo, E. Prioglio, D. Moscatelli, B. M. Colosimo, *Int. J. Bioprint.* **2024**, *10*, 394.
[80] T. Zhang, X. Cao, S. Zhang, Y. Chen, Y. Huang, M. Yu, X. Han, *Addit. Manuf.* **2024**, *95*, 104537.
[81] G. M. Fortunato, E. Batoni, A. F. Bonatti, G. Vozzi, C. De Maria, *Bioprinting* **2022**, *26*, 00195.
[82] H. Dong, B. Hu, W. Zhang, W. Xie, J. Mo, H. Sun, J. Shang, *Int. J. Bioprint.* **2022**, *9*, 629.
[83] S. G. Dennis, T. Trusk, D. Richards, J. Jia, Y. Tan, Y. Mei, S. Fann, R. Markwald, M. Yost, *J. Visual. Experim.* **2015**, *103*, 53156.
[84] "Advanced Solutions," can be found under https://www.advancedsolutions.com/biobot-basic (accessed: September 2024).
[85] "REGENHU," can be found under https://www.regenhu.com/3dbioprinting-solutions/ (accessed: September 2024).
[86] D. O. Adejumo, D. A. Fadare, R. A. Kazeem, O. M. Ikumapayi, A. Falana, A. S. Adedayo, D. A. Fadare, A. O. Adeoye, A. T. Ogundipe, E. S. Olarinde, *JESA* **2023**, *56*, 627.
[87] W. Zhao, T. Xu, *Biofabrication* **2020**, *12*, 045020.
[88] M. Shen, H. Yang, J. Cheng, M. Zhang, T. Hu, Y. Hu, *J. Mechan. Sci. Technol.* **2022**, *36*, 6329.
[89] J. Bodner, F. Augustin, H. Wykypiel, J. Fish, G. Muehlmann, G. Wetscher, T. Schmid, *Swiss Med Wkly* **2005**, *135*, 674.
[90] J. Lipskas, K. Deep, W. Yao, *Sci. Rep.* **2019**, *9*, 3746.
[91] K. Ma, T. Zhao, L. Yang, P. Wang, J. Jin, H. Teng, D. Xia, L. Zhu, L. Li, Q. Jiang, X. Wang, *J. Adv. Res.* **2020**, *23*, 123.
[92] H. Chen, X. Ma, T. Gao, W. Zhao, T. Xu, Z. Liu, *Biomed. Pharmacother.* **2023**, *158*, 114140.
[93] C. Zhou, Y. Yang, J. Wang, Q. Wu, Z. Gu, Y. Zhou, X. Liu, Y. Yang, H. Tang, Q. Ling, L. Wang, J. Zang, *Nat. Commun.* **2021**, *12*, 5072.
[94] L. Li, J. Shi, K. Ma, J. Jin, P. Wang, H. Liang, Y. Cao, X. Wang, Q. Jiang, *J. Adv. Res.* **2021**, *30*, 75.
[95] Z. Zhang, C. Wu, C. Dai, Q. Shi, G. Fang, D. Xie, X. Zhao, Y. J. Liu, C. C. L. Wang, X. J. Wang, *Bioact. Mater.* **2022**, *18*, 138.
[96] W. Zhao, C. Hu, T. Xu, S. Lin, Z. Wang, Y. Zhu, *Adv. Funct. Mater.* **2022**, *32*, 2207496.
[97] S. Vajjala, B. Majumder, A. Gupta, H. Surana, *O'Reilly* **2020**, *1*, 37.
[98] D. Khurana, A. Koli, K. Khatter, S. Singh, *Multimed. Tools Appl.* **2023**, *82*, 3713.
[99] A. F. Bonatti, F. Chiarello, G. Vozzi, C. De Maria, *3D Print. Addit. Manuf.* **2024**, *11*, 1495.
[100] E. Cambria, B. White, *IEEE Comput. Intell. Mag.* **2014**, *9*, 48.
[101] P. M. Nadkarni, L. Ohno-Machado, W. W. Chapman, *J. Am. Med. Inform. Assoc.* **2011**, *18*, 544.
[102] M. S. Khan, S. Sinha, U. T. Sheikh, D. Stricker, S. A. Ali, M. Z. Afzal, *ArXiv* **2024**, *37*, 7552.
[103] A. Badagabettu, S. S. Yarlagadda, A. B. Farimani, *ArXiv* **2024**, https://doi.org/10.48550/arXiv.2406.00144.
[104] A. H. Kyaw, S. H. Jeon, M. Smith, G. Neil, *ArXiv* **2024**, https://doi.org/10.48550/arXiv.2409.18390 .
[105] X. Yang, C. Zhu, *IEEE Access* **2024**, *12*, 88558.
[106] S.-H. Liao, *Expert Syst. Appl.* **2005**, *28*, 93.
[107] Y. Cao, Z. J. Zhou, C. H. Hu, S. W. Tang, J. Wang, *Decis. Support Syst.* **2021**, *150*, 113558.
[108] A. Saibene, M. Assale, M. Giltri, *Expert Syst. Appl.* **2021**, *177*, 114900.
[109] S. P. Leo Kumar, *Int. J. Prod. Res.* **2019**, *57*, 4766.
[110] C. Mota, S. Camarero-Espinosa, M. B. Baker, P. Wieringa, L. Moroni, *Chem. Rev.* **2020**, *120*, 10547.
[111] M. Yang, W. Dai, P. Jiang, *J. Eng. Design* **2023**, *34*, 691.
[112] R. Farahov, R. Burnashev, R. Grigoriev, I. Nasibullin, M. Bolsunovskaya, A. Enikeev, in *Int. Conf. of Young Specialists on Micro/Nanotechnologies and Electron Devices (EDM)*, IEEE, Piscataway, NJ **2022, pp. 555-559**.
[113] B. Ayan, D. N. Heo, Z. Zhang, M. Dey, A. Povilianskas, C. Drapaca, I. T. Ozbolat, *Sci. Adv.* **2020**, *6*, aaw5111.
[114] H. Ravanbakhsh, V. Karamzadeh, G. Bao, L. Mongeau, D. Juncker, Y. S. Zhang, *Adv. Mater.* **2021**, *33*, 2104730.
[115] S. Liu, A. Bernhardt, K. Wirsig, A. Lode, Q. Hu, M. Gelinsky, D. Kilian, *Compos B Eng* **2023**, *261*, 110804.
[116] A. S. Abdulwahab, R. I. Noorani, in *2024 the 8th Int. Conf. on Innovation in Artificial Intelligence*, ACM, NY, USA, **2024**, pp. 178–186.
[117] Y. S. Zhang, K. Yue, J. Aleman, K. Mollazadeh-Moghaddam, S. M. Bakht, J. Yang, W. Jia, V. Dell'Erba, P. Assawes, S. R. Shin, M. R. Dokmeci, R. Oklu, A. Khademhosseini, *Ann. Biomed. Eng.* **2017**, *45*, 148.
[118] S. Liu, L. Cheng, Y. Liu, H. Zhang, Y. Song, J. H. Park, K. Dashnyam, J. H. Lee, F. A. H. Khalak, O. Riester, Z. Shi, S. Ostrovidov, H. Kaji, H. P. Deigner, J. L. Pedraz, J. C. Knowles, Q. Hu, H. W. Kim, M. Ramalingam, *J. Tissue Eng.* **2023**, *14*, 20417314231187113.
[119] S. Fukuda, in *Expert Systems in Engineering Applications*, Springer, Berlin **1993**, pp. 307–314.
[120] K. H. Vining, D. J. Mooney, *Nat. Rev. Mol. Cell Biol.* **2017**, *18*, 728.
[121] V. D. Majstorović, *Comput. Ind.* **1990**, *15*, 43.
[122] C. Bell, in Maintaining and Troubleshooting Your 3D Printer **2014, pp. 85-127**.
[123] B. Mahadik, R. Margolis, S. McLoughlin, A. Melchiorri, S. J. Lee, J. Yoo, A. Atala, A. G. Mikos, J. P. Fisher, *Biofabrication* **2023**, *15*, 015008.
[124] H. B. Mamo, A. D. Tura, A. Johnson Santhosh, N. Ashok, D. K. Rao, *Mater. Today Proc.* **2022**, *57*, 768.
[125] A. Sedigh, D. DiPiero, K. M. Shine, R. E. Tomlinson, *Bioprinting* **2022**, *25*, e00190.
[126] R. Makkar, *Int. J. Stat. Appl. Math.* **2018**, *3*, 357.
[127] H. Kumar, in *Theoretical and Practical Advancements for Fuzzy System Integration*, IGI Global, Pennsylvania, USA, **2017, pp. 31-48**.
[128] C. Dumitrescu, P. Ciotirnae, C. Vizitiu, *Sensors* **2021**, *21*, 2617.
[129] A. Sedigh, M. R. Akbarzadeh-T, R. E. Tomlinson, *Biophysica* **2022**, *2*, 400.
[130] V. Keriquel, F. Guillemot, I. Arnault, B. Guillotin, S. Miraux, J. Amédée, J. C. Fricain, S. Catros, *Biofabrication* **2010**, *2*, 014101.
[131] Z.-H. Zhou, in *Machine Learning*, Springer, Berlin **2021**, pp. 1–55.
[132] M. Alloghani, D. Al-Jumeily, J. Mustafina, A. Hussain, A. J. Aljaaf, **2020**, pp. 3–21.
[133] L. Alzubaidi, J. Zhang, A. J. Humaidi, A. Al-Dujaili, Y. Duan, O. Al-Shamma, J. Santamaría, M. A. Fadhel, M. Al-Amidie, L. Farhan, *J Big Data* **2021**, *8*, 53.
[134] K. P. Murphy, In *Probabilistic Machine Learning: Advanced Topics*, The MIT Press, Cambridge, Massachusetts **2023**, pp. 3–340.
[135] C. Yu, J. Jiang, *Int. J. Bioprint.* **2020**, *6*, 253
[136] L. Yang, A. Shami, *Neurocomputing* **2020**, *415*, 295.

[137] T. Dietterich, *ACM Computing Surveys (CSUR)* **1995**, *27*, 326.
[138] R. Bagherpour, G. Bagherpour, P. Mohammadi, *Tissue Eng. Part B Rev.* **2024**, *31*, 31.
[139] D. Mohammadrezaei, L. Podina, J. De Silva, M. Kohandel, *Biofabrication* **2024**, *16*, 025016.
[140] Q. Qiao, X. Zhang, Z. Yan, C. Hou, J. Zhang, Y. He, N. Zhao, S. Yan, Y. Gong, Q. Li, *Biodes Manuf* **2023**, *6*, 464.
[141] J. Guan, S. You, Y. Xiang, J. Schimelman, J. Alido, X. Ma, M. Tang, S. Chen, *Biofabrication* **2022**, *14*, 015011.
[142] P. J. Tebon, B. Wang, A. L. Markowitz, A. Davarifar, B. L. Tsai, P. Krawczuk, A. E. Gonzalez, S. Sartini, G. F. Murray, H. T. Nguyen, N. Tavanaie, T. L. Nguyen, P. C. Boutros, M. A. Teitell, A. Soragni, *Nat. Commun.* **2023**, *14*, 3168.
[143] F. Safir, N. Vu, L. F. Tadesse, K. Firouzi, N. Banaei, S. S. Jeffrey, A. A. E. Saleh, B. Pierre, T. Khuri-Yakub, J. A. Dionne, *Nano Lett.* **2023**, *23*, 2065.
[144] S. Rafieyan, E. Ansari, E. Vasheghani-Farahani, *Biofabrication* **2024**, *16*, 045014.
[145] Z. Fu, V. Angeline, W. Sun, *Int. J. Bioprint.* **2021**, *7*, 434.
[146] K. Ruberu, M. Senadeera, S. Rana, S. Gupta, J. Chung, Z. Yue, S. Venkatesh, G. Wallace, *Appl. Mater. Today* **2021**, *22*, 100914.
[147] E. Reina-Romo, S. Mandal, P. Amorim, V. Bloemen, E. Ferraris, L. Geris, *Front. Bioeng. Biotechnol.* **2021**, *9*, 701778.
[148] H. Xu, Q. Liu, J. Casillas, M. Mcanally, N. Mubtasim, L. S. Gollahon, D. Wu, C. Xu, *J. Intell. Manuf.* **2022**, *33*, 995.
[149] X. Huang, W. L. Ng, W. Y. Yeong, *J. Intell.. Manuf.* **2024**, *35*, 2349.
[150] M. Tang, S. Jiang, X. Huang, C. Ji, Y. Gu, Y. Qi, Y. Xiang, E. Yao, N. Zhang, E. Berman, D. Yu, Y. Qu, L. Liu, D. Berry, Y. Yao, *Cell Discov.* **2024**, *10*, 39.
[151] J. M. Bone, C. M. Childs, A. Menon, B. Póczos, A. W. Feinberg, P. R. Leduc, N. R. Washburn, *ACS Biomater. Sci. Eng.* **2020**, *6*, 7021.
[152] D. Oh, M. Shirzad, M. C. Kim, E. J. Chung, S. Y. Nam, *Int. J. Bioprint.* **2023**, *9*, 308.
[153] K. Yao, J. Sun, K. Huang, L. Jing, H. Liu, D. Huang, C. Jude, *Int. J. Bioprint.* **2021**, *8*, 495.
[154] A. Sedigh, J. E. Tulipan, M. R. Rivlin, R. E. Tomlinson, *bioRxiv* **2020**, https://doi.org/10.1101/2020.10.08.331611.
[155] O. I. Abiodun, A. Jantan, A. E. Omolara, K. V. Dada, A. M. Umar, O. U. Linus, H. Arshad, A. A. Kazaure, U. Gana, M. U. Kiru, *IEEE Access* **2019**, *7*, 158820.
[156] M. Khashei, M. Bijari, *Expert Syst. Appl.* **2010**, *37*, 479.
[157] J. K. Basu, D. Bhattacharyya, T. Kim, *IJSEA* **2010**, *4*, 23.
[158] W. S. McCulloch, W. Pitts, *Bull. Math. Biophys.* **1943**, *5*, 115.
[159] X. H. Le, H. V. Ho, G. Lee, S. Jung, *Water* **2019**, *11*, 1387.
[160] A. G. Bors, *Online Symposium for Electronics Engineers* **2001**, *1*.
[161] A. Tsantekidis, N. Passalis, A. Tefas, in *Deep Learning for Robot Perception and Cognition*, Academic Press, Cambridge, MA **2022**, pp. 101–115.
[162] Y. Dai, P. Wang, A. Mishra, K. You, Y. Zong, W. F. Lu, E. K. Chow, P. M. Preshaw, D. Huang, J. R. J. Chew, D. Ho, G. Sriram, *Adv. Healthcare Mater.* **2025**, *14*, 2402727.
[163] X. Lin, Y. Rivenson, N. T. Yardimci, M. Veli, Y. Luo, M. Jarrahi, A. Ozcan, *Science* **2018**, *361*, 1004.
[164] Z. Xiaoxun, Z. Jianhong, H. Dongnan, H. Zhonghe, *Energy Procedia* **2019**, *158*, 6393.
[165] S. Kiranyaz, O. Avci, O. Abdeljaber, T. Ince, M. Gabbouj, D. J. Inman, *Mech. Syst. Signal Process* **2021**, *151*, 107398.
[166] S. Sokmen, S. Cakmak, I. Oksuz, *Biomed. Mater.* **2024**, *19*, 035038.
[167] E. Bisong, in *Building Machine Learning and Deep Learning Models on Google Cloud Platform*, Apress, Berkeley, CA, **2019**, pp. 443–473.
[168] H. Hewamalage, C. Bergmeir, K. Bandara, *Int. J. Forecast* **2021**, *37*, 388.
[169] J. C. Kimmel, A. S. Brack, W. F. Marshall, *IEEE/ACM Trans. Comput. Biol. Bioinform.* **2021**, *18*, 562.
[170] K. Sujigarasharma, S. Sharulatha, M. Lawanya Shri, E. Gangadevi, R. K. Dhanaraj, In *Computational Intelligence in Bioprinting*, Scrivener Publishing LLC, Austin, Texas **2024**, pp. 157–173.
[171] P. Geurts, A. Irrthum, L. Wehenkel, *Mol. BioSyst.* **2009**, *5*, 1593.
[172] S. M. Joy, R. M. Reich, R. T. Reynolds, *Int. J. Remote Sens.* **2003**, *24*, 1835.
[173] T. Windeatt, G. Ardeshir, *Intern. J. Pattern Recognit. Artif. Intell.* **2004**, *18*, 749.
[174] M. Kretowski, In *Evolutionary Decision Trees in Large-Scale Data Mining*, Vol. *59*, Springer International Publishing, Berlin, **2019** pp. 21–48.
[175] G. Zeng, *Commun. Stat. Theory Methods* **2024**, *54*, 701.
[176] A. Ziegler, I. R. König, *Wiley Interdiscip. Rev. Data Min. Knowl. Discov.* **2014**, *4*, 55.
[177] E. A. Freeman, G. G. Moisen, J. W. Coulston, B. T. Wilson, *Canadian J. For. Res.* **2015**, *46*, 323.
[178] P. Kumari, D. Toshniwal, *J. Clean. Prod.* **2021**, *279*, 123285.
[179] A. V. Konstantinov, L. V. Utkin, *Knowl Based Syst* **2021**, *222*, 106993.
[180] T. Chen, C. Guestrin, in *Proc. of the ACM SIGKDD Int. Conf. on Knowledge Discovery and Data Mining*, ACM, New York **2016**, pp. 785–794.
[181] Y. Jiang, G. Tong, H. Yin, N. Xiong, *IEEE Access* **2019**, *7*, 118310.
[182] B. Gaye, D. Zhang, A. Wulamu, *Math. Probl. Eng.* **2021**, *2021*, 5594899.
[183] P. Koch, B. Bischl, O. Flasch, T. Bartz-Beielstein, C. Weihs, W. Konen, *Evol. Intell.* **2012**, *5*, 153.
[184] L. Burghignoli, M. Rossetti, F. Centracchio, G. Palma, U. Iemma, *Int. J. Aeroacoust.* **2022**, *21*, 22.
[185] E. Brochu, V. M. Cora, N. de Freitas, *ArXiv* **2010**, https://doi.org/10.48550/arXiv.1012.2599.
[186] J. Krupa, M. Minutti-Meza, *J. Fin. Rep.* **2022**, *7*, 131.
[187] T. Nummi, *Int. Stat. Rev.* **2015**, *83*, 337.
[188] C. Y. J. Peng, B. D. Manz, J. Keck, *Am. J. Health Behav.* **2001**, *25*, 278.
[189] I. Kurt, M. Ture, A. T. Kurum, *Expert Syst. Appl.* **2008**, *34*, 366.
[190] K. Buza, A. Nanopoulos, G. Nagy, *Knowl Based Syst* **2015**, *86*, 250.
[191] O. Kramer, in *K-Nearest Neighbors*, Springer, Berlin, Heidelberg, **2013**, pp. 13–23.
[192] X. Dong, Z. Yu, W. Cao, Y. Shi, Q. Ma, *Front Comput Sci* **2020**, *14*, 241.
[193] P. Mahajan, S. Uddin, F. Hajati, M. A. Moni, *Healthcare* **2023**, *11*, 1808.
[194] J. Nathan Kutz, S. L. Brunton, in *Data-driven Science and Engineering: Machine Learning, Dynamical Systems, and Control*, Cambridge University Press, **2022**, pp. 168–252.
[195] A. Glielmo, B. E. Husic, A. Rodriguez, C. Clementi, F. Noé, A. Laio, *Chem. Rev.* **2021**, *121*, 9722.
[196] M. Ahmed, R. Seraj, S. M. S. Islam, *Electronics (Basel)* **2020**, *9*, 1295.
[197] I. J. Goodfellow, J. Pouget-Abadie, M. Mirza, B. Xu, D. Warde-Farley, S. Ozair, A. Courville, Y. Bengio, *Adv. Neural Inf. Process. Syst.* **2014**, *27*, 1.
[198] S. K. Chinnamgari, *R Machine Learning Projects: Implement Supervised, Unsupervised, and Reinforcement Learning Techniques Using R 3.5*, Packt Publishing **2019**, https://books.google.co.in/books?id=4dKDDwAAQBAJ.
[199] E. F. Morales, H. J. Escalante, in *Biosignal Processing and Classification Using Computational Learning and Intelligence: Principles, Algorithms, and Applications*, Academic Press, Cambridge **2021**, pp. 11–129.
[200] X. Li, A. Li, F. Feng, Q. Jiang, H. Sun, Y. Chai, R. Yang, Z. Wang, J. Hou, R. Li, *Animal Model Exp. Med.* **2019**, *2*, 107.
[201] L. P. Kaelbling, M. L. Littman, A. W. Moore, in *The Biology and Technology of Intelligent Autonomous Agents*, Springer, Berlin Heidelberg, **1995**, pp. 90–127.

[202] S. Dharmadhikari, N. Menon, A. Basak, *Addit. Manuf.* **2023**, *71*, 103556.
[203] K. K. Moncal, H. Gudapati, K. P. Godzik, D. N. Heo, Y. Kang, E. Rizk, D. J. Ravnic, H. Wee, D. F. Pepley, V. Ozbolat, G. S. Lewis, J. Z. Moore, R. R. Driskell, T. D. Samson, I. T. Ozbolat, *Adv. Funct. Mater.* **2021**, *31*, 2010858.
[204] I. T. Ozbolat, M. Hospodiuk, *Biomaterials* **2016**, *76*, 321.
[205] E. Davoodi, E. Sarikhani, H. Montazerian, S. Ahadian, M. Costantini, W. Swieszkowski, S. M. Willerth, K. Walus, M. Mofidfar, E. Toyserkani, A. Khademhosseini, N. Ashammakhi, *Adv. Mater. Technol.* **2020**, *5*, 1901044.
[206] X. B. Chen, A. Fazel Anvari-Yazdi, X. Duan, A. Zimmerling, R. Gharraei, N. K. Sharma, S. Sweilem, L. Ning, *Bioact. Mater.* **2023**, *28*, 511.
[207] S. Tian, R. Stevens, B. T. McInnes, N. A. Lewinski, *Micromachines* **2021**, *12*, 780.
[208] S. Tian, H. Zhao, N. Lewinski, *Bioprinting* **2021**, *23*, e00156.
[209] Y. Ma, M. A. Schutyser, R. M. Boom, L. Zhang, *Innov. Food Sci. Emerg. Technol.* **2021**, *73*, 102764.
[210] G. Percoco, L. Arleo, G. Stano, F. Bottiglione, *Addit. Manuf.* **2021**, *38*, 101791.
[211] J. Shi, B. Wu, B. Song, J. Song, S. Li, D. Trau, W. F. Lu, *Ann. Biomed. Eng.* **2018**, *46*, 1267.
[212] A. K. Ball, R. Das, S. S. Roy, D. R. Kisku, N. C. Murmu, *Soft comput* **2020**, *24*, 571.
[213] S. Jaemyung, M. Kang, L.i Zhangkang, K. Hitendra, K. Kangsoo, Park Simon S., *ArXiv* **2024**, https://doi.org/10.1101/2024.09.04.611131.
[214] N. R. Schiele, D. T. Corr, Y. Huang, N. A. Raof, Y. Xie, D. B. Chrisey, *Biofabrication* **2010**, *2*, 032001.
[215] D. Hakobyan, C. Médina, N. Dusserre, M. L. Stachowicz, C. Handschin, J. C. Fricain, J. Guillermet-Guibert, H. Oliveira, *Biofabrication* **2020**, *12*, 035001.
[216] B. Guillotin, A. Souquet, S. Catros, M. Duocastella, B. Pippenger, S. Bellance, R. Bareille, M. Rémy, L. Bordenave, J. Amédée j, F. Guillemot, *Biomaterials* **2010**, *31*, 7250.
[217] J. Qu, C. Dou, B. Xu, J. Li, Z. Rao, A. Tsin, *Phys. Fluids* **2021**, *33*, 071906.
[218] A. Zennifer, A. Subramanian, S. Sethuraman, *Bioprinting* **2022**, *27*, e00205.
[219] R. Levato, O. Dudaryeva, C. E. Garciamendez-Mijares, B. E. Kirkpatrick, R. Rizzo, J. Schimelman, K. S. Anseth, S. Chen, M. Zenobi-Wong, Y. S. Zhang, *Nat. Rev. Methods Prim.* **2023**, *3*, 47.
[220] W. Li, M. Wang, H. Ma, F. A. Chapa-Villarreal, A. O. Lobo, Y. S. Zhang, *iScience* **2023**, *26*, 106039.
[221] B. Zhao, M. Zhang, L. Dong, D. Wang, *Composites Communications* **2022**, *36*, 101395.
[222] X. Wang, J. Liu, R. Dong, M. D. Gilchrist, N. Zhang, *Virtual Phys Prototyp* **2024**, *19*, e2318774.
[223] D. Banerjee, Y. P. Singh, P. Datta, V. Ozbolat, A. O'Donnell, M. Yeo, I. T. Ozbolat, *Biomaterials* **2022**, *291*, 121881.
[224] N. I. Moldovan, N. Hibino, K. Nakayama, *Tissue Eng. Part B Rev.* **2017**, *23*, 237.
[225] M. H. Kim, D. Banerjee, N. Celik, I. T. Ozbolat, *Biofabrication* **2022**, *14*, 024103.
[226] B. Ayan, N. Celik, Z. Zhang, K. Zhou, M. H. Kim, D. Banerjee, Y. Wu, F. Costanzo, I. T. Ozbolat, *Commun. Phys.* **2020**, *3*, 183.
[227] J. G. Roth, L. G. Brunel, M. S. Huang, Y. Liu, B. Cai, S. Sinha, F. Yang, S. P. Pașca, S. Shin, S. C. Heilshorn, *Nat. Commun.* **2023**, *14*, 4346.
[228] C. Liu, Y. Chen, H. Chen, P. Zhang, *Int J Bioprint* **2024**, *10*, 1214.
[229] H. Gudapati, M. Dey, I. Ozbolat, *Biomaterials* **2016**, *102*, 20.
[230] I. T. Ozbolat, in *3D Bioprinting*, Elsevier, Amsterdam **2017**, pp. 125–163.
[231] J. Chang, X. Sun, *Front. Bioeng. Biotechnol.* **2023**, *11*, 1255782.
[232] R. D. Ventura, *Medical Lasers* **2021**, *10*, 76.
[233] H. Yang, K. H. Yang, R. J. Narayan, S. Ma, *Essays Biochem.* **2021**, *65*, 409.
[234] R. Raman, R. Bashir, in *Essentials of 3D Biofabrication and Translation*, Academic Press, Cambridge **2015**, pp. 89–121.
[235] S. S. Mahdavi, M. J. Abdekhodaie, H. Kumar, S. Mashayekhan, A. Baradaran-Rafii, K. Kim, *Ann. Biomed. Eng.* **2020**, *48*, 1955.
[236] J. Creff, R. Courson, T. Mangeat, J. Foncy, S. Souleille, C. Thibault, A. Besson, L. Malaquin, *Biomaterials* **2019**, *221*, 119404.
[237] N. Mehrabi, F. Morstatter, N. Saxena, K. Lerman, A. Galstyan, *ACM Comput. Surv.* **2021**, *54*, 1.
[238] I. Basharat, S. Shahid, *J Health Organ Manag* **2024**, https://doi.org/10.1108/JHOM-10-2023-0302.
[239] C. Mennella, U. Maniscalco, G. De Pietro, M. Esposito, *Heliyon* **2024**, *10*, 26297.
[240] M. Mohammad Amini, M. Jesus, D. Fanaei Sheikholeslami, P. Alves, A. Hassanzadeh Benam, F. Hariri, *Mach. Learn. Knowl. Extr.* **2023**, *5*, 1023.
[241] M. Filippi, M. Mekkattu, R. K. Katzschmann, *Trends Biotechnol.* **2024**, *43*, 290.
[242] A. S. Albahri, A. M. Duhaim, M. A. Fadhel, A. Alnoor, N. S. Baqer, L. Alzubaidi, O. S. Albahri, A. H. Alamoodi, J. Bai, A. Salhi, J. Santamaría, C. Ouyang, A. Gupta, Y. Gu, M. Deveci, *Informat. Fusion* **2023**, *96*, 156.
[243] S. Aminizadeh, A. Heidari, M. Dehghan, S. Toumaj, M. Rezaei, N. Jafari Navimipour, F. Stroppa, M. Unal, *Artif. Intell. Med.* **2024**, *149*, 102779.
[244] A. Retico, M. Avanzo, T. Boccali, D. Bonacorsi, F. Botta, G. Cuttone, B. Martelli, D. Salomoni, D. Spiga, A. Trianni, M. Stasi, M. Iori, C. Talamonti, *Physica Medica* **2021**, *91*, 140.
[245] L. C. Zuchowski, M. L. Zuchowski, E. Nagel, *NPJ Digit. Med.* **2024**, *7*, 230.
[246] V. Tucci, J. Saary, T. E. Doyle, *J Med Artif Intell* **2022**, *5*, 6664.
[247] O. Wysocki, J. K. Davies, M. Vigo, A. C. Armstrong, D. Landers, R. Lee, A. Freitas, *Artif Intell* **2023**, *316*, 103839.
[248] E. K. Oikonomou, R. Khera, *Hellenic J. Cardiol.* **2024**, *81*, 9.
[249] A. Fedorov, W. J. Longabaugh, D. Pot, D. A. Clunie, S. D. Pieper, D. L. Gibbs, C. Bridge, M. D. Herrmann, A. Homeyer, R. Lewis, H. J. Aerts, D. Krishnaswamy, V. K. Thiriveedhi, C. Ciausu, D. P. Schacherer, D. Bontempi, T. Pihl, U. Wagner, K. Farahani, E. Kim, R. Kikinis, *Radiographics* **2023**, *43*, 1.
[250] P. Esmaeilzadeh, *Artif. Intell. Med.* **2024**, *151*, 102861.
[251] Marketing Submission Recommendations for a Predetermined Change Control Plan for Artificial Intelligence/Machine Learning (AI/ML)-Enabled Device Software Functions, **2023**.
[252] M. Gharibshahian, M. Torkashvand, M. Bavisi, N. Aldaghi, A. Alizadeh, *Skin Res. Technol.* **2024**, *30*, 70016.
[253] M. Elbadawi, L. E. McCoubrey, F. K. H. Gavins, J. J. Ong, A. Goyanes, S. Gaisford, A. W. Basit, *Adv. Drug Deliv. Rev.* **2021**, *175*, 113805.
[254] E. Westphal, B. Leiding, H. Seitz, *J. Ind. Inf. Integr.* **2023**, *35*, 100517.
[255] E. Westphal, H. Seitz, *Addit. Manuf.* **2022**, *50*, 102535.
[256] A. Q. Wang, B. K. Karaman, H. Kim, J. Rosenthal, R. Saluja, S. I. Young, M. R. Sabuncu, *IEEE Access* **2024**, *12*, 53277.
[257] B. K. Karaman, E. C. Mormino, M. R. Sabuncu, *PLoS One* **2022**, *17*, 0277322.

Joao Vitor Silva Robazzi is a professor at the Federal Institute of Education, Science and Technology of São Paulo (IFSP) since 2016, where he coordinates the Maker Laboratory at the Sertãozinho campus and teaches microcontroller and embedded systems. He holds an M.Sc. in Industrial Engineering (Operations Research, 2018) and is currently pursuing a Ph.D. in Electrical Engineering (Dynamic Systems) at the University of São Paulo. His research focuses on optimizing 3D printing and bioprinting processes using machine learning, computer vision, robotics, and mechanical and electrical analysis. The goal is to improve print quality and enable intelligent fault detection in advanced manufacturing systems.

Irem Deniz Derman is a Ph.D. candidate in the Department of Engineering Science and Mechanics at Penn State University, USA. She received her M.Sc. degree from Istanbul Technical University in 2018. Her research interests include 3D bioprinting, biomaterials, induced pluripotent stem cells, and tissue engineering. Her current work focuses on advancing functional epithelial tissue engineering through multimodal 3D bioprinting strategies.

Deepak Gupta is a postdoctoral researcher at Penn State University (Pennsylvania, USA). He completed his master's and Ph.D. from the Department of Chemical Engineering at the Indian Institute of Technology Bombay (Mumbai, India) in 2022, and bachelor's from the Department of Chemical Engineering at the Indian Institute of Technology (BHU) Varanasi (Varanasi, India) in 2014. His research work focuses on biomaterials, tissue engineering, 3D bioprinting, and disease modeling.

Logan Haugh earned his Bachelor of science degree in biomedical engineering from Pennsylvania State University in 2025. There, he worked as an undergraduate research assistant where he specialized in cell culture, microbiology assay, and 3D printing. Currently, he is pursuing a Master of Science in Chemical and Biomolecular Engineering from the University of Pennsylvania. Logan is particularly interested in translational biomedical research, including gene and cell therapies.

Yogendra Pratap Singh is an Assistant Professor at the School of Health Science and Technology, VIT Vellore, India, and a former Postdoctoral Scholar at Penn State University. He earned his Ph.D. from IIT Guwahati, focusing on silk-based biomaterials for osteochondral regeneration. His research integrates 3D bioprinting, immunomodulatory biomaterials, and stem cell technologies for regenerative medicine. Dr. Singh has authored over 25 publications, holds two patents, and serves on youth editorial boards of Bioactive Materials and the International Journal of Bioprinting. His current interests include immune-compatible implants, bioinspired engineering, and translational strategies for diabetes and neural repair.

Vaibhav Pal is currently a Ph.D. candidate in the Department of Chemistry at Pennsylvania State University, working in the Ozbolat Lab. He received his bachelor's and master's degrees in Chemistry from the Indian Institute of Science Education and Research (IISER) Mohali in 2020. His research focuses on developing microgel-based printable biomaterials for rapid vascularization and immunomodulation in regenerative medicine. He has co-authored multiple peer-reviewed publications and actively contributes to academic service and science outreach.

Yasar Ozer Yilmaz is a Research Scholar in the Ozbolat Lab at Penn State University. He holds a master's degree in Biotechnology and Bioengineering from the University of Kent, UK, and a bachelor's in Chemical Engineering from Marmara University, Türkiye. His research focuses on the development of lab-on-a-chip and bioprinting platforms for disease modeling and drug screening. He specializes in biofabrication techniques and microfluidic system integration to recreate complex tissue environments. His interdisciplinary background supports his goal of advancing innovative solutions in tissue engineering, regenerative medicine, and personalized healthcare applications.

Suihong Liu, earned a joint Ph.D. from Shanghai University (China) and TU Dresden (Germany), and is currently serving as a postdoctoral scholar in Ozbolat Lab at Penn State University. His research interests include intelligent-biofabrication of functional tissue analogs, high-throughput bioprinting of biologics, and the development of albumen-derived, nutrient-rich bioactive biomaterials for cellular agricultureadvancing sustainable and health-oriented cultivated meat systems.

Andre Luis Dias is a professor at the Federal Institute of Education, Science and Technology of São Paulo, currently serving as Research and Innovation Director at the Sertãozinho campus. His research interests include intelligent fault diagnosis, industrial communication networks, machine learning, and deep learning for industry applications. He holds a Ph.D. in 2019 and M.Sc. in 2014 in Electrical Engineering focused on Dynamic Systems from the University of São Paulo. From 2007 to 2016, he worked as an engineer at SIEMENS, where he was involved in process automation and drives, digital factory technologies, and energy management.

Rogério Andrade Flauzino was born in Franca, São Paulo, Brazil, in 1978. He holds both a Bachelor's and a Ph.D. degree in Electrical Engineering from the University of São Paulo (USP), São Carlos campus, where he completed his doctoral studies in 2007. Currently serving as an Associate Professor at USP, his research focuses on dielectrics, fault detection, and the integration of intelligent systemssuch as machine learning and computational intelligencefor diagnostics and decision-making in dynamic systems.

Ibrahim Tarik Ozbolat is a Dorothy Foehr Huck and J. Lloyd Huck Chair in 3D Bioprinting and Regenerative Medicine and Professor of Engineering Science and Mechanics, Biomedical Engineering and Neurosurgery, and a member of the Huck Institutes of the Life Sciences at Penn State University. Dr. Ozbolat's main area of research is in 3D Bioprinting. He has been working on several aspects of bioprinting, such as bioprinting processes, bioink materials, bioprinters, and post-bioprinting tissue maturation for manufacturing more than a dozen tissues and organs. Dr. Ozbolat is a leading scientist with over 190 publications, including two books in his domain. Due to his notable contributions to bioprinting, he has received several prestigious international and national awards.